KINETIC AND MECHANISTIC ANALYSIS OF ELECTROCHEMICAL REDUCTION IN ELECTRON DEFICIENT AROMATIC HALIDES

A Thesis

submitted by

A. MUTHUKRISHNAN

for the award of the degree

of

DOCTOR OF PHILOSOPHY

DEPARTMENT OF CHEMISTRY
INDIAN INSTITUTE OF TECHNOLOGY MADRAS
CHENNAI - 600 036

JULY 2010

THESIS CERTIFICATE

This is to certify that the thesis entitled **"Kinetic and Mechanistic Analysis of Electrochemical Reduction in Electron Deficient Aromatic Halides"** submitted by **A. Muthukrishnan** to the Indian Institute of Technology Madras for the award of degree of **Doctor of Philosophy** is a bonafide record of research work carried out by him under my supervision. The contents of this thesis, in full or in parts, have not been submitted to any other Institute or University for the award of any degree or diploma.

Chennai -600036 Prof. M. V. Sangaranarayanan

Date: (Research Guide)

ACKNOWLEDGEMENTS

I would like to express my deep and utmost gratitude to ***Prof. M. V. Sangaranarayanan*** *for allowing me to work under his guidance. I owe my deepest gratitude for his valuable guidance, kindness and most of all for his patience. I am grateful to him for his constant encouragement and support. The thesis would not be possible without his constant support and valuable discussions. He is friendly, helpful and it has been my great pleasure to work under his guidance.*

I would like to acknowledge Prof. ***R. Dhamodharan****, Head, Department of Chemistry for allowing me to use the facility in this department. I also thank the former Heads in the department of Chemistry. My thanks and appreciation goes to my thesis committee members,* ***Prof. D. Loganathan****,* ***Prof. Sanjay kumar****, and* ***Prof. K. Hariharan*** *for their valuable comments and suggestions during the doctoral committee meetings.*

The thesis could have never been completed without the love and support of my friends throughout the years. I would like to extend my thanks to ***R. Elayaraja, K. Senthil Kumar****,* ***V. Vimalan*** *and* ***Ramesh Kumar****, who created a pleasant atmosphere during my stay in IIT Madras.*

I would like to thank my labmates ***G. Nandhini*** *and* ***M. Vinoth kumar*** *for their support and spending their valuable time with me.*

I would like to acknowledge ***Council of Scientific and Industrial Research, India*** *for their Fellowship and* ***Indian Institute of Technology Chennai*** *for providing me the facilities.*

A. Muthukrishnan

ABSTRACT

KEYWORDS: *[reductive cleavage, convolution potential sweep voltammetry, dissociative electron transfer, 4-fluorobenzonitrile, methylfluorobenzoate, halopentafluorobenzene, stepwise reduction, concerted mechanism, Density functional calculations, potential energy diagram]*

The reduction of carbon-fluorine bond in 4-fluorobenzonitrile in acetonitrile as the solvent, is analyzed using Convolution Potential Sweep Voltammetry and the dependence of the transfer coefficient on potential is investigated within the framework of Marcus-Hush quadratic activation-driving force theory. The validity of stepwise mechanism is inferred from solvent reorganization energy estimates as well as bond length calculations. The electrodimerization of 4-fluorobenzonitrile was noticed at higher scan rates and the minimum concentration for the electrodiemrization has been estimated as 4mM. A novel method of calculating the standard reduction potential of the 4-fluorobenzonitrile is proposed.

The electrochemical reduction of methylfluorobenzoates at glassy carbon electrodes is analyzed using the convolution potential sweep voltammetry (CPSV). The stabilization of the radical anion due to the electron-withdrawing group is shown to lead to intra-molecular stepwise dissociative electron transfer. While methyl 2-fluorobenzoate (*ortho* isomer) follows EC mechanism, the methyl 4-fluorobenzoate (*para*- isomer) undergoes electro-dimerization prior to C-F bond cleavage. The first order rate constant for the EC mechanism and the dimerization rate constant for the electro-dimerization are deduced from the classical as well as convolution potential sweep voltammetry. A plausible mechanism of dimerization is suggested. The influence of the electron-withdrawing groups is illustrated by comparing the reduction behaviour of methylfluorobenzoates

with 4-fluorobenzonitrile. The potential energy surfaces and electron density mapping employing Gaussian 03 calculations provide further support for the validation of the mechanism pertaining to C-F bond cleavages.

The mechanistic analysis pertaining to the reductive cleavage of C-X (X =Cl,Br,I) bonds in halopentafluorobenzenes has been investigated at glassy carbon electrodes using convolution potential sweep voltammetry. The quadratic activation-driving force relation has been found valid, with potential-dependent transfer coefficients. The charge density analysis using density functional calculations, estimation of intrinsic barriers and standard reduction potentials indicate that the mechanism can not be classified unambiguously either as stepwise or concerted in these compounds. The non-linear behaviour of the transfer coefficient with potential may indicate the change in mechanism from stepwise to concerted pathway. From various diagnostic criteria, the C-X bond cleavage mechanism appears to be border-line between stepwise and concerted.

TABLE OF CONTENTS

Chapter 2 Mechanistic analysis of electrochemical reduction of 4-fluorobenzonitrile

Chapter 3 Analysis of C-F bond cleavages in methylfluorobenzoates - Fragmentation and dimerization of anion radicals

LIST OF TABLES

LIST OF FIGURES

LIST OF SYMBOLS AND ABBREVIATIONS

a_{RX} radius of the *RX* molecule, ´

A surface area of the electrode, cm^2

b order of the reaction

$C_O(0,t)$ surface concentration of the oxidized species at time *t*, M

$C_R(0,t)$ surface concentration of the reduced species at time *t*, M

C_b bulk concentration, M

CPSV Convolution Potential Sweep voltammetry

D diffusion coefficient, cm^2s^{-1}

D_P interaction energy between the fragments, eV

D_{RX} dissociation energy of the R-X bond, eV

e_0 electronic charge, C

E^0 standard reduction potential, V

E_p peak potential, V

$E_{p/2}$ half peak potential, V

$E^0_{RX/RX^{\bullet -}}$ standard reduction potential of RX (stepwise mechanism), V

$E^0_{RX/R^{\bullet}+X^-}$ standard reduction potential of RX (concerted mechanism), V

f_R force constant of the reactant, Nm^{-1}

f_P force constant of the products, Nm^{-1}

F Faraday constant, 96500 $Cmol^{-1}$

Fc ferrocene

G_P free energy of products, eV

G_R free energy of reactants, eV

$\Delta G_0^{\#}$ intrinsic barrier, eV

G_P^0 standard Gibbs free energy of products, eV

G_R^0 standard Gibbs free energy of reactants, eV

$\Delta G_b^{\#}$ activation barrier of the reverse reaction, eV

$\Delta G_f^{\#}$ activation barrier of the forward reaction, eV

ΔG^0 standard free energy of the reaction, eV

ΔG_{sol}^0 standard free energy of solvation, eV

$\Delta_{tr} G_{X,Y\to Z}^0$ standard Gibbs transfer free energy of compound X from solvent Y to Z, eV

i current, A

I convoluted current, $As^{1/2}$

I_l limiting convoluted current, $As^{1/2}$

IP ionization potential, eV

k first order rate constant s^{-1}

k_d dimerization rate constant, mol^{-1} lit s^{-1}

k_{ET} heterogeneous electron transfer rate constant, cm s^{-1}

n number of electrons involved in the reaction

R Universal gas constant, $JK^{-1}mol^{-1}$

RX organic halide

ΔS^0 entropy change of the reaction under standard conditions, eV

t time, s

Δt time interval between two voltammetric points, t

T temperature, T

v scan rate, Vs^{-1}

w_R work done in bringing the reactant from bulk to surface of the electrode, eV

w_P work involved in transfer of the products from reaction zone to bulk, eV

α transfer coefficient or symmetry factor

ε_o optical dielectric constant

ε_s static dielectric constant

λ_s solvent reorganization energy, eV

λ_i inner reorganization energy, eV

φ_r electrical potential at the reaction site, V

CHAPTER 1

INTRODUCTION AND SCOPE OF THE PRESENT INVESTIGATION

SECTION 1.1 INTRODUCTION TO ELECTROCHEMICAL REDUCTION OF ORGANIC COMPOUNDS

The reductive cleavage of organic compounds continues to be a fascinating topic of research on account of diverse mechanistic pathways- mediated by the solvent characteristics and magnitude of the driving force. Among various organic substrates, aromatic halides are especially interesting in view of the difficulty in their reduction as one passes from carbon-fluorine to carbon-iodine bonds. It is customary to anticipate that these reductions lead to the neutral radical and the corresponding halide anion. The stabilization of these radical anions is controlled by several factors such as (i) carbon-halogen bond energy (ii) presence of electron-withdrawing groups in the aromatic moiety; (iii) polarity of the solvent medium etc. The reduction of the organic halides (RX) may in general be represented as

$$RX + e \rightleftarrows RX^{\bullet -} \rightarrow R^{\bullet} + X^{-} \qquad (1.1)$$

$$RX + e \rightarrow R^{\bullet} + X^{-} \qquad (1.2)$$

In the conventional nomenclature of electron transfer processes at electrodes, it is customary to designate the above as EC mechanism wherein ‘E’ refers to the electron transfer while ‘C’ denotes the chemical reaction. One would anticipate that the relative rates of the initial electron transfer and the chemical reaction would dictate

the overall mechanism. It is of interest to compare the reduction of aliphatic and aromatic halides in order to comprehend the role of the aromatic ring as well as the substituents.

1.1.1. Reduction of aliphatic halides

In the reduction of alkyl halides studied by Andriuex et al (Andrieux *et al*, 1986 a; Andrieux *et al*, 1986 b), it was observed that the reduction of 1-bromobutane, 2-bromobutane, *tert*-butylbromide led to two cyclic voltammetric waves each, thus confirming the formation of corresponding neutral radical and carbanion. On the other hand, electrolysis of 1-bromodecane yielded decane and 1-decene as the products while the reduction of iodoethane (Dahm and Peters, 1994) led to a mixture of ethane, butane and ethylene in different proportions. The reduction of CCl_4 has been studied by various investigators (Wawzonek and Duty, 1961; Baizer and Chruma, 1972; Karrenbrock and Schafer, 1978; Shono *et al*, 1981; Shono *et al*, 1982; Shono *et al*, 1984; Sibille *et al*, 1986). The reduction of CCl_4 at glassy carbon electrodes leads to the formation of two successive two-electron transfer peaks. The first peak indicates the formation of $CHCl_3$ and the second peak denotes the reduction of $CHCl_3$ to CH_2Cl_2. The kinetics and mechanism of the reduction of CCl_4 was analyzed by Pause and coworkers (Pause *et al*, 2000) in dimethyformamide (DMF) and also in DMF-H_2O binary solvents (Prasad and Sangaranarayanan, 2004 b). Interestingly, different types of aldehydes and ketones can be prepared by the electrogenerated CCl_3^- formed from the reduction of CCl_4. The vicinal halides undergo two-electron reduction to yield olefins. The reduction of *meso* 2,3-dibromobutane at Hg electrodes resulted in *trans*-butene while *d,l*-2,3-dibromobutane

led to *cis*-butene, thus indicating the role of stereochemistry in the reduction of aliphatic halides. The reduction of vicinal dibromides at carbon electrodes yielded the corresponding olefin as was demonstrated by Andrieux and coworkers (Andrieux *et al*, 1994 a). The carbanion formed by the two-electron reduction undergoes a rearrangement in the case of vinyl halides (Miller and Riekena, 1969; Fry and Mitnick, 1969; Elving *et al*, 1961; Yoshida *et al*, 1986). The reduction of acetalinic halides is potential dependent and in the case of 6-bromo 1-phenyl 1-hexyne, a variety of products is formed upon reduction (McNamee *et al*, 1977). In general, most of the aliphatic halides undergo de-halogenation followed by protonation in polar solvents. The reduction of haloacetonitrile leads to dimerization due to the presence of the electron-withdrawing CN group (Cardinale *et al*, 2002). The silver electrode shows a catalytic activity for the reduction of aryl bromides and substituted aryl bromides. A recent study by Isse and coworkers (Isse *et al*, 2009 a, Isse *et al*, 2009 b, Durante *et al*, 2009) led to the inference that Ag electrodes result in the reduction of aryl bromides at more positive potentials in comparison with the glassy carbon electrode.

1.1.2. Reduction of aromatic halides

Andrieux and coworkers investigated (Andrieux *et al*,1979, Andrieux *et al*, 1986 b) the mechanism of the reduction of aromatic halides. The halobenzenes and halopyridines undergo two-electron irreversible reductions to form the corresponding protonated compound. The reduction of bromobenzene at cadmium-coated stainless steel electrode gives aldehydes (Saboureau *et al*, 1989). The reduction of fluorobenzene is rendered difficult since the C-F bond energy is higher; however, it can be reduced in an indirect manner using mercury cathodes in diglyme containing a

mixture of tetrabutylammonium tetrafluoroborate and dimethylpyrrolidinium tetrafluoroborate (Miller and Vajtner, 1985). The reduction of different halogen-substituted benzenes yield monohalogens at first and subsequently, further reduction to dehalogenated compounds in a stepwise manner. For example *p*-fluoroiodobenzene and *p*-bromoiodobenzene form respectively, fluorobenzene and bromobenzene. These mono halides finally lead to benzene at still higher negative potentials. The reduction of 5-bromo-1,3-dichloro-2-iodobenzene at carbon electrode leads to removal of halides from the benzene ring in the sequence iodine < bromine < chloro(1) < chloro(2) (Prasad and Sangaranarayanan, 2004 c) and iodine being the easiest to reduce. The substituted aromatic halides such as halonitrobenzene and halocyanobenzenes increase the life time of intermediate radical anion and this can be inferred from Electron Spin Resonance studies. The mechanism of reduction of pentafluoronitrobenzene and pentachloronitrobenzene at glassy carbon in DMF has been investigated by Andrieux and coworkers (Andrieux *et al*, 1994 b). The reduction of halogenated aromatic carbonyl compounds yields the dehalogenated alcohols viz. pentafluorobenzaldehyde on reduction yields both pentafluorobenzyl alcohols and 2,3,4,5-tetrafluorobenzayl alcohol when Hg is employed as the electrode (Drakesmith, 1972).

1.1.3. Reduction of polyhalides

The electrochemical reduction at specific position in 1,2-dimethyl-4,5,6,6-tetrachlorospiro [2.3] hexadiene at mercury electrode and deuterium oxide on monodehalogenation forms 1,2-dimethyl-4,5,6,trichloro-6-deuteriospiro [2.3] hexadiene. (Semmelhack *et al*, 1972). Strelow and coworkers reduced 1,1,3,3-

tetrachlorodispirocyclobutanes and obtained 1,3- dichlorodispirobicyclo [1.1.0] butanes (Lund and Hammerich, 2001). The energetics of the reduction of polychlorinated ethylenes and the possible mechanism of the dehalogenation of polychlorinated ethylenes have been analyzed by *ab initio* electronic structure methods (Bylaska *et al*, 2008). The reduction of poly chlorinated biphenyls and polychlorinated naphthalenes employing 'interrupted voltammogram' provides valuable insights regarding the nature of chlorines most susceptible to reduction. Farwell and coworkers (Farwell *et al*, 1975) studied a variety of polychlorinated biphenyls and naphthalenes using this strategy.

1.1.4. Electrochemical techniques for elucidation of reaction mechanism

It is customary to employ the cyclic voltammetry or square wave voltammetry for obtaining kinetic and mechanistic information of electro-organic reactions. The three-electrode assembly depicted in Figure 1.1 has been extensively employed in conjunction with the Faraday cage wherever necessary. The divided and undivided cells have both been employed in this context. The present day Electrochemical workstations provide easy analysis of experimental data as well as simulation of the voltammograms. The preferred electrode material in such studies is the glassy carbon electrode on account of the wide potential window accessible for experimental studies. On account of environmental concerns and the possibility of the reaction of radicals with mercury leading to mercurated compounds (Brown and Taylor, 1974; Mbarak and Peters, 1982), Hg has not been preferred as the working electrode. The choice of solvents is dictated by two considerations viz (i) its ability to dissolve the

species and (ii) stability during the reaction. Acetonitrile and dimethylformamide have been the most popular solvents for electrochemical studies.

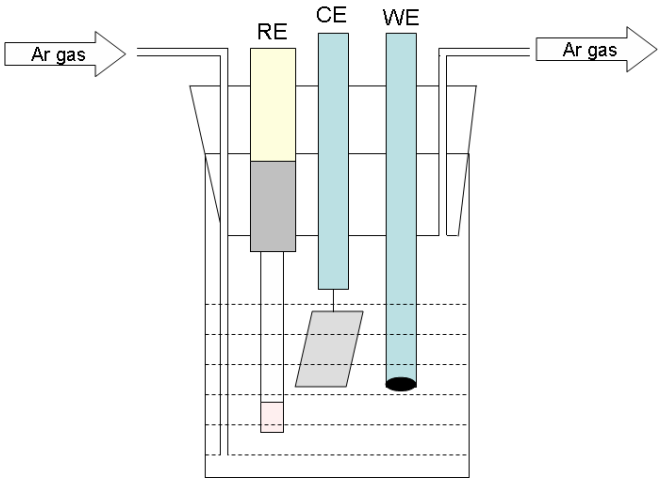

Figure 1.1 Schematic diagram of a single compartmental cell customarily employed for studying electrochemical reductions. The symbols RE, CE and WE refer respectively to the reference, counter and working electrodes.

SECTION 1.2 METHODS FOR ELUCIDATION OF THE REDUCTION MECHANISM

As mentioned earlier, the cyclic voltammetric techniques or its variants such as Convolution Potential Sweep Voltammetry (CPSV) have been extensively employed for kinetic and mechanistic studies; hence it is appropriate to indicate the experimental quantities of interest: (i) the peak potential and peak width estimates under different control variables and (ii) working curves arising from the classical Nicholson and Shain analysis for various schemes. As a complimentary to these experimental data, quantum chemical calculations provide a rationale into the product formation from the perspective of geometric and energetic considerations. The digital simulation of cyclic voltammograms with reasonable molecular parameters using commercial software such as DIGISYM as well as user-friendly more generalized softwares for mechanistic analysis and geometry of the electrodes viz EChem++ developed by Speiser (Ludwig and Speiser, 2004) deserve mention in this context.

1.2.1. Dependence of the peak potential and peak width on scan rates

The dependence of the peak potential on the scan rate (v) plays a central role in comprehending the mechanism of the electron transfer process and provides the rate constants and standard electrode potentials as appropriate. As is well-known, the peak potential is independent of the scan rates for completely-reversible reactions and hence the value of $\partial E_p/\partial \log(v)$ is zero. In the case of entirely irreversible processes, $\partial E_p/\partial \log(v) > 29.4$. As mentioned earlier, the reduction of organic halides at electrodes generally follows the EC mechanism and a further sub-division is also

sometimes employed depending upon the relative rates of the two steps viz electron transfer and bond breaking: (i) stepwise pathway (eC) wherein the bond breaking chemical reaction is the rate determining step and (ii) concerted pathway (Ec) wherein the initial electron transfer is the rate determining step. In eC and Ec mechanisms, the capital letters denotes the rate- determining step (Testa and Reinmuth, 1961). In the case of substrates exhibiting EC mechanism, the variation of the E_p with scan rate is represented by the following equation (Parker, 1985)

$$\frac{\partial Ep}{\partial \log(v)} = \frac{1}{1+b} \ln(10) \frac{RT}{F} \tag{1.3}$$

where R, T and F denote the universal gas constant, absolute temperature and Faraday respectively, b being the order of the reaction. For stepwise electron transfer processes, the slope ($\partial E_p/\partial \log(v)$) is ~ 29.4mV and in the case of concerted processes, this value is > 60mV.

The constancy of the transfer coefficient (α) is an indication of the applicability of the Butler-Volmer equation and hence its estimation from the peak width measurements is non-trivial. For concerted processes, the equation for the peak width is given by Nicholson and Shain as

$$|E_{p/2} - E_p| = 47.5 / \alpha \tag{1.4}$$

where $E_{p/2}$ is the half peak potential. For concerted electron transfer reactions, the peak width is always > 95.6mV and α is < 0.5 while in the case of the stepwise mechanism, the peak width ~ 47.8mV (Nadjo and Savéant, 1973). The intermediate values pertaining to $\partial E_p/\partial \log(v)$ as well as $E_{p/2} - E_p$ indicate that the kinetics of the reactions is controlled by both the processes. Table 1.1 provides the diagnostic criteria for different mechanistic pathways.

Table 1.1 The magnitude of $\partial E_p/\partial \log(v)$ and $|E_{p/2} - E_p|$ for various processes

Mechanism of electron transfer	$\partial E_p/\partial \log(v)$ (mV)	$E_{p/2} - E_p$ (mV)	Inference
E mechanism	~0	56.5	Reversible process
Stepwise	29.4	47.8	Initial electron transfer step is faster
Concerted	>60	>95.6	Electron transfer is the rate-determining step
Electrodimerization	19.4	60	Initial electron transfer is faster and the dimerization of radical anions is the rate-determining step

1.2.2. Investigation of reaction mechanism using theoretical working curves

Nicholson and Shain (Nicholson and Shain, 1964) developed a comprehensive theory for the voltammetric response of several commonly encountered reaction schemes and provided tabular compilations and/or diagnostic working curves for estimating the rate constants, transfer coefficients etc. The stepwise reduction of organic molecules leads to a stable radical anion which can be identified within the time scale of the experiment. At high scan rates, the appearance of the reversible peak is the indicative of the formation of the stable radical anion. The ratio between the anodic and cathodic peak potentials (or the difference between the anodic and cathodic peak potentials) can also be employed for estimating the rate constants with the help of the theoretical working curves (Nicholson and Shain, 1964; Nicholson, 1965).

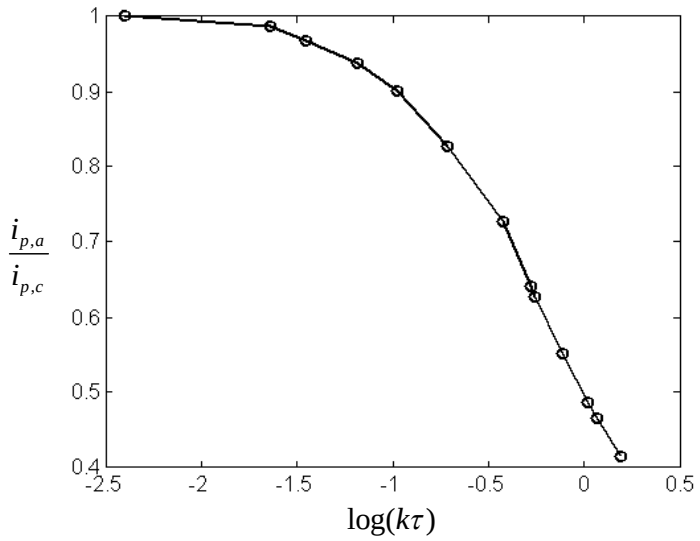

Figure 1.2: Estimation of the rate constants (k) using the ratio between anodic and cathodic peak currents using the working curve approach of Nicholson and Shain (Nicholson and Shain, 1964). τ denotes the time between the peak potential and switching potential. The points denote the predicted values while the line is drawn as a guide to the eye.

The standard rate constant for concerted electron transfer schemes is related to the peak potential (E_p), standard reduction potential (E^0) and scan rate (v) as

$$E_p = E^0 - \frac{RT}{nF}\left[0.78 - \ln\left(\sqrt{\frac{k}{a}}\right)\right] \tag{1.5}$$

where $a = nFv/RT$. The estimation of the standard reduction potentials for irreversible electron transfer processes will be indicated later. It is possible to deduce the rate constants for reversible charge-transfer processes followed by chemical reactions, from the ratio of anodic and cathodic peak currents using the working curves. This methodology is illustrated in Figure 1.2.

1.2.3. Convolution Potential Sweep Voltammetry (CPSV)

The convolution potential sweep voltammetry constitutes a versatile technique in the elucidation of kinetic parameters since (i) all the data points of the voltammogram are taken into consideration; (ii) no *a priori* assumption of the current-potential equation is required; (iii) the dependence of the transfer coefficient on potential arises naturally and (iv) accurate estimates of the standard rate constants are possible.

The convolution current $I(t)$ is related to the experimental voltammetric current $i(t)$ via a semi- integral as (Imbeaux and Savéant, 1973; Savéant and Tessier, 1975 a; Nadjo and Savéant, 1973)

$$I(t) = \frac{1}{\sqrt{\pi}} \int_0^t \frac{i(u)}{(t-u)^{\frac{1}{2}}} du \tag{1.6}$$

The convoluted current encompasses the properties of the current as well as charge and the convoluted current has the dimension Amperes second$^{1/2}$. While several numerical algorithms can be employed for computing the above semi-integral, the following algorithm suggested by Lawson and Maloy (Lawson and Maloy, 1974) is especially convenient on account of easy implementation

$$I(t) = \frac{1}{\sqrt{\pi}} \sum_{j=1}^{j=k} \frac{i(j\Delta t)\Delta t}{\sqrt{k\Delta t - j\Delta t + 0.5\Delta t}} \tag{1.7}$$

wherein Δt denotes time difference between adjacent points in voltammograms. As shown in Figure 1.3, a sigmoidal shape for the dependence of the convoluted current on potential arises in general with a limiting value designated as the limiting convoluted current (I_l) viz.

$$I_l = nFAC_b\sqrt{D} \tag{1.8}$$

where C_b is the bulk concentration of the reactant, D denotes its diffusion coefficient, A is the surface area of the electrode, 'n' being the number of electrons involved.

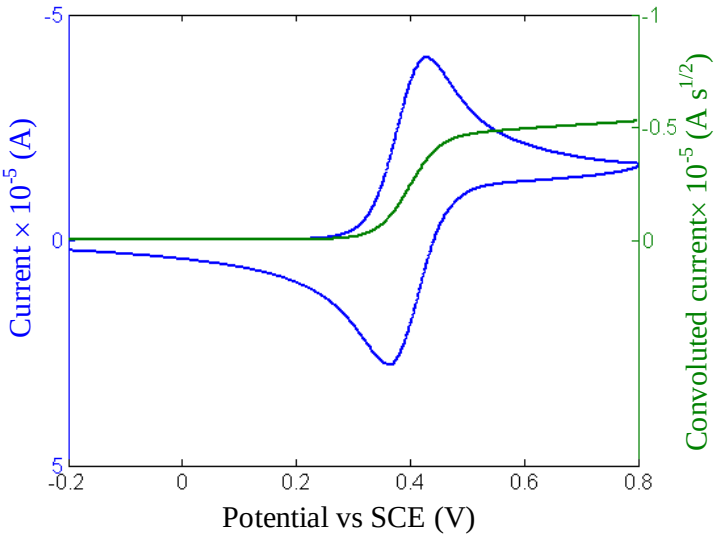

Figure 1.3: Cyclic voltammogram of Ferrocene at Glassy Carbon electrodes at a scan rate of 0.1Vs^{-1}; supporting electrolyte: 0.1M TBAP; solvent: acetonitrile. The green line indicates the convolution current for forward segment of the cyclic voltammogram.

The merit of the CPSV consists in explicit evaluation of the surface concentrations of the oxidized $C_O(0,t)$ and reduced species $C_R(0,t)$ using the following equations:

$$C_O(0,t) = \frac{I_l - I(t)}{nFAD_o^{1/2}} \tag{1.9}$$

and

$$C_R(0,t) = \frac{I(t)}{nFAD_R^{1/2}} \tag{1.10}$$

These equations enable the estimation of the electron transfer rate constants as indicated below for irreversible electron transfer processes. The relation between the voltammetric current $i(t)$ and surface concentrations is

$$i(t) = FAk(E)\left[C_O(0,t) - \theta C_R(0,t)\right] \tag{1.11}$$

where $\theta = k_b/k_f$. Combining the preceding equations, it is possible to derive the expression for the logarithmic rate constant as given in equation 1.12, assuming the diffusion coefficients of oxidized and reduced species to be equal viz.

$$\ln(k_{ET}) = \ln(\sqrt{D}) - \ln\frac{I_l - I(t)}{i(t)} \tag{1.12}$$

Thus k_{ET} can be estimated as a function of the electrode potential. In order to obtain the standard electrode potentials, a graphical procedure is employed using the variation of the electrode potential with current viz.

$$E = E^0 + \frac{RT}{F}\ln\left[\frac{I_l - I}{I}\right] \tag{1.13}$$

In the case of a reversible charge transfer reaction followed by an irreversible chemical reaction, an analogous analysis leads to the estimation of rate constants from the intercept of *I-E* plot i.e

$$E = E^0 + \frac{RT}{2F}\ln k + \frac{RT}{F}\ln\left(\frac{I_l - I}{i}\right) \tag{1.14}$$

The advantages of CPSV can be further illustrated in the cases of systems which undergo electro-dimerization. The *I-E* equation in such dimerization systems is (Savéant and Tessier, 1975 a)

$$E = E^0 + \frac{RT}{3F}\ln\left(\frac{2k_d}{3FA\sqrt{D}}\right) + \frac{RT}{F}\ln\left[\frac{I_l - I}{i^{2/3}}\right] \tag{1.15}$$

from which the dimerization rate constant k_d is obtainable. It may be noted that the linear variation of logarithmic rate constant with the potential suggests that the Butler-Volmer kinetics is valid with a constant value of the transfer coefficient. On the other hand, the non-linear dependence implies that the transfer coefficient is dependent upon the electrode potential and the quadratic activation-driving force relation of

Marcus-Hush theory is valid (Marcus and Sutin, 1985). The potential dependent transfer coefficient follows as

$$\alpha = -\frac{RT}{F}\frac{d\ln(k_{ET})}{dE} \tag{1.16}$$

It is imperative to emphasize the crucial role of α in the elucidation of the reaction mechanism. For most of the simple inorganic ions, the electron transfer follows the outer sphere electron transfer and α is in general ≥ 0.5. The estimated transfer coefficient is independent of the potential. This value *inter alia* implies that the activation energy barrier is symmetric and the perturbation of the potential energy surface by the applied potential is uniform for the reactants and products. However, for reactions of organic compounds on electrode surfaces, α is seldom constant and varies from 0 to1 depending on the mechanism of the reaction. For stepwise mechanisms, α is expected to be > 0.5 and for concerted processes, α is < 0.5. If the transfer coefficient varies linearly with the potential, the customary Marcus theory is valid; when this dependence itself is non-linear, it suggests more involved reaction mechanisms where several competing factors operate. While the CPSV has the advantage of employing scan rates ranging from millivolts per second to megavolts per second, an equally versatile technique in the analysis of electrochemical systems is offered by the Electrochemical Impedance Spectroscopy. (Barsoukov and Macdonald, 2005).The data analysis involves postulating an appropriate equivalent circuit and deducing the system parameters such as charge transfer resistance, double layer capacitance, ohmic resistance, constant phase elements etc by fitting of the experimental data using the Nyquist and/ or Bode plots. This technique (cf. Macdonald, 1977) has been exploited to a significant extent in the Underpotential deposition of metals (Retter *et al*, 2003), electrochemical supercapacitors (Girija and Sangaranarayanan, 2006) etc. The application of the electrochemical impedance

spectroscopy to the elucidation of the reaction mechanism of electro-organic reactions however has not been extensive presumably due to the de-coupling of various factors by judicious choice of the supporting electrolyte and solvents.

1.2.4. Quantum chemical calculations

The quantum chemical calculations employing density functional theory (DFT) provide further insights into the reaction mechanism. A particularly popular approach in this context is offered by the Gaussian 03 software (Frisch *et al*, 2004) whereby several energetic parameters can be estimated for the reactant and solvent in vacuum as well as for chosen solvents under varying levels of sophistication. These DFT calculations are especially convenient for distinguishing between the stepwise and concerted pathways of the reductive cleavage of organic halides. Further, the bond lengths of the cleaving carbon-halogen bonds estimated from the DFT is useful in determining the mechanism. The quantum chemical calculations are exploited in the following manner: The optimization of the neutral molecule and anion radical is carried out and the bond lengths are calculated from the optimized geometry. In the case of aromatic halides, the electron initially goes to π^* orbital of the molecule and forms a radical anion; it is then transferred to the σ^* orbital of the C-X bond. There are two types of intermediates (i) anion radical intermediate and (ii) radical-ion pair intermediate. These can also be designated as π and σ anion complexes. The bond length of the cleaving bond of radical-ion pair is always grater than radical anion. Hence for compounds which undergo stepwise reduction, the C-X bond length will not vary significantly before and after the electron transfer, whereas, in the case of concerted mechanisms, the bond length of the radical anions will be larger. This

methodology involving the calculation of bond lengths has been illustrated for the reduction of haloacetonitriles (Cardinale *et al*, 2002) and the occurrence of concerted mechanism has been inferred.

Another parameter obtainable from the quantum chemical calculations is the partial atomic charge of the cleaving halogen atom. In haloacetonitriles (chloro, bromo and iodo), the charge on the halide anion radical is > 0.7 indicating the predominant negative charge on them. Thus the cleavage is facilitated. In order to visualize the geometrical effects, the Lower Unoccupied Molecular Orbital (LUMO) of neutral molecule and the Singly Occupied Molecular Orbital (SOMO) of the anion radical are also sometimes constructed for further confirmation of the mechanism.

SECTION 1.3 THEORIES OF ELECTRON TRANSFER PERTAINING TO REDUCTIVE CLEAVAGE OF ORGANIC HALIDES

The theories of electron transfer at metal electrodes have a chequered history. The classical formulation due to Butler-Volmer and Gurney (Bard and Faulkner, 2001) predicts a current-potential response for the reaction $ox + ne \underset{k_b}{\overset{k_f}{\rightleftharpoons}} red$ as

$$i = FAk^0[C_O(0,t)e^{-\alpha f(E-E^0)} - (C_R(0,t)e^{(1-\alpha) f(E-E^0)}] \quad (1.17)$$

where k^0 is the standard heterogeneous rate constant, $f = F/RT$ and E^0 denotes the equilibrium or standard potential. It has been shown recently that the above equation can be derived from Onsager's non-equilibrium thermodynamics formalism (Sethi and Sangaranarayanan, 2008). Further, analogous equations hold good for electron transfer at liquid/liquid interfaces too (Volkov and Deamer, 1996). For completely irreversible processes, it is possible to discard either of the two exponential terms in equation (1.17) and resort to a plot of ln(i) vs (E-E^0). This Tafel polarization method then yields the standard rate constant *vis a vis* exchange current density as well as the transfer coefficient. Thus a linear variation of the logarithmic rate constant with potential suggests the validity of the Butler-Volmer kinetics.

1.3.1. Marcus-Hush Kinetics

The non-linear dependence of ln(k_{ET}) on E for a variety of organic compounds on electrode surfaces has led to an alternate formulation of the electron transfer processes pioneered by Marcus.

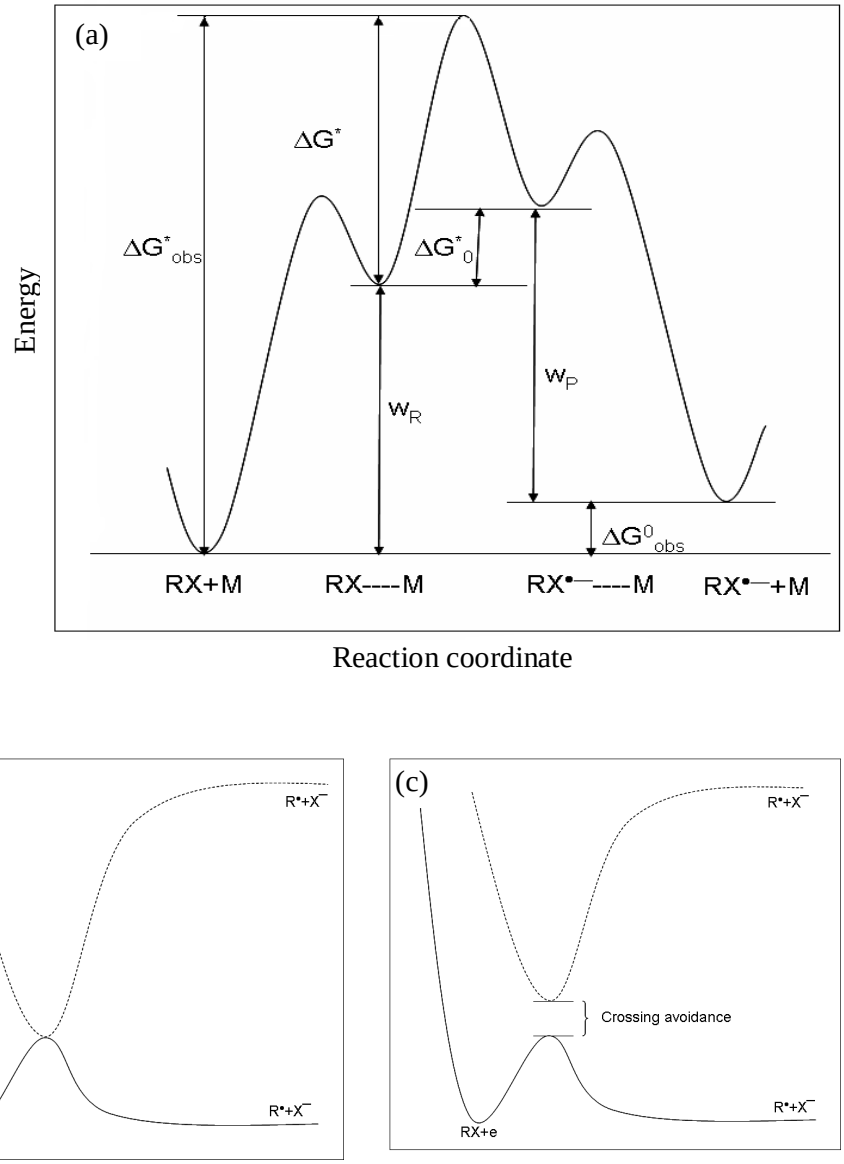

Figure 1.4 Schematic potential energy diagram for outer sphere electron transfer. (a) Energetic components associated with the outer sphere electron transfer. (b) Strong coupling between the reactant and the electrode produce leading to the decrease in the probability of the formation of products (c) Weak coupling between the electrode and the reactant leading to a more facile formation of products.

One of the central features of this theory is the quadratic dependence of the activation energy on driving force (in contrast to the linear dependence given by the Butler-Volmer equation). The validity of the Born-Oppenheimer approximation and adiabatic outer sphere nature underlies the Marcus-Hush theory (Marcus, 1956; Hush, 1958; Hush, 1961; Marcus, 1963; Marcus, 1968; Marcus, 1977; Marcus and Sutin, 1985). As can be seen from Fig 1.4, the work terms involving the reactants (w_r) and products (w_p) play a central role in the analysis. Consequently, the precise role played by the solvent media, extent of alteration of the activation energy, intrinsic barrier of the system etc naturally arise in this analysis.

The total Gibbs free energy of the reactants (G_R) and products (G_P) are given by considering the various vibrational modes constitutes the internal reorganization energy and solvent or external reorganization energy

$$G_R = G_R^0 + w_R + \frac{1}{2}\lambda_s (x - x_R)^2 + \frac{1}{2}\sum f_R (y - y_R)^2 \tag{1.18}$$

$$G_P = G_P^0 + w_P + \frac{1}{2}\lambda_s (x - x_P)^2 + \frac{1}{2}\sum f_P (y - y_P)^2 \tag{1.19}$$

G_R^0 and G_R^0 denote the standard Gibbs free energies of the reactants and products respectively. w_R denotes the work required to bring the reactants (precursor complex) to the reaction zone. w_P represents the work involved in transporting the product from the surface to bulk. The reorganization energy comprises of two contributions viz (i) inner reorganization energy (λ_i) and (ii) outer (or solvent) reorganization energy (λ_s) (Taube, 1970). The inner reorganization energy arises due to the change in the bond lengths and bond angles on account of electron transfer. The solvent reorganization energy is estimated from changes in solvation effects. The harmonic approximation is useful in calculating the reorganization energy. For estimating the internal

reorganization energy, all the vibrational modes are included and considered to be additive. In the analysis propounded by Marcus, the solvent reorganization energy is given by

$$\lambda_s = \frac{e_0^2}{2a_{RX}}\left(\frac{1}{\varepsilon_o} - \frac{1}{\varepsilon_s}\right) \tag{1.20}$$

ε_o and ε_s denote respectively the optical and static dielectric constant of the solvent. a_{RX} is the radius of the molecule. The calculation of activation free energy by minimization of the free energy profiles leads to the following quadratic equations for the Gibbs free energy of activation:

$$\Delta G_f^{\#} = w_R + \Delta G_0^{\#}\left(1 + \frac{\Delta G^0 - w_R + w_P}{4\Delta G_0^{\#}}\right)^2 \tag{1.21}$$

$$\Delta G_b^{\#} = w_P + \Delta G_0^{\#}\left(1 + \frac{\Delta G^0 - w_R + w_P}{4\Delta G_0^{\#}}\right)^2 \tag{1.22}$$

Here, $\Delta G^0 = G_R^0 - G_P^0$ or $\Delta G^0 = E - E^0$ and is the standard Gibbs free energy change of the process. $\Delta G_0^{\#}$ is the standard free energy of activation at zero driving force and is also referred to as the intrinsic barrier. This intrinsic barrier depends only upon the structural parameters of the species and is not influenced by the driving force. The intrinsic barrier is related to the reorganization energies as

$$\Delta G_0^{\#} = \frac{\lambda_i + \lambda_s}{4} \tag{1.23}$$

After replacing the work terms w_R and w_P by $zF\varphi_r$ and $(z-1)F\varphi_r$ respectively where φ_r denotes the electrical potential at the reaction site the final expression for the current-potential relation is given by

$$\frac{i}{FA} = Z\exp\left[-\frac{zF\varphi_r}{RT} - \frac{G_0^{\#}}{RT}\left(1 + F\frac{E - E^0 + \varphi_r}{4G_0^{\#}}\right)^2\right]\left\{[C_R]_0 - [C_P]_0\exp\left(\frac{F}{RT}(E - E^0)\right)\right\} \tag{1.24}$$

A is the surface area of the electrode and $[C_R]_0$ and $[C_P]_0$ are the surface concentrations of the reactants and products respectively while the charge number of the reactant is z. The symmetry factor or transfer coefficient (α) is now estimated from

$$\alpha = \frac{\partial \Delta G_f^{\#}}{\partial \Delta G^0} \tag{1.25}$$

$$\alpha = 0.5\left(1 + F\frac{E - E^0 - \varphi_r}{4\Delta G_0^{\#}}\right) \tag{1.26}$$

The quadratic activation driving force relationship has been investigated in the case of reduction of organic halides using Marcus theory (Marcus and Sutin, 1985). While carrying out cyclic voltammetric experiments, the driving force can be altered by changing the scan rates which is equivalent to varying the electrode potentials. The experimental verification of Marcus-Hush model has been carried out for a series of nitro-derivatives in DMF (Peover and Powell, 1967) as well as thiocarbonates.

While the Butler-Volmer and Marcus kinetic laws have profound importance in phenomenological analysis of electron transfer reactions at electrode surfaces, quantum chemical approaches of diverse sophistication (Bockris and Khan, 1979) have been propounded in order to comprehend the role of adiabaticity. In this context, a recent Monte Carlo simulation for estimating the transmission coefficient for low overpotentials is noteworthy in view of incorporating the electrode-reactant coupling within a random walk perspective.(Kuznetsov *et al*, 2002).

1.3.2. Marcus-Savéant theory for dissociative electron transfer

The term 'dissociative' indicates that the bond breaking occurs on account of the electron transfer process. Thus, the bond breaking and the electron transfer steps are concerted. Due to bond breaking, the outer sphere mechanism of Marcus-Hush is not directly valid and the harmonic oscillator approximation also does not hold good. In order to circumvent these limitations, an alternate approach for the dissociative electron transfer theory was developed by Wentworth for the reduction of alkyl halides in the *gas phase* (Wentworth *et al*, 1969). Savéant and his coworkers in a series of papers have developed a comprehensive theory of dissociative electron transfer processes in the *solution phase* (Savéant, 1987; Savéant, 1990; Savéant, 1993). The potential energy vs reaction coordinate diagram is depicted in Figure 1.5 for dissociative electron transfer occurring at electrode surfaces.

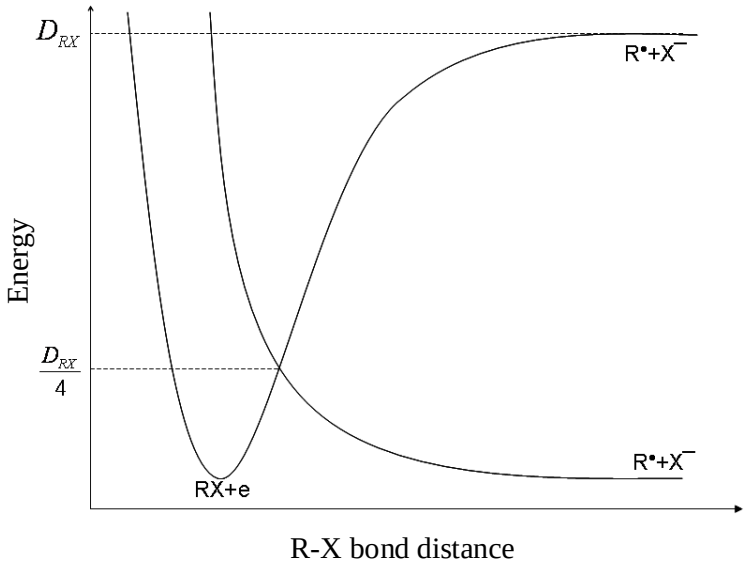

Figure 1.5 Marcus-Savéant Model for dissociative electron transfer processes depicting the dissociation energy of the *RX* bond.

The most salient feature of this analysis is the incorporation of the dissociation energy of the *RX* bond in the expression for the intrinsic barrier viz.

$$\Delta G_0^{\#} = \frac{D_{RX}}{4} + \frac{\lambda_i + \lambda_s}{4} \tag{1.27}$$

The transfer coefficient varies linearly with the potential as in the case of the Marcus theory. Its value being > 0.5 or < 0.5 has interesting implications regarding diagnostic criteria of electron transfer processes.

1.3.3. Extended Marcus-Savéant theory for fragmental interactions

It is of interest to enquire the nature of interactions among the fragments and their stabilization (or otherwise) arising from the polarity of the medium. In an earlier formalism of Marcus-Savéant, the interactions between the fragments are considered to be repulsive. This need not always be true and the presence of the electron-withdrawing groups and the extent of dipolar interactions will dictate the mechanism of electron transfer. The compounds which possess electron-withdrawing groups create a partial positive charge on the radical center which leads to the interaction between fragments in the polar media. These are designated as charge-dipole or ion-radical interactions. In order to incorporate these ion-radical interactions, the activation driving force relationship is modified as

$$\Delta G^{\#} = \frac{\left(\sqrt{D_{RX}} - \sqrt{D_P}\right)^2}{4}\left(1 + \frac{\Delta G^0 - D_P}{4\Delta G_0^{\#}}\right)^2 \tag{1.28}$$

where, D_P denotes the ion-radical interaction energy. The corresponding potential energy profile is depicted in Figure 1.6. The expression for the intrinsic barrier becomes

$$\Delta G_0^{\#} = \frac{\left(\sqrt{D_{RX}} - \sqrt{D_P}\right)^2}{4} + \frac{\lambda}{4} \qquad (1.29)$$

in stead of equation (1.27). While the ion-radical interaction is not altered by the driving force, the intrinsic barrier decreases significantly. If the ion-radical interaction energy is about 1% of the bond dissociation energy, the intrinsic barrier decreases by ~ 15%. The haloacetonitriles (Cardinale *et al*, 2002) and carbon tetrachloride (Pause *et al*, 2000) constitute illustrative examples for these ion-radical fragmental interactions.

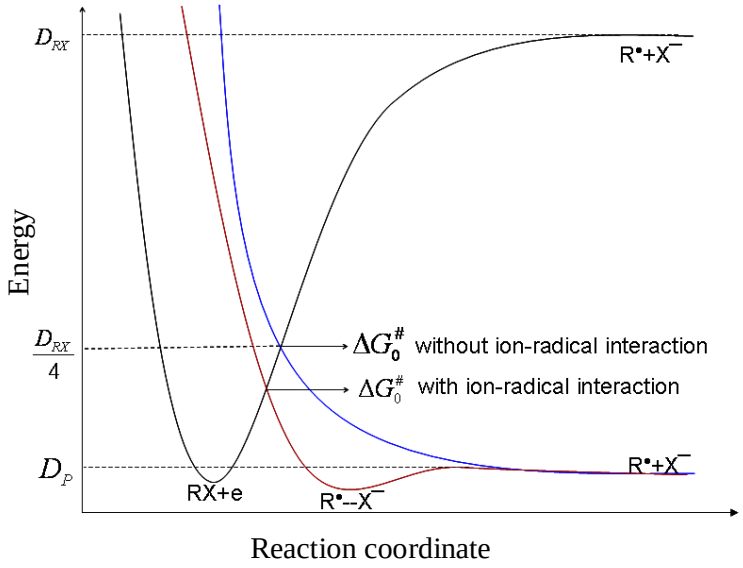

Figure 1.6 Marcus –Savéant potential energy profile for the dissociative electron transfer reactions containing ion-radical interactions.

1.3.4. Competition between stepwise and concerted mechanism

As mentioned earlier, the reductive cleavage of halides can occur either via the stepwise or concerted mechanisms. However, in some cases, the transition from one

mechanism to the other is feasible by changing the driving force. The driving force can be varied either by changing the electrode potential (through the scan rates in cyclic voltammetry) or by altering the temperature. This change in mechanism from stepwise to concerted has been observed in the investigation of the electrochemical reduction of sulphonium cations at carbon electrodes in acetonitrile (Andrieux *et al*, 1994 c).

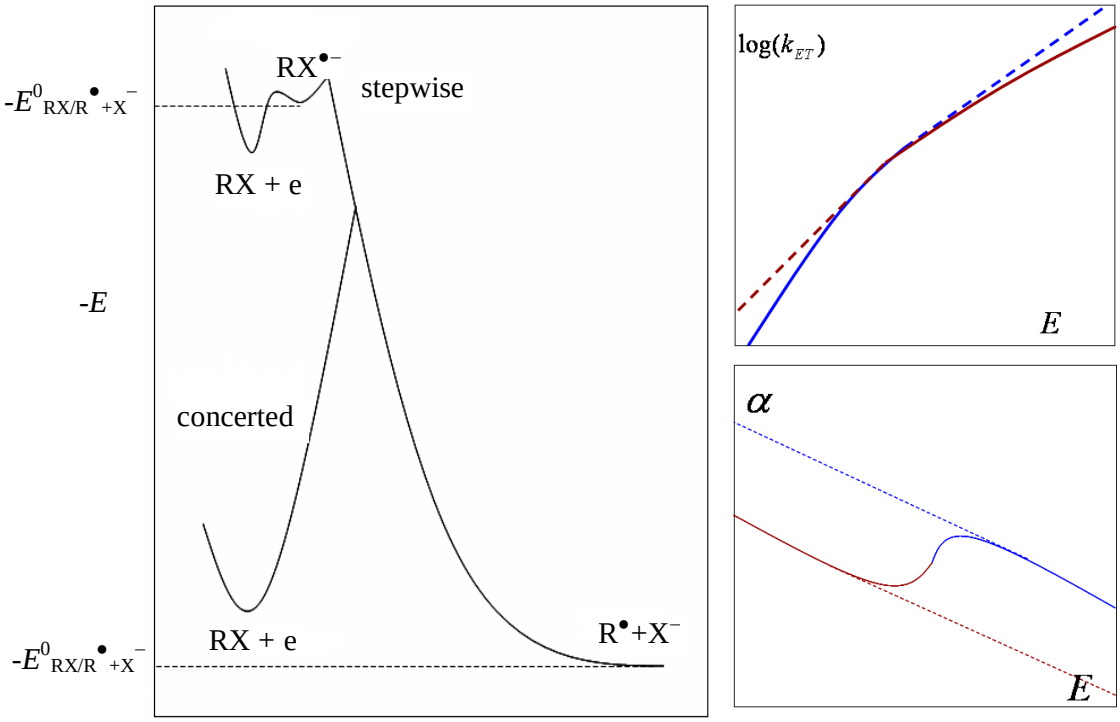

Figure 1.7 (a) Schematic variation of the energy profile for the transition between concerted and stepwise mechanisms. (b) The variation of the rate constant with potential and (c) the dependence of the transfer coefficient on potential. The blue line indicates the stepwise pathway while the red line indicates the concerted mechanism. (Costentin *et al*, 2006).

The reduction of chloro and bromobenzene at carbon electrode in DMF follows stepwise mechanism while that of iodobenzene (Pause *et al*, 1999) changes from concerted to stepwise upon an increase in the scan rate. The mechanistic shift between the three isomers of the cyano benzylchlorides has been recently identified by Costentin and coworkers (Costentin *et al*, 2009) wherein the *orhto* and *para* isomers follows concerted mechanism and the *meta* isomer forms stable intermediate radical anion (stepwise pathway). The peculiar dependence of the transfer coefficient on potential is indicative of this mechanistic transition (Figure 1.7).

1.3.5. Electron transfer at chemically modified electrodes

While the analysis of electron transfer at metal/electrolyte interface is concerned with estimating the rate constants, transfer coefficients and activation energies, the mechanism of charge transport at redox polymer electrodes has been a frontier area of research during the past three decades, in view of the immense potentialities in electrocatalysis (Anson *et al*, 1991; Chidsey and Murray, 1986; Fritsch-Faules and Faulkner, 1989). The formulation of the diffusion migration equations and solution of the same under different potential perturbations have been a central theme in this context (Savéant, 1986). Analogously, the study of electron transfer through monolayer-covered electrodes has several interesting applications. In particular, the study of electron transfer kinetics of cytochrome *c* immobilized on the alkanethiol monolayers at electrode surfaces is of immense relevance to diverse processes in bio-electrochemistry (Leopold and Bowden, 2002; Nakano *et al*, 2007).

SECTION 1.4 METHODS FOR ESTIMATING STANDARD REDUCTION POTENTIAL OF ORGANIC HALIDES

In contrast to reversible electron transfer processes, the estimation of standard reduction potentials is not straight forward in the case of organic halides which undergo irreversible electron transfer reactions. Among several methods available for estimating E^0 in this context, the following deserve mention: (a) from thermochemical cycles; (b) with the help of voltammetry at microelectrodes using high scan rates and (c) employing the potential-dependent transfer coefficients obtained using CPSV.

1.4.1. Estimation of E^0 from thermochemical cycles

This method can be illustrated briefly for stepwise and concerted mechanisms. In the case of compounds which follow stepwise mechanism, the standard reduction potential can be denoted as $E^0_{RX/RX^{\bullet -}}$. On the other hand, for concerted processes, it is denoted as $E^0_{RX/R^{\bullet}+X^-}$. Fu and coworkers (Fu *et al*, 2005) demonstrated the method using the thermochemial cycles in order to estimate the oxidation potential of organic molecules and the radicals.

The parametric equation for E^0 in terms of the solvation energies (ΔG^0_{sol}) and adiabatic ionization potential (*IP*) has been deduced as (Fu *et al*, 2005)

$$E^0_{RX^{\bullet -}/RX}(vs\ NHE) = IP + \frac{1}{23.06}(-T\Delta S^0 + \Delta G^0_{sol1} - \Delta G^0_{sol2}) - 4.44 \qquad (1.30)$$

where ΔS^0 is the change in entropy.

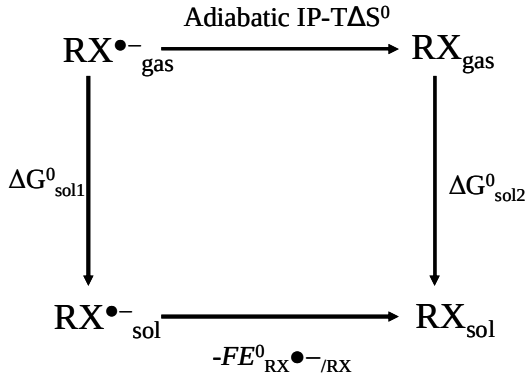

Scheme 1.1 Thermochemical cycle for estimating the oxidation potentials.

In the case of dissociative electron transfer reactions (concerted), an alternate thermochemical cycle (Scheme 1.2) is postulated wherein the dissociation energy (D_{RX}) of the organic halides is included.

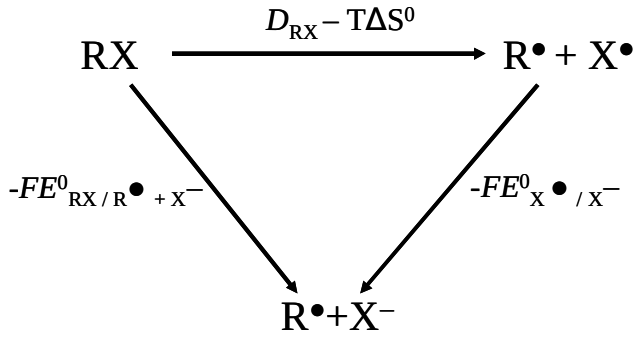

Scheme 1.2 Thermochemical cycle for estimating the standard reduction potential in the case of disscociative electron transfer reactions

The equation pertaining to E^0 follows from the above thermochemical cycle as

$$E^0_{RX/R^{\bullet}+X^-} = -D_{RX} + T\Delta S^0 + E^0_{X^{\bullet}/X^-} \qquad (1.31)$$

where $E^0_{X^{\bullet}/X^-}$ is tabulated the standard reduction potential of the halides. The oxidation of the organic halides and radicals following outer sphere mechanism can be calculated using the equation (1.30).

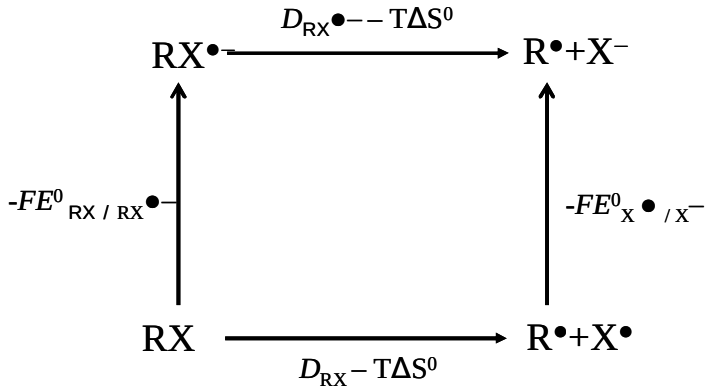

Scheme 1.3 Thermochemical cycle for estimating E^0 for stepwise reduction of organic halides.

An alternate thermochemical cycle depicted in Scheme 1.3 can also be made use of estimating the reduction potential of organic molecules. The standard reduction potential follows as

$$-FE^0_{RX/RX^{\bullet-}} = (D_{RX^{\bullet-}} - D_{RX}) + T(\Delta S^0_{RX \rightarrow R^{\bullet}+X^{\bullet}} - \Delta S^0_{RX^{\bullet-} \rightarrow R^{\bullet}+X^-}) + E^0_{X^{\bullet}/X^-} \quad (1.32)$$

where $D_{RX^{\bullet-}}$ is the bond dissociation energy of the radical anion. The thermodynamic parameters appearing in the above equation may be estimated from the DFT based approaches.

1.4.2. Estimation of E^0 from high scan-rate cyclic voltammetry at microelectrodes

An accurate experimental method for obtaining the standard reduction potential involves the use of cyclic voltammetry at microelectrodes. For stepwise reductive

electron transfer schemes, the radical anion is more stable which is again oxidized (before it undergoes decomposition or fragmentation) by employing very high scan rates. In a typical illustration of this technique, nitrobenzene derivatives (Prasad and Sangaranarayanan, 2005 a) exhibiting irreversible cyclic voltammograms at low scan rates yielded reversibility at larger scan rates. Even radical anions that are not very stable and arise from concerted mechanisms can also be trapped or oxidized at microelectrodes using large scan rates. The reductive cleavage of 4-nitrobenzylchloride in DMF exhibits two peaks viz. the first peak denotes the reversible reduction of nitro group while the second peak indicates that pertaining to chlorine. In order to obtain the standard reduction potential for chlorine, scan rates ~ 100,000 Vs^{-1} at Pt microelectrodes has been employed (Andrieux et al, 1992).

1.4.3. Estimation of E^0 from potential-dependent transfer coefficients

It follows from the equation (1.26) that α=0.5 when E=E^0. Thus, from the variation of α with E, the potential corresponding to α=0.5, becomes E^0 as depicted in Figure 1.8. If the dependence of α is more involved, non-linear regression analysis need to be invoked for obtaining E^0. It may be noted that there exist a subtle relation between the standard potentials and peak potentials and its nature is dictated by the mechanism of the reduction.

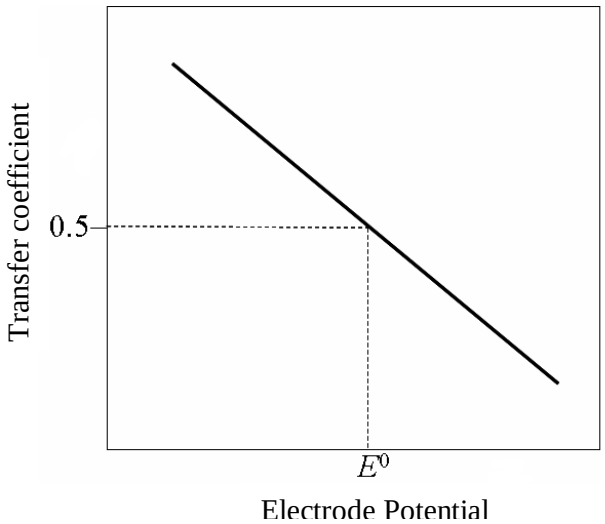

Figure 1.8 Schematic illustration of the transfer coefficient method for estimating E^0 in dissociative electron transfer reactions

1.4.4. Solvent effect

In all electron transfer processes, the solvent plays a crucial role on account of its ability to solvate the reactants. In reductive cleavages, the stabilization of anion radicals is influenced by the polarity of solvents. As mentioned earlier, in organic halides, the electron is first transferred to π* orbital of the molecule and then it is transferred to σ* orbital of the cleaving bond. The π-anion complex is a radical anion intermediate while the σ-anion complex constitutes an ion-radical pair. The solvents affect both the intermediates- albeit differently. In polar solvents, the radical anions or π-anion complex are highly stabilized while the σ-anion complex dissociates into solvent-separated ion and radical. The solvents solvate the two fragments to varying extent leading to the bond dissociation. The radical anions are however not stable in non-polar solvents since the anion radicals are more polar. On the other hand, the σ-

anion complex is stabilized since the bond dissociation leads to the charged particles that are unstable in non-polar medium. Furthermore, the polar solvents promote the stepwise pathway while the non-polar solvents facilitate the dissociative electron transfer.

The solvation influences not only the mechanism of the reaction but also their rates. The increase in the polarity of the solvents leads to enhancement in the stabilization of the intermediate radical anion thus leading to a decrease in the rate constant. The concerted mechanism occurs via σ-anion complex and the rate constants increase as the polarity increases. In the study of the reduction of nitro and cyanobenzylhalides (Costentin *et al*, 2004), the rate constants decrease while passing from acetonitrile to water on account of the stepwise mechanism. Further, a change in mechanism from one solvent to another is also not improbable. The solvation of leaving anion and ion-pairing of anion radicals in binary solvents for the reduction of haloanthracenes, halonitrobenzenes and haloacetophenones constitutes a typical example (Andrieux *et al*, 1995). The change in the mechanism due to the solvation effect also studied by Jaworski and coworkers (Jaworksi *et al*, 2009). In this study, the reduction of 1-chloro-10-methyltribenzotriquinacene in benzonitrile follows stepwise mechanism and it follows dissociative concerted electron transfer in acetonitrile and DMF, arising from the stronger solvation effect offered by acetonitrile and DMF.

SECTION 1.5 SCOPE AND OBJECTIVE OF THE PRESENT INVESTIGATION

1.5.1. Motivation for the present investigation

The electrochemical reduction of carbon-halogen bonds has been investigated using voltammetric techniques such as Cyclic voltammetry, Square wave voltammetry etc. However, each technique provides new challenges and novel insights into the kinetics and mechanism. The reduction of aromatic halides in the presence of electron-withdrawing groups offers several interesting possibilities. The flow chart provided in the Scheme 1.4 for distinguishing between the step wise and concerted mechanism is an illustration of the power of the cyclic voltammetry in the mechanistic analysis of electron transfer processes.

The reduction of organic chlorides, bromides and iodides have been extensively studied under different conditions but the study on fluorides have been scarce on account of the inherent difficulty arising from the strength of the C-F bond. The reduction occurs at large negative potentials which is almost near the reduction potentials of solvents and supporting electrolyte. It is of interest to investigate whether this limitation can be overcome by choosing reactants having electron-withdrawing groups such as –CN, $-COOCH_3$, $-NO_2$ etc. The study involving the reduction of fluoromethylarenes (Andrieux *et al*, 1997 a) by Andrieux and coworkers follows stepwise reduction for each fluorine. Thus it will be interesting to study substrates with fluorine in different positions of the aromatic ring.

1.5.2. Objectives of the study

The objectives of the present investigation are as follows:

(i) To investigate the electrochemical reduction of 4-fluorobenzonitrile using CPSV and quantum chemical calculations;

(ii) To analyse the electrochemical reduction of *ortho* and *para* isomers of methylfluorobenzoates with the help of the classical Nicholson and Shain method as well as CPSV;

(iii) To investigate the electrochemical reduction of chloro, bromo and iodo pentafluorobenzene using CPSV and quantum chemical calculations.

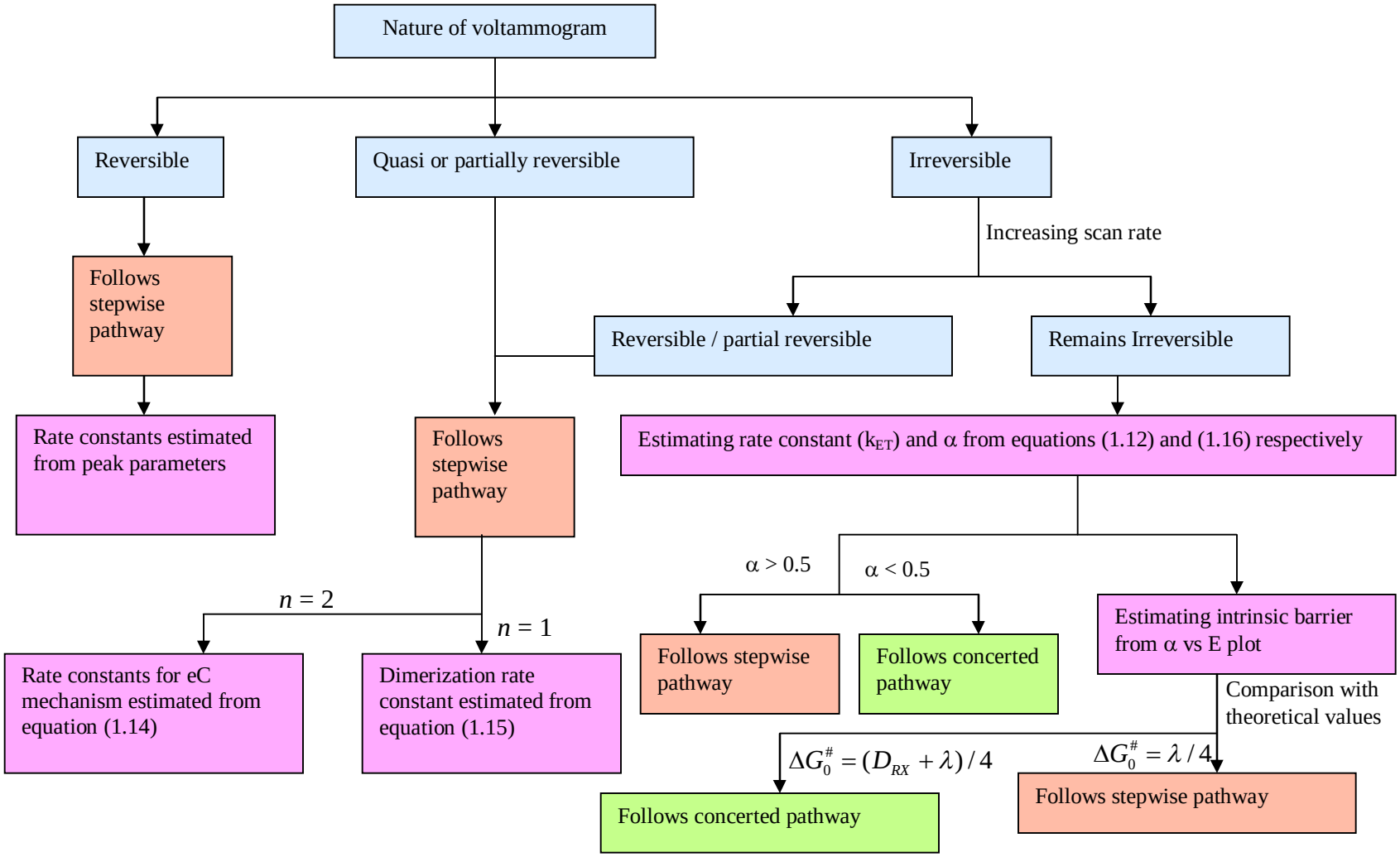

Scheme 1.4 A flow chart for distinction between concerted and stepwise mechanism.

CHAPTER 2

MECHANISTIC ANALYSIS OF ELECTROCHEMICAL REDUCTION OF 4-FLUOROBENZONITRILE

SECTION 2.1 INTRODUCTION

The electrochemical reductive cleavage of carbon-halogen bonds is influenced by different thermodynamic and structural factors. In general, aromatic halides follow the stepwise mechanism while concerted mechanism occurs in the case of aliphatic halides. The analysis of carbon-fluorine bonds is especially challenging since the reduction of these compounds occurs at potentials wherein the solvent and /or supporting electrolytes undergo decomposition. In order to circumvent this limitation, the methodology of redox catalysis has been employed (Andrieux *et al*, 1979).

The electrochemical reduction of aromatic chlorides, bromides and iodides has been investigated by several research groups as indicated in Chapter 1. However, the study on the reduction of aromatic fluorides has been rare. The bond energy of the carbon-halogen bonds follow the sequence (in $kJmol^{-1}$) C-I (213) < C-Br (276) < C-Cl (339) < C-F (448) for aliphatic compounds. The reduction of C-F bond is studied in trifluoromethylarenes by Combellas and coworkers (Combellas *et al*, 1996) in liquid ammonia at -38°C. The reduction of all three fluorines which occurs in a stepwise manner has also been studied for substituted trifluoromethylbenzenes at 20°C using DMF as solvent (Andrieux *et al*, 1997). The intramolecular dissociative electron

transfer model was applied for this system to deduce the rate constant and symmetry factor. The reduction of phenacyl fluoride (Elvinga and Leone, 1957) at dropping mercury electrode gives two polarographic waves indicating the defluorination and the acetophenone reduction, along with the pH dependence of the reduction.

The halobenzenes (RX) in general undergo irreversible electron transfer reactions wherein the electrons donated by the electrode is initially transferred to the π^* orbital of the halobenzenes thereby forming the corresponding radical anions. This is followed by a subsequent transfer to the σ^* orbital of the carbon-halogen bond yielding the radical ($R^{\bullet}$) and the halide anion (X^-). Since the redox potential of the radical ion ($R^{\bullet}$) is more positive than that of the halobenzene (RX), the reduction of the resulting radical becomes more favourable. The anion then abstracts a proton preferably from solvent (Webster, 2004) thus forming a neutral molecule.

The objectives of this Chapter are

(i) to analyze the reduction of carbon-fluorine bond in 4-fluorobenzonitrile using CPSV;

(ii) to demonstrate the occurrence of stepwise mechanism using bond length calculations and solvent reorganization energies from quantum chemical calculations;

(iii) to estimate the standard reduction potential of 4-fluorobenzonitrile using Gibbs transfer free energies and to deduce the standard reduction potential of of $F^{\bullet}$ in acetonitrile.

SECTION 2.2 KINETICS OF THE REDUCTION OF 4-FLUOROBENZONITRILE

2.2.1. Cyclic voltammetry

The cyclic voltammetric experiments were carried out using the CH Instruments 660A, USA in a single-compartment electrochemical cell thermostatted at 298 K. The working electrode was a glassy carbon electrode of 3 mm diameter (CH Instruments, USA) polished with 0.3, 0.1 and 0.05 μ graded γ-alumina slurry and sonicated in methanol before each experiment. The Ag/Ag^+ electrode was employed as the quasi-reference electrode, while the counter electrode was a platinum wire. Under identical conditions of the solvent and supporting electrolyte, the potential of the Ag/Ag^+ quasi-reference electrode was calibrated with reference to the Fc/Fc^+ couple. The substrate 4-fluorobenzonitrile (Sigma-Aldrich) and the supporting electrolyte tetrabutylammonium perchlorate (TBAP) (Sigma-Aldrich) were employed without further purification. Acetonitrile (HPLC grade, SRL India) distilled over calcium hydride as per the protocols in the literature (Armarego and Chai, 2003) and protected by 3 Å molecular sieves in argon atmosphere was employed. High purity argon was passed through the solution to remove the dissolved oxygen before each experiment. The uncompensated solution resistance was measured before the experiment and the ohmic drop was compensated leaving the residual resistance of 35Ω for scan rate below 1 Vs^{-1} and 50Ω above the scan rate of 1 Vs^{-1}. Figure 2. 1 depicts a typical cyclic voltammogram for the reduction of 4-fluorobenzonitrile in acetonitrile (ACN) containing 0.1 M TBAP at a scan rate of 0.3 Vs^{-1}. The wave remains irreversible up to a scan rate of 0.7 Vs^{-1}. The small reversible peak appearing at the scan rate of 1 Vs^{-1}

indicates the existence of the radical anion (Figure 2.2) whose life-time is 10^{-4} seconds or higher.

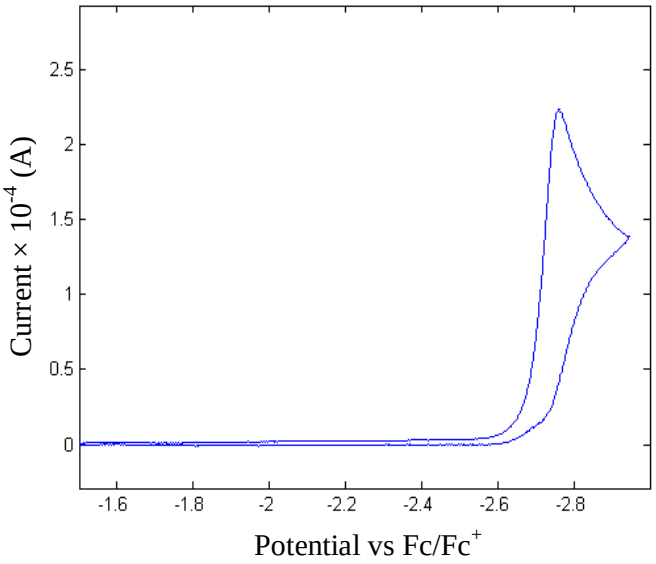

Figure 2.1 Background subtracted Cyclic Voltammogram of 4-fluorobenzonitrile (1 mM) in acetonitrile. Supporting electrolyte: 0.1 M TBAP. (Scan rate 0.3 Vs^{-1}).

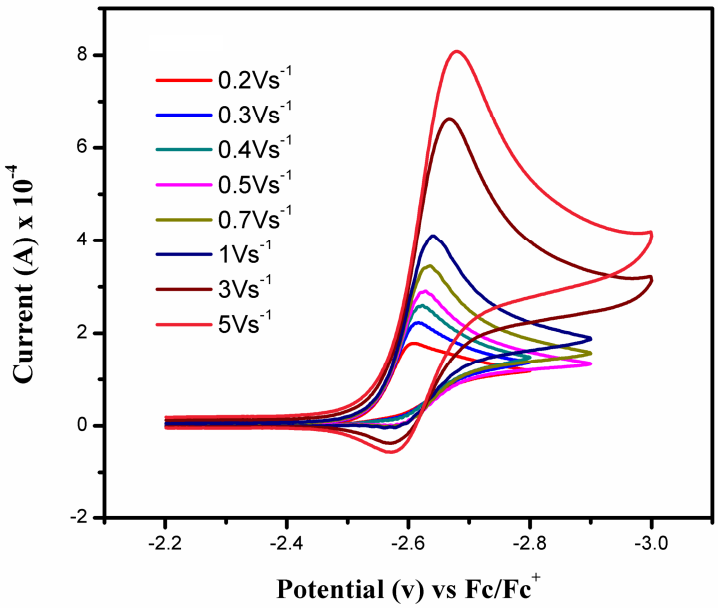

Figure 2.2 Background subtracted cyclic voltammogram of 4-fluorobenzonitrile at different scan rates.

The ratio between cathodic and anodic peak currents indicates the extent of the reversibility. The value of $i_{p,c}/i_{p,a}$ is 2.92 at the maximum scan rate of 5 Vs^{-1}. Since C-F bond dissociation energy is higher, the peak potential corresponding to it is more negative (-2.76 V vs Fc/Fc^{+} at 0.3 Vs^{-1}) than other halides. The peak potential varies with log(v) in a linear manner and the mean slope is 49.3 mV. The peak width ranges from 44 mV (at 0.1 Vs^{-1}) to 68 mV (at 5 Vs^{-1}). From the above characteristics of the cyclic voltammogram, it is inferred that the electron transfer step is rapid while the follow-up reaction is the rate-determining step (Nadjo and savéant, 1973).

2.2.2. Effect of concentration

It is of interest to enquire whether the reduction of 4-fluorobenzonitrile apart from yielding the reduced product can also undergo dimerization to yield 4,4'-dicyanobiphenyl since the latter product in fact was found by Houser et al when the solvent employed was DMF (Houser *et al*, 1973). Further, the dimer formation was noticed whenever the concentration exceeded 0.5 mM. In order to investigate the mechanism of dimer formation, the concentration of 4-fluorobenzonitrile was varied employing the scan rate as high as 30 Vs^{-1}. A plausible mechanism of dimerization suggested by Houser and coworkers is shown below:

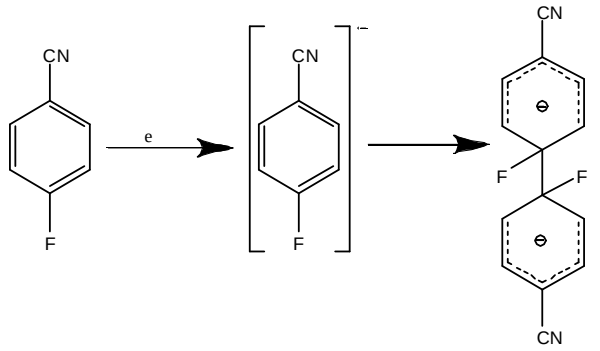

Scheme 2.1 Dimerization of 4-fluorobenzonitrile anion radicals

Interestingly, as the substrate concentration is enhanced (higher than 4 mM), additional anodic peaks indicating the formation of the dimer appear (cf. Figure 2.3). Further, these peaks become more prominent as concentration is further increased. These additional anodic peaks arise due to the oxidation of 4,4'-dicyanobiphenyl- formed by the reduction of 4-fluorobenzonitrile. This implies that the minimum threshold concentration required for the dimer formation is 4 mM. Hence it is appropriate to employ the mechanistic analysis pertaining to the results at 1 mM concentration of 4-fluorobenzonitrile since dimer formation does not occur at this concentration. It may be pointed out here that when repetitive scans were carried out at concentrations higher than 4 mM, the corresponding cathodic peaks (due to the reduction of two CN groups in the dimer) arise thus confirming the formation of dimer.

2.2.3. Convolution Potential Sweep Voltammetry

The scan rate normalized voltammograms for the scan rates ranging from 0.1 Vs^{-1} to 5 Vs^{-1} are provided given in Figure 2.4(a). The CPSV is particularly useful in the elucidation of the reaction mechanism. The advantage of CPSV has its origin in the existence of simple mathematical relationships between the reactant concentration at the electrode surface and the convoluted current. The convoluted current (I) is related to the experimentally observed current (i) through the convolution integral given in the equation (1.6). Using the numerical integration with the help of the Lawson-Maloy algorithm (cf. equation 1.7) the dependence of the convoluted current on potential is deduced (Figure 2.4 b). The MATLAB program written for obtaining the convolution current is provided in the Appendix-A.

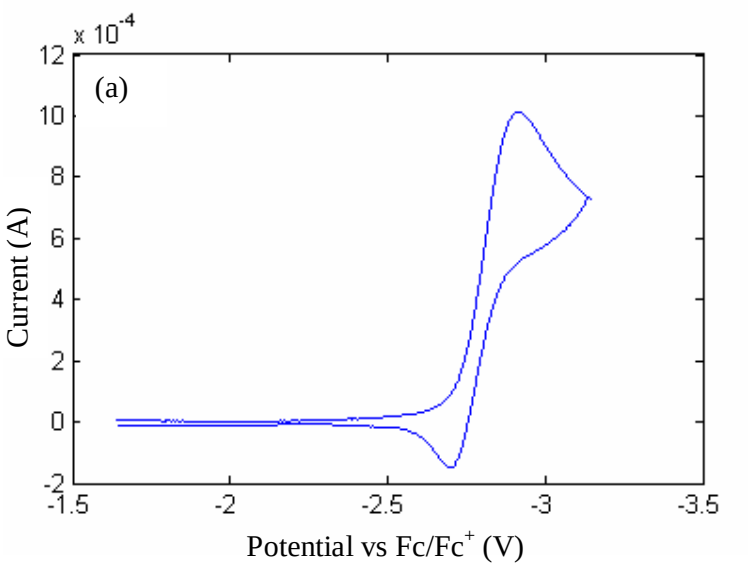
x 10^-4
(a)
Current (A)
Potential vs Fc/Fc+ (V)

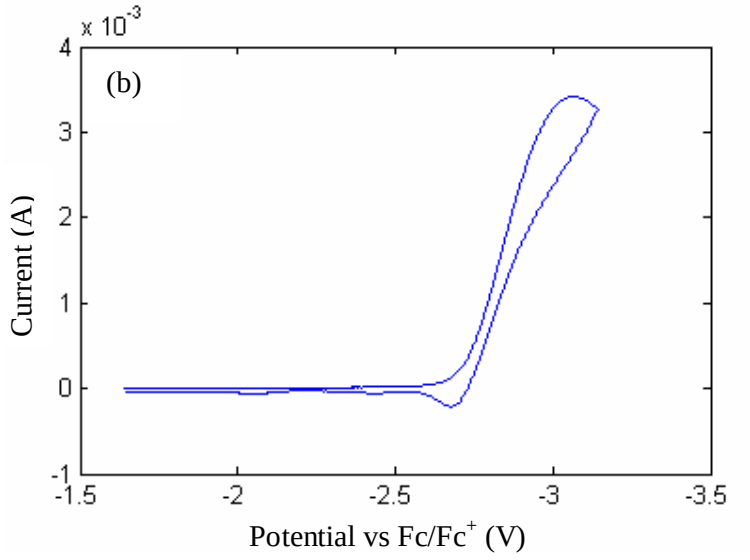
x 10^-3
(b)
Current (A)
Potential vs Fc/Fc+ (V)

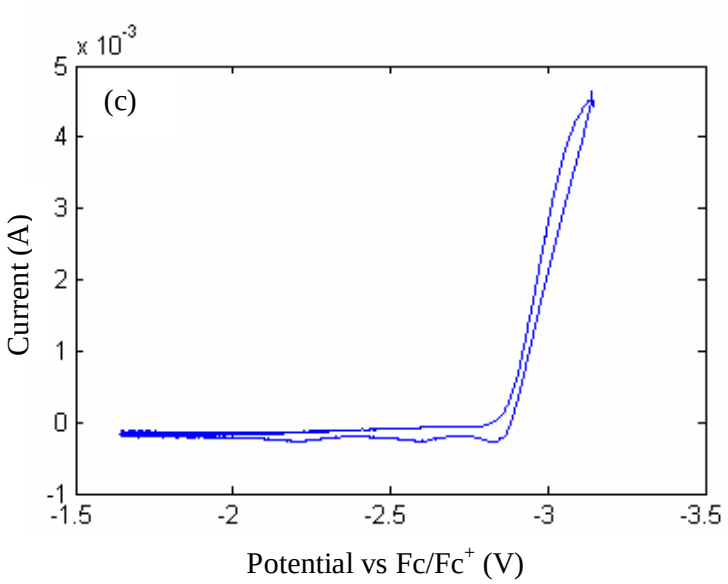

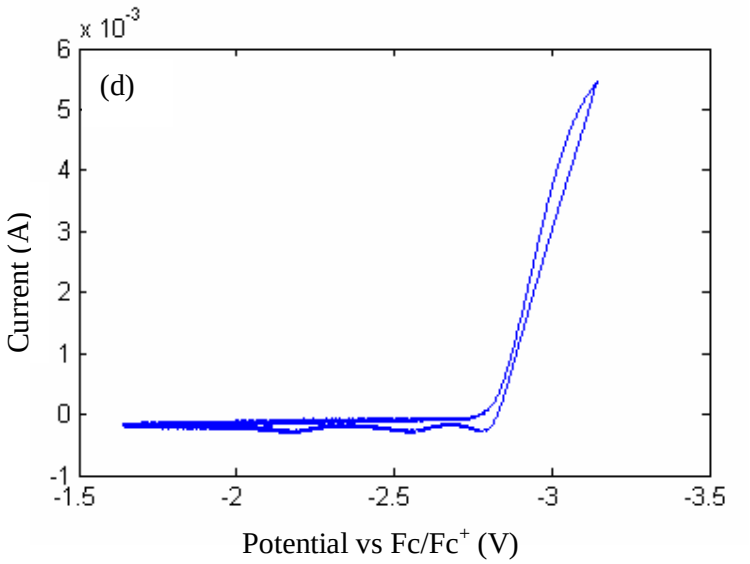

Figure 2.3 Background subtracted Cyclic Voltammograms of 4-fluorobenzonitrile in acetonitrile. Supporting electrolyte: 0.1 M TBAP (Scan rate 30 Vs^{-1}). (a) 1 mM, (b) 4 mM, (c) 7 mM and (d) 9 mM.

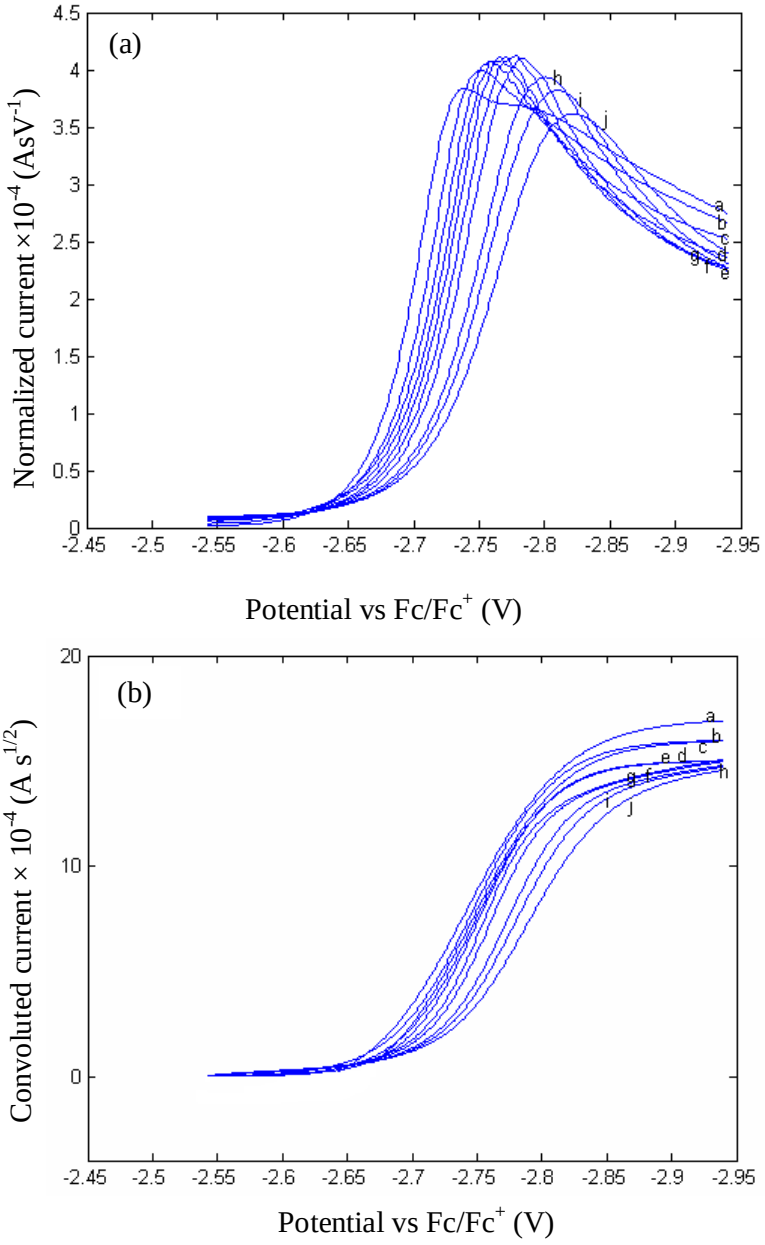

Figure 2.4 (a) The scan-rate normalized cyclic voltammogram of 4-fluorobenzonitrile. (b) The dependence of the convoluted current on potential. (a) 0.1 Vs^{-1} (b) 0.2 Vs^{-1} (c) 0.3 Vs^{-1} (d) 0.4 Vs^{-1} (e) 0.5 Vs^{-1} (f) 0.7 Vs^{-1} (g) 1 Vs^{-1} (h)2 Vs^{-1} (i) 2.994 Vs^{-1} (j) 5 Vs^{-1}.

A typical sigmoidal curve is obtained with a plateau at large negative potentials. The plateau region indicates the limiting value of the convolution current (I_l) given by eqn (1.8). The diffusion coefficient (D) is deduced from I_l as 4.64×10^{-4} cm^2 s^{-1}. The surface area of the electrode (A) is 7.065 mm^2.

2.2.4. Dependence of the transfer coefficient on potential

The availability of the convoluted current enables the accurate estimation of the heterogeneous electron transfer rate constant from equation (1.12). As seen from Figure 2. 5, the plot of $\ln(k_{ET})$ vs potential is non-linear which indicates the validity of Marcus-Hush theory of quadratic activation driving force- relationship with a potential-dependent transfer coefficient. It is noticed from Figure 2.6 that the transfer coefficient varies linearly with potential. It is customary to look for two distinct regimes concerning the magnitude of the transfer coefficient viz > 0.5 and < 0.5. These two regimes have interesting connotations in the elucidation of the reaction mechanism as has been pointed out earlier (Prasad and Sangaranarayanan, 2004). The transfer coefficient is estimated using the equation (1.16). Since it is > 0.5 at all the scan rates employed, the follow-up reaction viz the conversion of the radical ion into the corresponding halide anion controls the overall rate of the reaction.

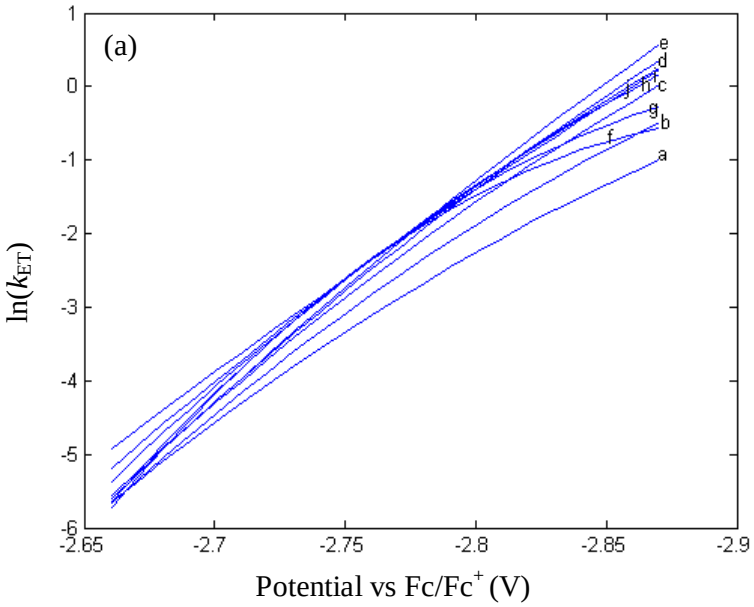

Figure 2.5 The dependence of the heterogeneous electron transfer rate constant on potential at different scan rates for (a) 0.1 Vs^{-1} (b) 0.2 Vs^{-1} (c) 0.3 Vs^{-1} (d) 0.4 Vs^{-1} (e) 0.5 Vs^{-1} (f) 0.7 Vs^{-1} (g) 1 Vs^{-1} (h) 2 Vs^{-1} (i) 2.994 Vs^{-1} (j) 5 Vs^{-1}. (k_{ET} in cm s^{-1})

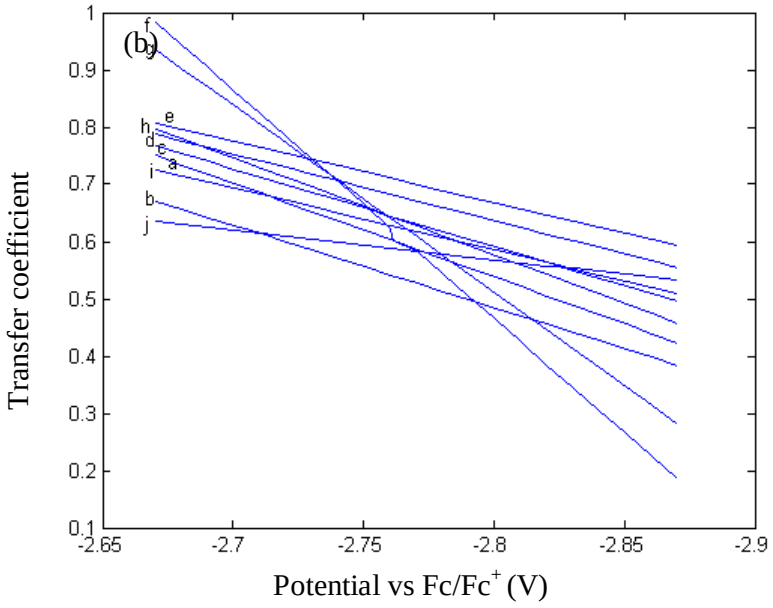

Figure 2.6 Estimated transfer coefficients for the scan rates given in Figure 2.5.

SECTION 2.3 MECHANISTIC ANALYSIS - ELECTROCHEMICAL REDUCTION OF 4-FLUOROBENZONITRILE

2.3.1. Methodology for quantum chemical calculations

Quantum chemical calculations are employed for estimating the bond length, bond energy and electron densities. The calculations were performed using Gaussian 03 software employing the Becke three parameter hybrid exchange in conjunction with the correlation functional developed by Lee, Yang and Parr (B3LYP) (Becke, 1993; Lee *et al*, 1988) The structure of 4-fluorobenzonitrile was optimized using 6-31+G(d) basis set (McLean *et al*, 1980; Raghavachari *et al*, 1980). The optimization was verified using frequency calculations and carried out until no imaginary frequencies were noticed. Similarly, the anion radicals are optimized using open shell (unrestricted) model UB3LYP/6-31+G(d) while the neutral molecule was optimized with a closed shell model (restricted). The additional polarizable and diffuse functions may not make significant contributions to estimated values. The input parameters of the solvent (acetonitrile) are: (i) atomic radii from UAO model; (ii) cavity model: GePol; (iii) dielectric constant (ε) = 36.64; (iv) dielectric constant at infinite frequency (ε_∞) = 1.806; (v) radius of acetonitrile = 2.155 Å. In order to estimate the total charge density, the Gaussian 03 version was used. For this purpose, the cubes were generated for total density and the electrostatic potential (ESP) was obtained with the help of the Gaussview 3.09. The ESP is mapped on the surface of the total electron density in order to generate the corresponding contour diagrams. The potential energy diagram is constructed using single point energy calculations of various C-F bond lengths with step size of 0.05 Å. The input file (Z-matrix) is prepared from Gauss view software version 3.09 and analogously for the output file.

The electrostatic potential map was drawn by generating the *cube* files by Gaussian Utilities. The red and blue colours indicate respectively the electron-rich and the electron-deficient regions.

2.3.2. Estimation of the solvent reorganization energy

The estimation of the solvent reorganization energy provides further insights regarding the stepwise and concerted reaction mechanism. The algebraic expression for total reorganization energy (λ) is different for stepwise and concerted processes. In the case of concerted pathways, the solvent reorganization energy is given by

$$\lambda = D_{C-F} + \lambda_s \tag{2.1}$$

and $D_{\text{C-F}}$ denotes the dissociation energy of carbon-fluorine bond. On the other hand, for stepwise mechanism, $\lambda = \lambda_s + \lambda$. The experimental reorganization energy can be estimated from the α vs E-E^0 plot wherein the slope equals 1/(2λ) derived from equation (1.26). A straight-forward comparison of λ between the experimental value and theoretical value provides an unambiguous inference of the reaction mechanism. In the case of 4-fluorobenzonitrile, λ values deduced from the slope of α vs E-E^0 plot range from 0.12eV to 0.91eV (The estimation of E^0 is discussed in the section 2.4). The C-F bond dissociation energy from the potential energy profile constructed with the help of B3LYP/6-31+g(d) basis set yields a value of 6.92 eV. The solvent reorganization energy λ_s (cf. equation 1.20) using equation $\lambda_s = 2.08/a_{RX}$ is 0.53 eV where a_{RX}, the radius of the reactant is 3.96 Å. The addition of C-F bond dissociation energy with λ_s yields a value of 7.45 eV which is completely at variance with the mean reorganization energy of ca. 0.37 eV estimated from the experimental α vs E-E^0 plot. Hence the concerted mechanism is not valid in this case; λ_i is quite small and

hence may be neglected. Thus it is appropriate to compare λ_s (0.53 eV) with the value of 0.37 eV deduced above. Since the two values are in gross agreement with each other, the reduction of 4-flouorobenzonitrile follows a stepwise mechanism.

2.3.3. Distinction between concerted and stepwise mechanism using bond-lengths and electron density mapping

As indicated in Chapter 1, the estimation of the appropriate bond-lengths can provide a method of distinguishing between stepwise and concerted mechanisms. In the stepwise mechanism, an intermediate anion radical is formed whereas for concerted reactions, direct bond-breaking occurs. Hence the variation in bond length of anionic radical will not be significant in the stepwise mechanism. However, in the case of concerted pathways, owing to the breaking of bonds, bond-length becomes much larger than its initial value (before the occurrence of electron transfer). A previous study (Cardinale *et al*, 2002) on haloacetonitriles demonstrated the validity of the concerted pathway from computed bond lengths. The bond-length for 4-fluorobenzonitrile and its anion radical was estimated as 1.35 Å and 1.38 Å respectively (Figure 2.7). Since there is no significant difference between the two values, the stepwise mechanism is inferred. This is in conformity with the results obtained from CPSV.

The electrostatic potential (ESP) map is used to predict the variation of the electron density from neutral molecule to the anion radical. The ESP for 4-fluorobenzonitrile is depicted in Figure 2.8. While a significant negative charge is found in the CN group of the neutral 4-fluorobenzonitrile, no significant negative charge is found on the fluorine atom. The extent of negative charges is significant for the anion radical,

indicating the delocalization of electrons over the benzene ring leading to more stable anion radical. Thus the electrostatic potential mapping also implies the occurrence of the stepwise mechanism.

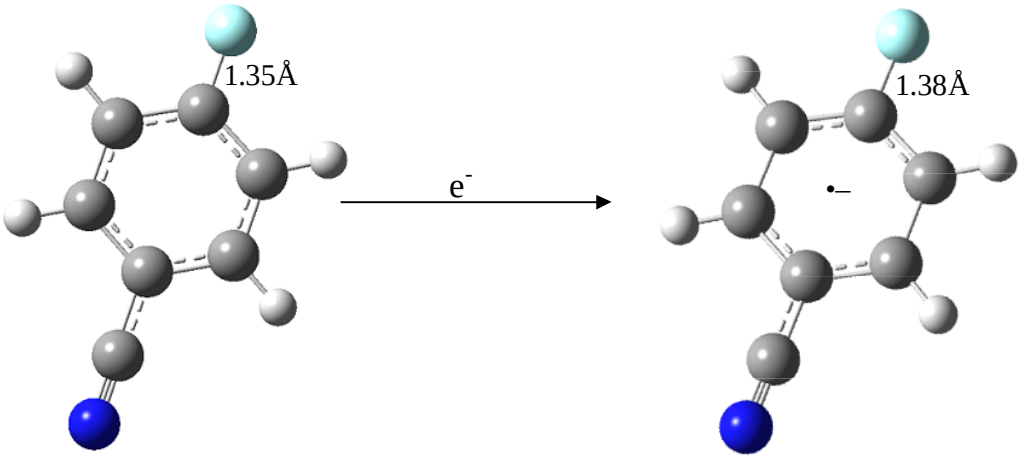

Figure 2.7 C-F bond lengths before and after electron transfer in the case of 4-fluorobenzonitrile.

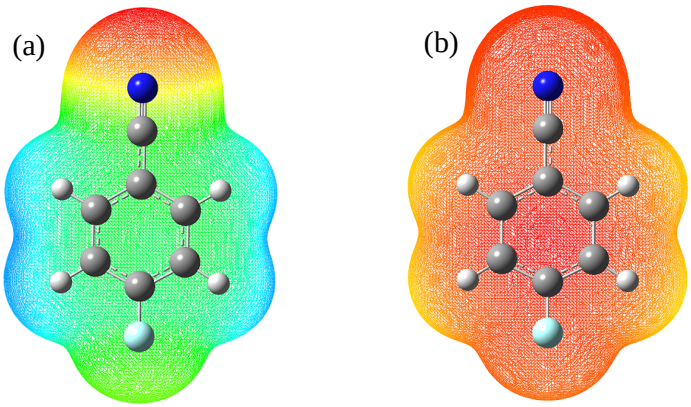

Figure 2.8 Electrostatic potential of 4-fluorobenzonitrile (a) and its anion radical (b) mapped onto the surface of the electron density of 0.004 unit. The blue portions represents the positive part of the electrostatic potential while the red portions denotes the negative part.

SECTION 2.4 ESTIMATION OF THE STANDARD REDUCTION POTENTIAL OF 4-FLUOROBENZONITRILE

2.4.1. Theoretical standard reduction potentials using thermochemical cycles

The estimation of standard reduction potentials of organic compounds is a non-trivial exercise since their electron transfer reactions are in general irreversible and a clear elucidation of their reaction mechanisms is a pre-requisite. In chapter 1, several methods have been described for obtaining the standard reduction potentials. For 4-fluorobenzonitrile, a thermochemical cycle is constructed as shown in Scheme 2.2.

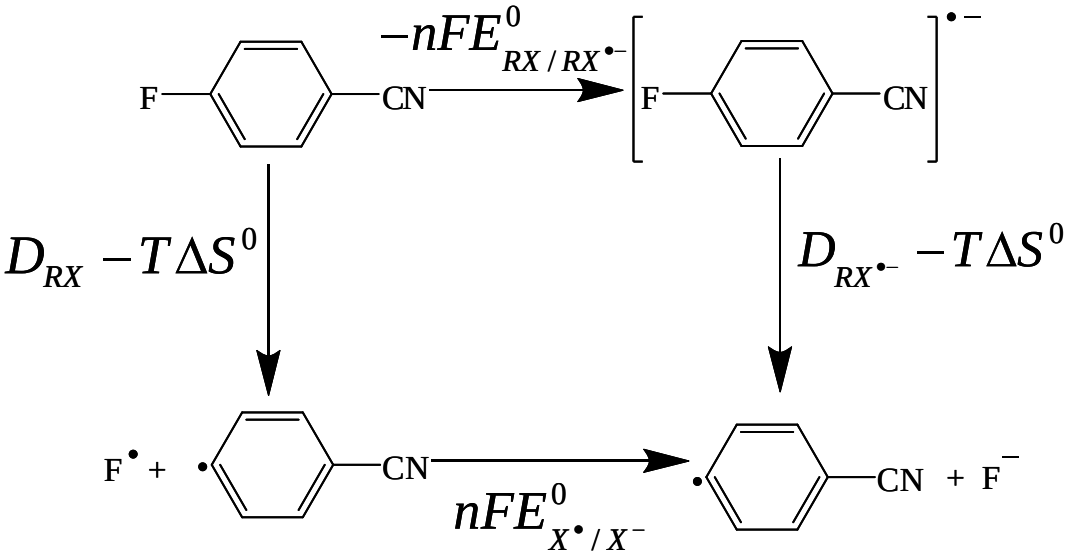

Scheme 2.2 Thermochemical cycle for estimating the standard reduction potential for 4-fluorobenzonitrile.

The bond dissociation energy of the neutral and the anionic radical in acetonitrile is obtained from the potential energy diagram for the optimized geometry deduced earlier. Further, the bond dissociation energies of the neutral molecule and the anionic

radical using B3LYP/6-31+g(d) are 6.92 eV and 1.52 eV respectively. In order to evaluate the standard reduction potential of $RX/RX^{\bullet -}$, equation (1.32) is employed. $E^0_{X^\circ / X^-}$ denotes the standard reduction potential of the fluorine radical (cf. equation 1.32). The appropriate entropy changes are estimated from the individual entropies of the reactants and products as

$$\Delta S^0_{RX \rightarrow R^\bullet + X^\bullet} = (S^0_{R^\circ} + S^0_{X^\bullet}) - S^0_{RX} \tag{2.2}$$

$$\Delta S^0_{RX^{\bullet -} \rightarrow R^\bullet + X^-} = (S^0_{R^\circ} + S^0_{X^-}) - S^0_{RX^{\bullet -}} \tag{2.3}$$

However, the standard reduction potential of $F^\bullet$ needs to be estimated in *acetonitrile*. The standard reduction potential of a system in non-aqueous solvents can be related to that in *water* using the Gibbs transfer free energies. Following the methodology advocated by Pause *et al* (Pause *et al*, 2000)

$$E^{0,AN}_{F^\bullet / F^-}(vs\ SHE) = E^{0,H_2O}_{F^\bullet / F^-}(vs\ SHE) - E^{0,H_2O}_{Ag^+ / Ag}\ (vs\ SHE) - \left(\Delta_{tr} G^0_{F^-, H_2O \rightarrow AN} + \Delta_{tr} G^0_{Ag^+, H_2O \rightarrow AN}\right) + 0.68 \tag{2.4}$$

where $\Delta_{tr} G^0_{F^-, H_2O \rightarrow AN}$ and $\Delta_{tr} G^0_{Ag^+, H_2O \rightarrow AN}$ denote respectively the Gibbs transfer free energy of F^- and Ag^+ from water to acetonitrile. The Gibbs transfer free energies of the above are reported as 16.99 kcalmol^{-1} and -7.42 kcalmol^{-1} respectively **(**Marcus, 1997). The addition of 0.68 ensures the conversion of the potentials from Ag/AgCl reference to SHE scale. The standard reduction potentials of $F^\bullet/F^-$ and Ag^+/Ag redox couples in water have been reported as 2.85 V and 0.799 V respectively (Weast, 1979). Consequently, the standard reduction potential of $F^\bullet/F^-$ in acetonitrile follows as 2.32 V with respect to SHE. (Another method of estimating the standard reduction potential of $X^\bullet/X^-$ in acetonitrile is given in Appendix-B). From these values, $E^0_{RX/RX^{\bullet -}}$ in acetonitrile follows as -2.90 V with reference to SHE. In order to compare the above estimate with that from the experimental cyclic voltammetric analysis, it is

essential to convert the former with reference to the Fc/Fc^+ couple. For this purpose, another thermo-chemical cycle is constructed as shown in Scheme 2.2.

2.4.2.Estimation of standard potential for Fc/Fc^+

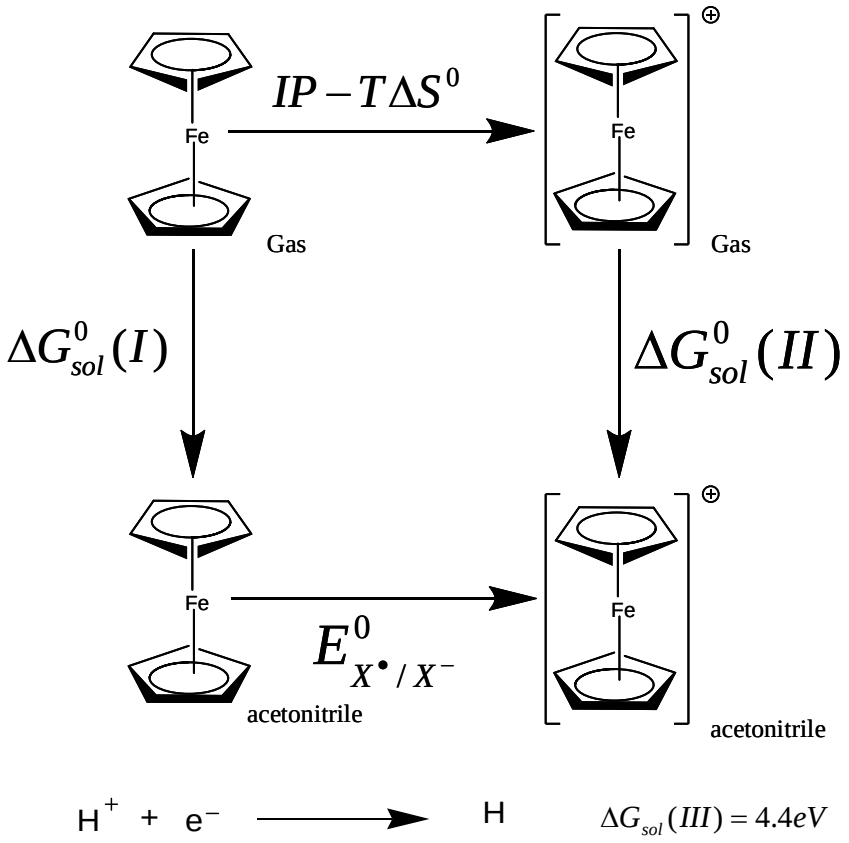

Scheme 2.3 Thermochemical cycle for estimating the potential of Fc/Fc^+ in acetonitrile vs SHE.

The ionization potential of ferrocene (*Fc*) in the gas phase was estimated from the B3LYP/6-31+g(d) method as 6.91 eV in agreement with the experimental value of 6.86 eV deduced from electron spectroscopy (Rabalais *et al*,1972). In order to obtain the correct value of ionization potential in the solution phase, a correction factor of 0.28 eV needs to be added (Fu *et al*, 2005). Consequently, the ionization potential of ferrocene in the solution phase is 7.19eV. Further, the value of TΔS for the conversion of *Fc* to Fc^+ is -1.128 kcalmol^{-1} at 298 K as indicated above. The Gibbs solvation free

energies of Fc and Fc^+ estimated using the polarizable continuum model along with the B3LYP/6-31+g(d) basis set are 2.64 kcalmol^{-1} and -52.51 kcalmol^{-1} respectively after employing the scaling factor of 1.2 suggested by Fu et al (Fu *et al*, 2005) (cf. equation 1.30).

Thus, E^0_{Fc/Fc^+} in acetonitrile follows as 0.417 V vs SHE wherefrom $E^0_{RX/RX^{\bullet -}}$ is calculated to be –2.48 V with reference to the ferrocene/ferrocenium couple. The above methodology of estimating the standard redox potential of compounds requires further refinement regarding the influence of basis sets and subtle effects of standard states involved in the solvation free energy calculations. Nevertheless, by a judicious combination of B3LYP methodology with thermochemical cycles, the computation of the standard redox potentials of any species in a given solvent is indeed feasible.

SECTION 2.5 SUMMARY

The reduction of 4-fluorobenzonitrile in acetonitrile is analysed using CPSV. The potential-dependent rate constants and the transfer coefficients were analyzed with the help of Marcus-Hush theory of outer sphere electron transfer reactions. The transfer coefficient and reorganization energy calculations confirms the step-wise reductive cleavage. The dimerization of 4-fluorobenzonitrile was found to occur at higher scan rates and is concentration-dependent with the threshold concentration being 4 mM. A novel method to calculate the standard reduction potentials for compounds undergoing stepwise reductions has been proposed.

CHAPTER 3

ANALYSIS OF C-F BOND CLEAVAGES IN METHYLFLUOROBENZOATES – FRAGMENTATION AND DIMERIZATION OF ANION RADICALS

SECTION 3.1 INTRODUCTION

The reductive cleavage of C-X bonds (where X= F, Cl, Br, I, O, S etc) constitutes a fascinating area of research in the study of electron transfer reactions in view of the crucial role played by the functional group, dielectric properties of the solvent and magnitude of the driving force (Maran *et al*, 2001; Savéant, 2000; Houman, 2008). While there are compounds which follow solely stepwise or concerted electron transfer pathways, there exist cases where the mechanism itself depends upon the driving force and a transition from one mechanism to the other is feasible (Andrieux *et al*, 1997 b; Pause *et al*, 1999; Andrieux *et al*, 1994; Andrieux *et al*, 1994; Antonello and Maran, 1999).

The C-F bond cleavage reactions in aromatic substrates is rendered difficult on account of the high activation energy barriers and hence their study has been restricted to a smaller number of aromatic compounds. The reductive de-fluorination of 1,3 difluorobenzene (Miller and Vajtner, 1985), pentafluoronitrobenzene (Andrieux *et al* 1994) on mercury electrodes and fluoromethylarenes (Andrieux *et al*, 1997) on glassy carbon electrodes deserves mention in this context. Alternately, the C-F bond

reductions can be accomplished with the help of suitable redox catalysts such as anthracene, phenanthrene, benzonitrile, chrysene etc (Andrieux *et al*, 1979). A different strategy for carrying out the reduction of C-F bonds consists in introducing electron-withdrawing groups in the aromatic ring e.g fluorobenzonitrile (Houser *et al*, 1973). Although electron-withdrawing groups such as -CN, $-NO_2$, $-COOCH_3$ etc are expected to facilitate C-F bond cleavages, a proper choice of the compounds is warranted since the *para*-substituted fluorocompounds may dimerize rather than undergoing simple reduction. Further, all methylhalobenzoates (excluding the fluoro) undergo Ullmann type of coupling on reactive nickel surfaces (Yasuhara *et al*, 1998), sacrificial anodes such as zinc, iron, aluminium etc (Fillon *et al*, 2002; Gomes *et al*, 2002). It is hence of interest to investigate the electron transfer processes in methylfluorobenzoates. In aromatic fluorocompounds, the radical anions dissociate to form the neutral radicals and corresponding anions. The neutral radicals lead to defluorinated compounds, upon abstraction of a proton (Webster, 2004). In the case of substrates undergoing dimerization, the logarithmic analysis of the convoluted current provides the dimerization rates and for acetophenone, the dimerization rate constant has been deduced as 4×10^5 mol^{-1} lit s^{-1} by Savéant and Tessier (Savéant, and Tessier, 1975 b). Since the C-CN bond breaking (in stead of C-F bond cleavage) occurs in the case of *meta* –fluorobenzonitrile (Houser *et al*, 1973), the *ortho* and *para* isomers of methylfluorobenzoates are chosen in the present study.

The convolution potential sweep voltammetry (CPSV) is a valuable technique since (i) the entire data points of the voltammogram can be made use of and (ii) no *a priori* assumption of the governing rate laws is required. While the linear free energy relation is the basis of the Butler-Volmer equation for simple electron transfer

processes, the kinetics of dissociative electron transfer reactions is customarily investigated using the quadratic activation-driving force relation via the Marcus-Hush formalism (Savéant and Tessier, 1975). In this Chapter, we investigate the mechanism of C-F bond cleavages in methyl 2-fluorobenzoate (OFMB) and methyl 4-fluorobenzoate (PFMB) using CPSV and quantum chemical calculations.

SECTION 3.2 METHODOLOGY

3.2.1. Experimental

The experimental protocol regarding the cyclic voltammetry, cell design and electrodes was as mentioned in Chapter 2. The methodology for purification of the solvent ACN was identical with that indicated in Chapter 2. The supporting electrolyte tetrabutylammonium perchlorate (TBAP) (Sigma-Aldrich, electrochemical grade) was used without further purification. The reactants methyl 2-fluorobenzoate and methyl 4-fluorobenzoate (Sigma-Aldrich) were used as received. The 4,4'-biphenyldicarboxylic acid (Sigma-Aldrich) was used as received.

3.2.2. Preparation of 4,4'-biphenyldicarboxylic dimethylester

In order to prepare the 4,4'-biphenyldicarboxylic dimethylester, 0.5 g of the corresponding acid was dissolved using excess volume of thionyl chloride and was refluxed under moisture-free conditions until the reaction mixture became homogeneous. The reaction mixture was cooled to 0ºC and 15 ml of methanol was slowly added. The whole solution was poured into ice cold water and the extraction was carried out with ethyl acetate, followed by (i) drying with anhydrous Na_2SO_4 and (ii) evaporation of the solvent. The compound (4,4'-biphenyldicarboxylic dimethylester) was re-crystallized from a mixture of ethanol and dichloromethane. The characterization of the compound (Figures 3.1 and 3.2) was carried out using NMR and FTIR studies: ^{1}H NMR (400 MHz, $CDCl_3$) δ 3.95 (6H, s), 7.69 (4H, d), 8.13 (4H, d); FTIR data: the C-O stretching frequency (di-ester at 1721 cm^{-1} and 4,4'-biphenyldicarboxylic acid at 1677 cm^{-1}).

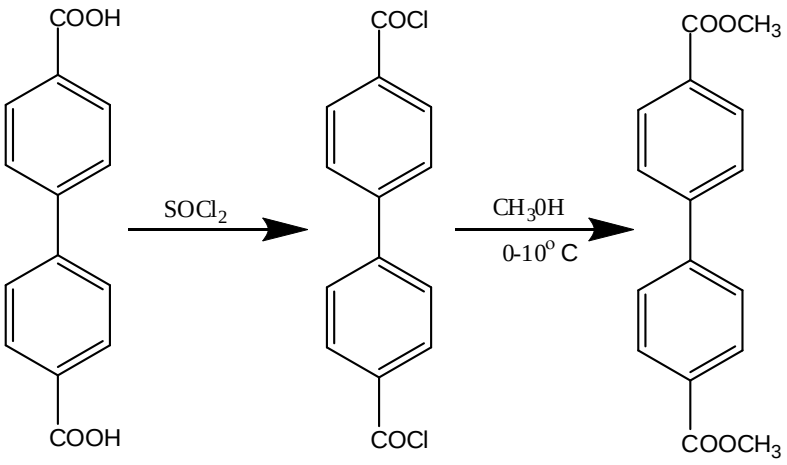

Scheme 3.1 Methodology employed for the preparation of 4,4'-biphenyldicarboxylic dimethylester.

3.2.3. Density functional Calculations

The quantum chemical calculations were carried out using Gaussian 03 [Frisch *et al*, 2004] with the help of Becke three-parameter hybrid exchange correlation of Lee, Yang and Parr (B3LYP) and the 6-311++g(d,p) basis set wherein the Polarizable Continuum Model (PCM) was employed for the solvent. The deduced molecular orbital coefficients were employed for constructing the Singly Occupied Molecular Orbitals (SOMO) pertaining to the neutral species and the radical anions.

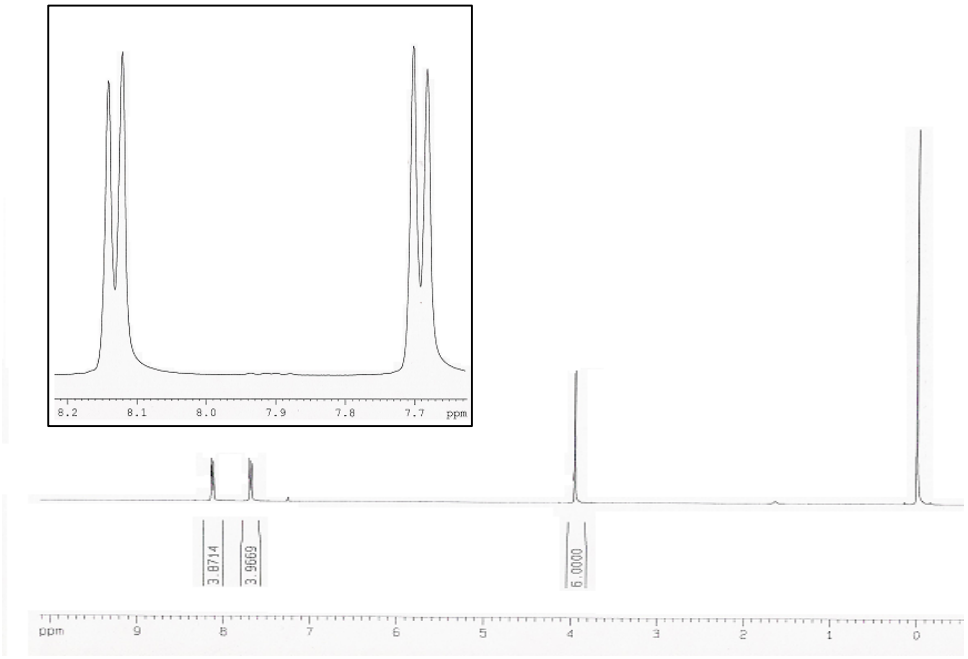

Figure 3.1 ^{1}H-NMR spectrum of the 4,4'-biphenyldicarboxylic dimethylester. The inset depicts the splitting of the aromatic protons.

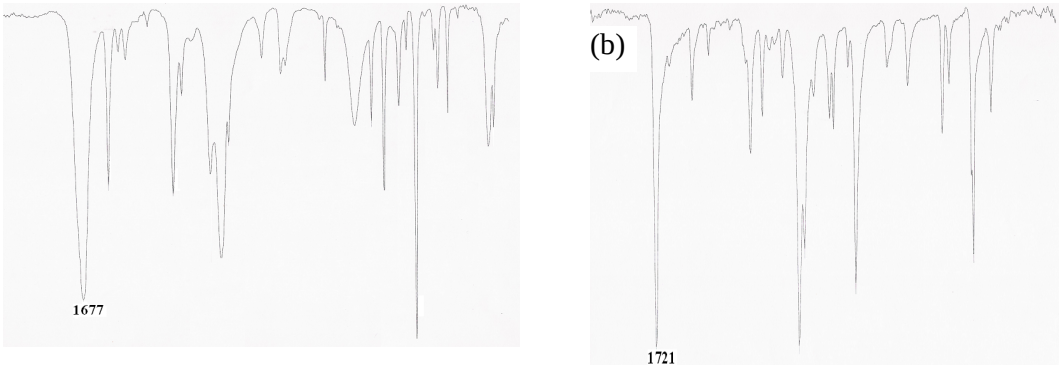

Figure 3.2 The FTIR spectrum of (a) 4,4'-biphenyldicarboxylic acid and (b) 4,4'-biphenyldicarboxylic dimethylester.

SECTION.3.3 REDUCTION OF METHYL 2-FLUOROBENZOATE

A typical cyclic voltammogram of Methyl 2-fluorobenzoate (OFMB) at the scan rate of 0.05 Vs^{-1} is shown in Figure 3.3. In the case of OFMB, a single irreversible cathodic peak at -2.183 V is noticed.

3.3.1. Peak potential and peak width measurements

In order to obtain more insights into the mechanism of electron transfer process in OFMB, the influence of the scan rate needs to be analyzed in a systematic manner. For this purpose, low scan rates (in the range 0.01 Vs^{-1} to 0.05 Vs^{-1}) as well as high scan rates (> 10 Vs^{-1}) were employed. Further, the experimental data at *high scan rates* indicate a reversible (diffusion-controlled) behaviour while a kinetically controlled behaviour was noticed at lower scan rates (Figure 3.4). The reversible peak occurring at high scan rates suggests the presence of a stable radical anion and thus the cyclic voltammogram depicted in Figure 3.3 implies the occurrence of EC mechanism ($RX + e \rightleftharpoons RX^{\bullet -} \xrightarrow{k} R^{\bullet} + X^{-}$) represented in Scheme 3.2. The peak potential shifts cathodically with increase in the scan rate and the slope of $E_{p,c}$ vs log(v) plot i.e $\partial E_{p,c}/\partial \log(v)$ is estimated as 25 mV consistent with the anticipated value of 29.6 mV for a first order chemical reaction. It is hence inferred that the electrochemical reduction occurs via the first order elimination of fluoride ion and that the decomposition of radical anion is the rate determining step (Parker *et al*, 1981; Nadjo *et al,* 1973). The transfer coefficient is deduced from peak width ($E_{p/2} - E_p$) value and equals 0.81.

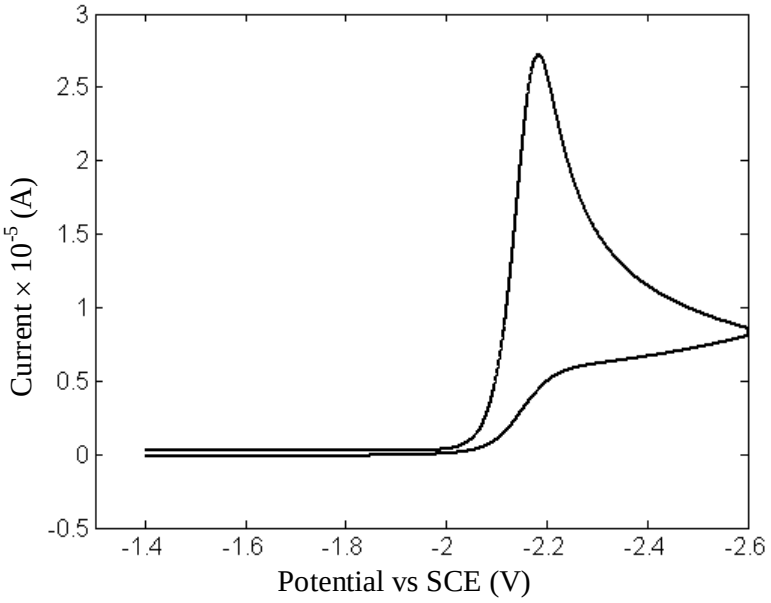

Figure 3.3 Cyclic voltammograms of methyl 2-fluorobenzoate (1 mM) at 50 mVs^{-1}. The current refers to the background-subtracted values. Supporting electrolyte is 0.1 M TBAP.

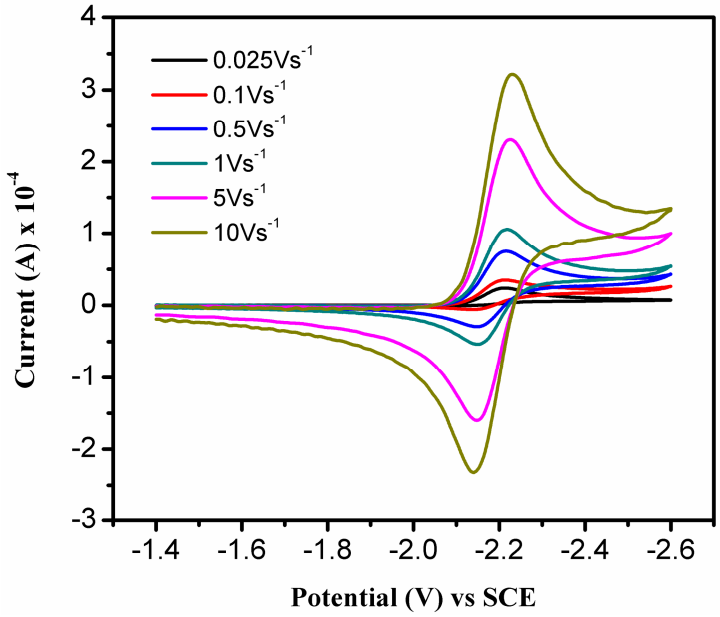

Figure 3.4 Backgound subtracted cyclic voltammogram of Methyl 2-fluorobenzoate at different scan rates.

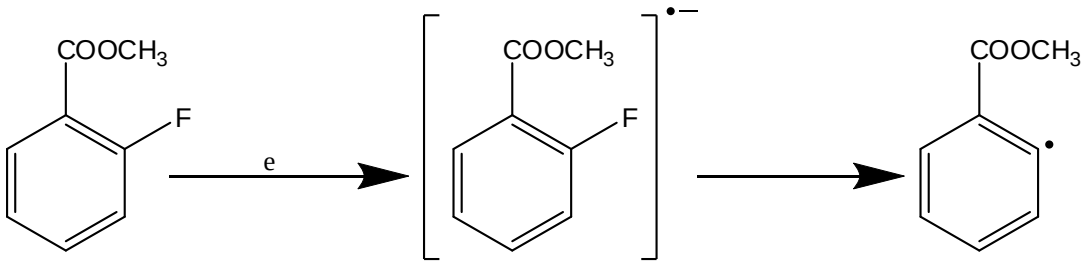

Scheme 3.2 Dissociation of OFMB via the EC mechanism.

3.3.2. Estimation of standard reduction potential and rate constants using CPSV

The classical cyclic voltammetric analysis due to Nicholson and Shain (Nicholson and Shain, 1964) is valuable since tabular compilations and working curves have been provided as diagnostic criteria for different types of electron transfer processes. However, when a wide range of scan rates is employed, the CPSV is preferable. The convolution current (I) is related to the voltammetric current (i) through the convolution integral (Savéant and Tessier, 1975) as given by equations (1.6) and equation (1.7). The convoluted current employing Lawson-Maloy algorithm (Lawson-Maloy, 1974) is depicted in Figure 3.5.

A typical sigmoidal curve is noticed with a plateau at large negative potentials. This represents the limiting convolution current represented by equation (1.8) The diffusion coefficient (D) estimated from limiting convoluted current is 0.83×10^{-5} cm^2s^{-1} while the number of electrons (n) involved in this reduction is two (n =2). In order to estimate E^0, the regime where the diffusion control occurs (high scan rates) is made use of equation (1.13) (Imbeaux and Savéant, 1973).

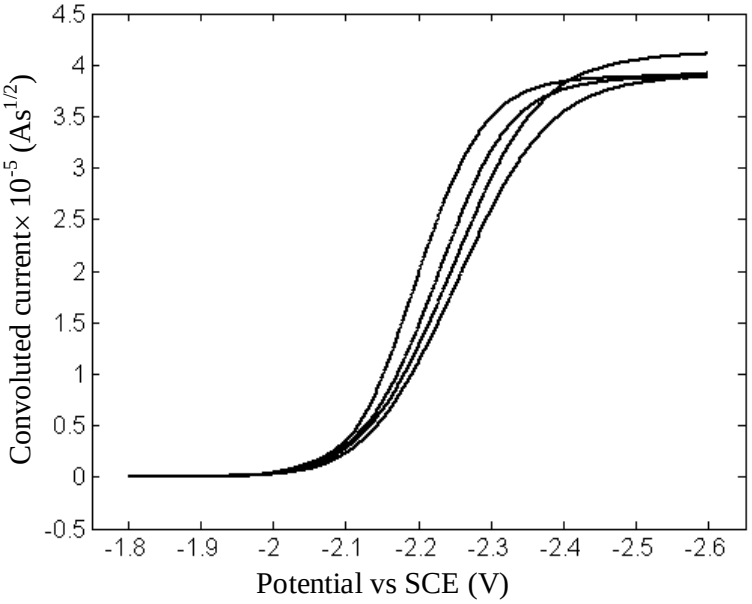

Figure 3.5 The convoluted current for the reduction of methyl 2-fluorobenzoate at high scan rates. The scan rates are 20 Vs^{-1}, 30 Vs^{-1}, 40 Vs^{-1} and 50 Vs^{-1}.

Thus, the intercept of the plot of $\ln\left[\frac{I_l - I}{I}\right]$ vs E at high scan rates region (Figure 3.6) provides E^0 as -2.190 V. This value is in agreement with E^0 estimated as -2.157 V from the arithmetic mean of anodic and cathodic peak potentials viz. $E^0=(E_{p,a}+E_{p,c})/2$, at high scan rates. The slope deduced from the plot of Figure 3.6 is 28 mV for scan rates ranging from 10 Vs^{-1} to 50 Vs^{-1} and is consistent with the theoretical value of 25.6 mV for the systems under diffusion control. The availability of the standard reduction potential (E^0) can then be exploited to deduce the value of the uni-molecular rate constant (k) as shown in equation (1.14). At scan rates in the range of 0.01 Vs^{-1} to 0.05 Vs^{-1}, the slope of $\ln((I_l-I)/i)$ vs E plot is 29 mV (Figure 3.7), in gross agreement with the theoretical value of 25.6 mV for systems solely under kinetic control.

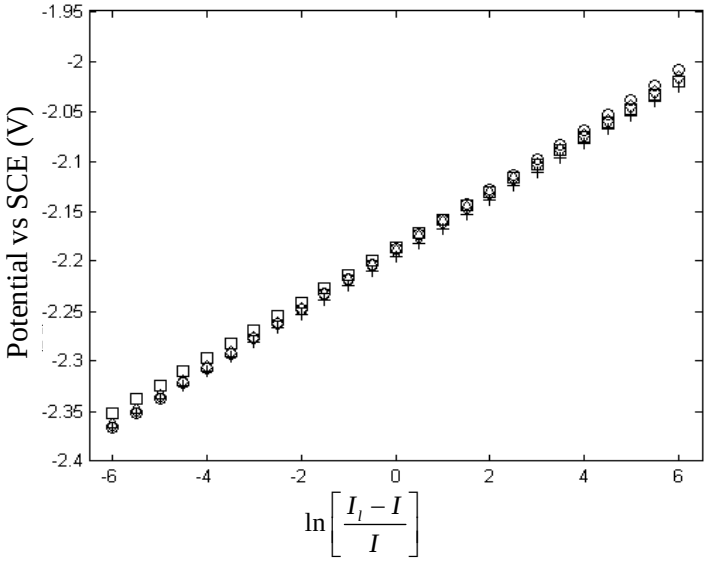

Figure 3.6 Estimation of the standard electrode potentials from the convoluted current at high scan rates for methyl 2-fluorobenzoate. The scan rates are as follows: 10 Vs^{-1} (+), 20 Vs^{-1} (o), 40 Vs^{-1} (□) and 50 Vs^{-1} (◊)

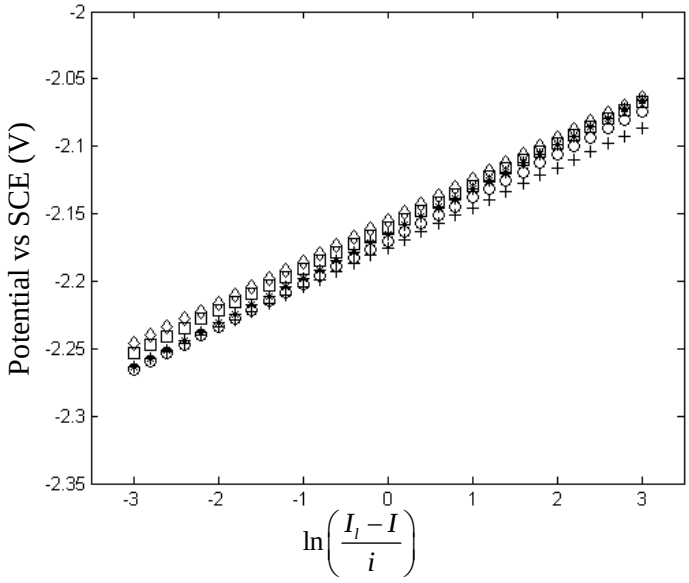

Figure 3.7 The dependence of the convoluted current on potential deduced from the data at low scan rates for methyl 2-fluorobenzoate. The scan rates are 10 mVs^{-1} (+), 20 mVs^{-1} (o), 30 mVs^{-1} (∗), 40 mVs^{-1}(□) and 50 mVs^{-1} (◊)

The rate constant k follows as 10.87 s^{-1} for the above range of scan rates; the dimensionless kinetic parameter λ is given by

$$\lambda = \frac{RT}{F}\frac{k}{v} \tag{3.1}$$

v being the scan rate employed. Thus, the value of log(λ) ranges from 0.77 to 0.92 for OFMB and for systems solely under kinetic control, log (λ) should be greater than 0.28 (Nadjo and Savéant, 1973),. We may recall that the reductive cleavage of 1-chloro-2,4-dinitrobenzene (Prasad and Sangaranarayanan, 2005 a) follows EC mechanism and the reversible behaviour was noticed at high scan rates in the cyclic voltammetric analysis. Further, the rate constants ranging from 1.6×10^{8} s^{-1} to 4.0×10^{-3} s^{-1} have been reported for reductive cleavage of various organic compounds such as halobenzophenone, halobenzonitrile, halonitrobenzene etc (Grimshaw, 2000).

3.3.3. Estimation of the rate constants from the classical Nicholson and Shain method

It is of interest to enquire whether the above rate constants pertaining to the EC mechanism of OFM0B can also be deduced from the classical analysis of Nicholson and Shain (Case VI). This analysis (Nicholson and Shain, 1964; Nicholson, 1966) provides a tabular compilation of the dimensionless current function χ(at) (where $a=nFv/RT$) as well as a working curve for the ratio between the anodic and cathodic peak currents ($i_{p,a}/i_{p,c}$) as a function of ($k\tau$), where k denotes the rate constant, τ being the time elapsed from the peak potential to the switching potential. The rate constant (k) estimated by fitting the calculated $i_{p,a}/i_{p,c}$ values with theoretical curve given in Figure 1.2 of Nicholson and Shain analysis (the methodology is given in the Section 1.2.2) as 13.18 s^{-1}, in gross agreement with the value of 10.87 s^{-1} deduced from CPSV. Furthermore, when the ratio k/a is large (i.e low scan rates), it is possible to

estimate the rate constants from the shift of the peak potential using equation (1.5) of chapter 1.

Employing the experimental peak potentials at the scan rates ranging from 0.01 Vs^{-1} to 0.05 Vs^{-1} in the above equation leads to the mean rate constant as 11.65 s^{-1}. Thus, the rate constants deduced from the ratio of the peak currents, shift of the peak potentials and CPSV analysis are consistent with each other.

SECTION.3.4 REDUCTION OF METHYL 4-FLUOROBENZOATE

The cyclic voltammogram for the reduction of methyl 4-fluorobenzoate (PFMB) is depicted in Figure 3.8. For PFMB, an irreversible cathodic peak at -2.298 V appears along with two additional anodic peaks.

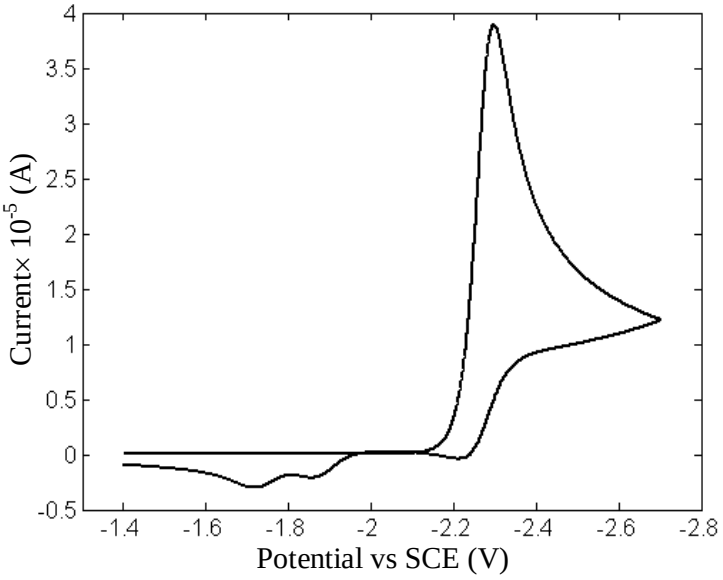

Figure 3.8 Background subtracted cyclic voltammogram of methyl 4-fluorobenzoate (1 mM) in acetonitrile at 0.5 Vs^{-1}. The supporting electrolyte is 0.1 M TBAP.

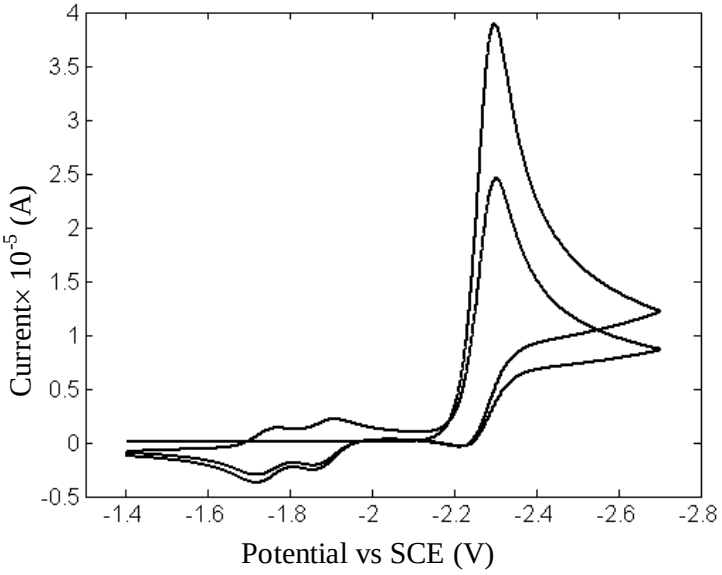

Figure 3.9 Background subtracted multi cyclic voltammograms of methyl 4-fluorobenzoate at 0.1 Vs^{-1} depicting the reversibility of anodic peaks.

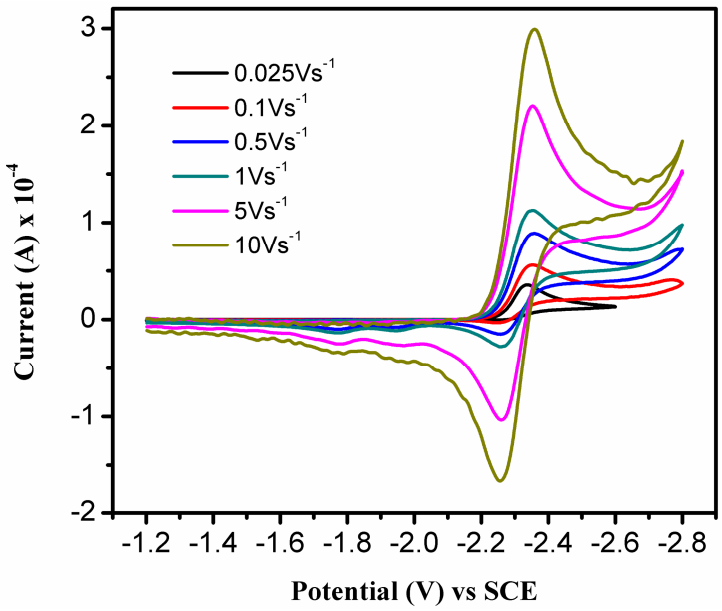

Figure 3.10 Background subtracted cyclic voltammogram of Methyl 4-fluorobenzoate at different scan rates.

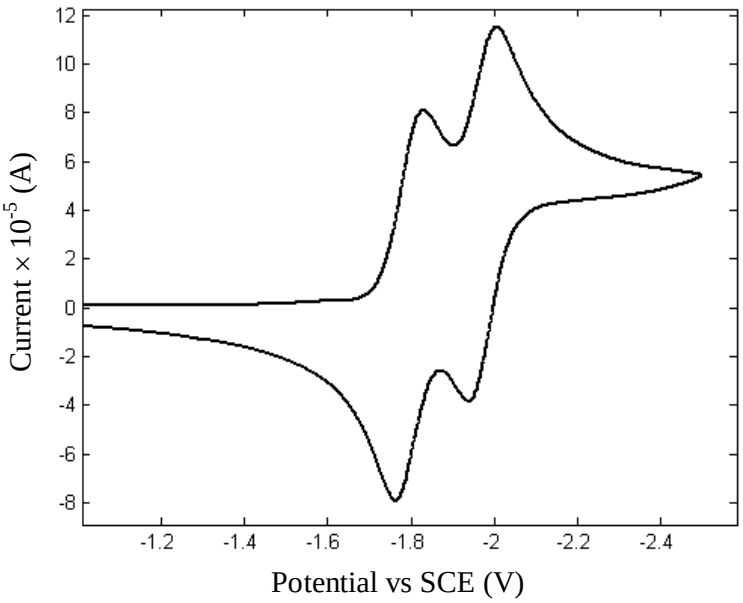

Figure 3.11 Background subtracted cyclic voltammograms of 4,4'-biphenyldicarboxylicdimethylester at 0.1 Vs^{-1}. The supporting electrolyte is 0.1 M TBAP.

3.4.1. Mechanism of electrodimerization of methyl 4-fluorobenzoate

In the case of PFMB, two additional anodic reversible peaks which appear in the cyclic voltammogram (Figures 3.8 and 3.9) may be attributed to the formation of dimers subsequent to the C-F bond cleavage. At higher scan rates, the peak becomes reversible (Figure 3.10). In order to confirm the origin of the anodic peaks, the cyclic voltammogram of the authentic sample of 4,4'-biphenyldicarboxylic dimethylester (prepared as mentioned in the experimental section) was also obtained (Figure 3.11). The occurrence of the two anodic peaks in the cyclic voltammogram of the authentic sample validates the dimerization hypothesis. The dimerization mechanism may occur via two plausible methods as given below.

(A) Coupling of radical anions with subsequent elimination of fluoride ions viz.

$$RX + e \rightarrow RX^{\bullet -}$$
$$2RX^{\bullet -} \rightarrow [RX]_2^{2-}$$
$$[RX]_2^{2-} \rightarrow RR + 2X^-$$

(B) Coupling of neutral radicals preceded by elimination of fluoride ions

$$RX + e \rightarrow RX^{\bullet -}$$
$$RX^{\bullet -} \rightarrow R^{\bullet} + X^-$$
$$2R^{\bullet} \rightarrow RR$$

Scheme 3.3 The two plausible mechanisms for dimerization of PMFB

In order to distinguish between the paths A and B, there exist two diagnostic criteria viz (i) the variation of the peak current ratio with the concentration of the reactant and (ii) the dependence of the peak potential on scan rates. If the ratio ($i_{p,a}/i_{p,c}$) is independent of the concentration, it is inferred that the dimerization occurs via the coupling of the neutral radicals. On the other hand, the decrease of the peak current

ratio with increase in the concentration is suggestive of the mechanism as the coupling of radical anions.

Table 3.1 provides the dependence of the peak current ratio on the reactant concentration wherein the decrease of $i_{p,a}/i_{p,c}$ is noticed, thus suggesting the coupling of radical anions as the most likely method of dimer formation. This inference is consistent with the mechanism of dimerization occurring via the coupling of (i) 4-fluorobenzonitrile radical anions on platinum as postulated by Houser et al (Houser *et al*, 1973) and (ii) pentafluoronitrobenzene radical anions on glassy carbon by Andrieux et al (Andrieux *et al*, 1994).

Table 3.1 The ratio between the anodic and cathodic peak currents as a function of the concentration of PMFB at the scan rate of 0.1 Vs^{-1} and switching potential of -2.6 V.

C_b (Mm)	$i_{p,a}/i_{p,c}$
0.99	0.398
1.96	0.347
2.91	0.313
3.85	0.304
4.76	0.291
5.66	0.287
6.54	0.289
7.41	0.287
8.26	0.287

The origin of the concentration dependence is attributed to the second order kinetics arising in the second step of the Scheme 3.3 (A) given as

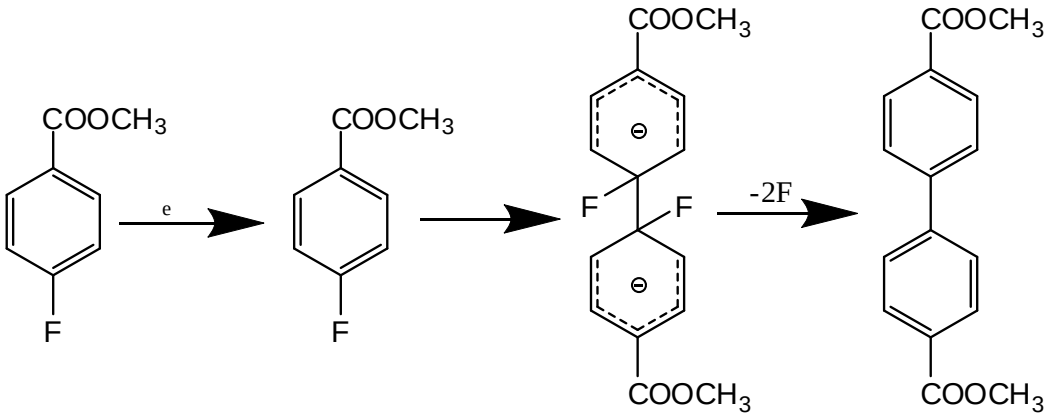

Scheme 3.4 Dimerization of PFMB via the second order radical anion coupling

3.4.2. Peak potential and peak width measurements

The variation of the peak potential with scan rates also provides a diagnostic criterion for distinguishing between the two pathways of dimerization. In this case, the variation E_p with log(v) has been postulated (equation 1.3) wherein b denotes the order of the reaction. If the pathway as suggested by (A) occurs, b=2 and hence $\partial E_p/\partial \log(v)$ should be 19.7 mV. The experimental value for PFMB is 18 mV, thus supporting the mechanism A wherein the rate determining step is the second order dimerization of radical anions. The transfer coefficient follows as 0.74 from peak width measurements.

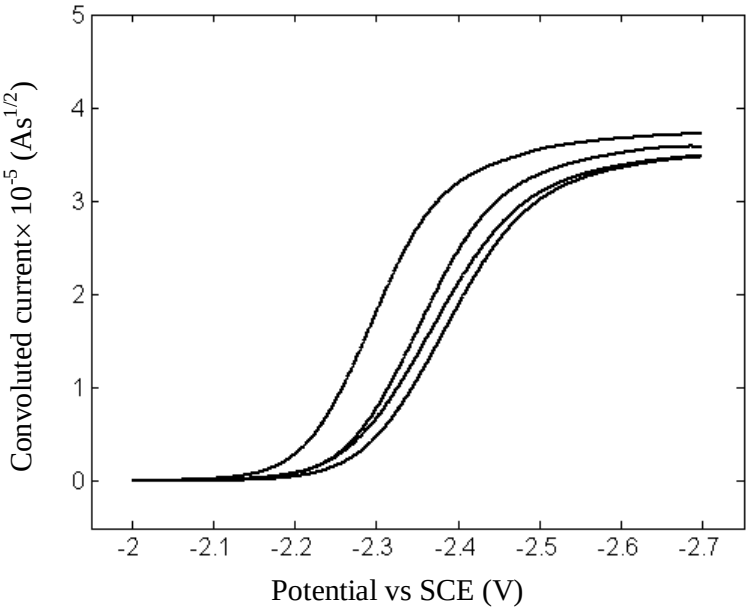

Figure 3.12 The convoluted current for the reduction of methyl 4-fluorobenzoate at high scan rates. The scan rates are 20 Vs^{-1}, 30 Vs^{-1}, 40 Vs^{-1} and 50 Vs^{-1}.

3.4.3. Standard Reduction potentials and dimerization rate constants

The potential-dependent convoluted current is depicted in Figure 3.12. As in the earlier case, the standard reduction potential (E^0) follows from the high scan rate data as -2.277 V (Figure 3.13) and is in agreement with that obtained from the cathodic and anodic peak potentials (-2.279 V). Further, the standard reduction potentials of OFMB and PFMB are comparable to that of ethyl 3-fluorobenzoate (Gennaro *et al*, 1996). The dimerization rate constant (k_d) is estimated form the convoluted current while the voltammetric current is given by equation (1.15). The dimensionless kinetic parameter is defined as $\lambda_d = \frac{RT}{F}\frac{k_d C_b}{v}$. The diffusion coefficient (D) for PFMB is estimated as 2.50×10^{-5} cm^2s^{-1} using equation (1.8), Using the above-mentioned value of E^0 and the intercept from the plot of $\ln\left[\frac{I_l - I}{i^{2/3}}\right]$ vs E of Figure 3.14, a typical

dimerization rate constant (k_d) is deduced as 1.38×10^6 $mol^{-1}lit$ s^{-1} and the corresponding dimensionless parameter (λ_d) as 2.95. The estimated parameters from cyclic voltammogram are given in Table 3.2

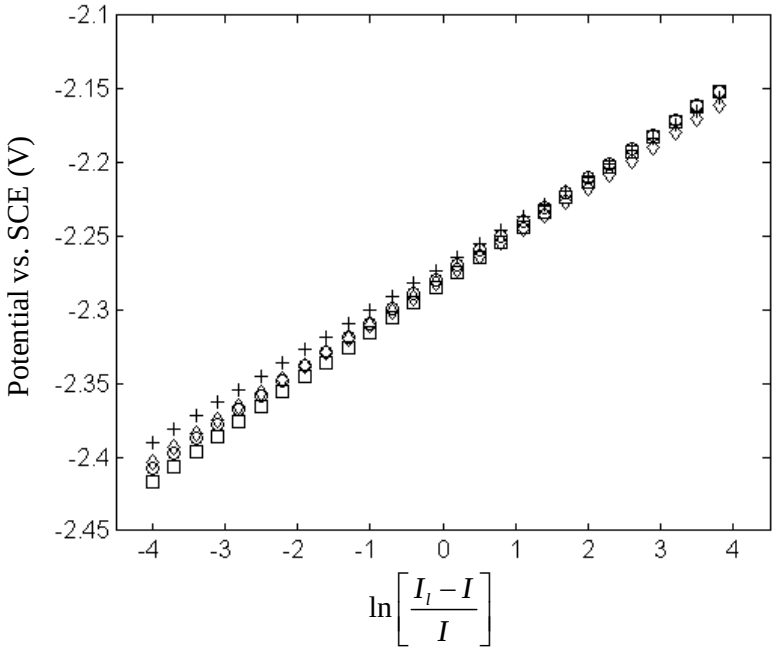

Figure 3.13 Estimation of the standard electrode potentials from the convoluted current at high scan rates for methyl 4-fluorobenzoate. The scan rates are as follows: 10 Vs^{-1} (+), 20 Vs^{-1} (o), 40 Vs^{-1} (□) and 50 Vs^{-1} (◊)

Table 3.2 Parameters derived from the cyclic voltammetric data

Parameters	Methyl 2-fluorobenzoate	Methyl 4-fluorobenzoate
E^0 vs. SCE (V)	-2.190	-2.277
α	0.81	0.74
D (cm^2s^{-1})	0.83×10^{-5}	2.50×10^{-5}
rate constants	10.87 s^{-1}	1.38×10^6 mol^{-1} lit s^{-1}

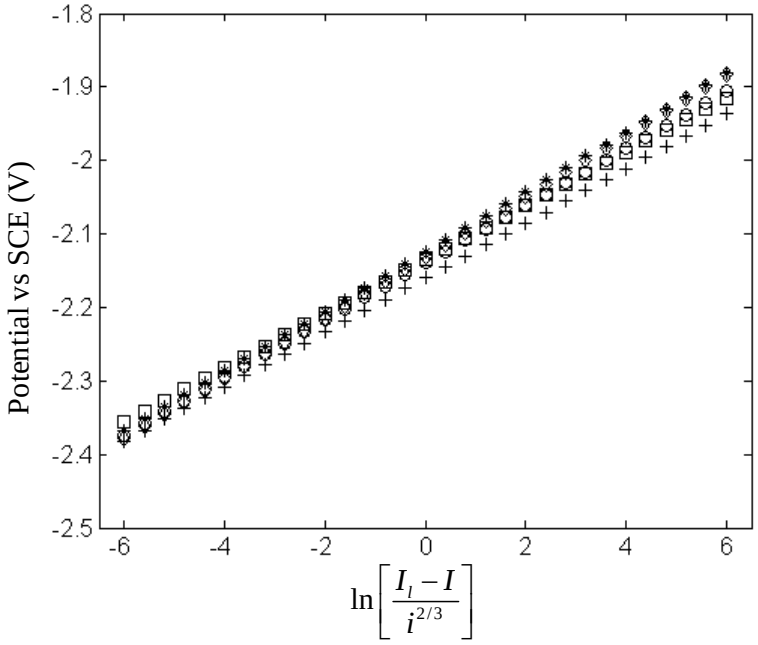

Figure 3.14 The dependence of the convoluted current on potential deduced from the data at low scan rates for methyl 4-fluorobenzoate. The scan rates are 10 mVs^{-1} (+), 20 mVs^{-1} (o), 30 mVs^{-1} (∗), 40 mVs^{-1}(□) and 50 mVs^{-1} (◊)

SECTION 3.5 MECHANISTIC ANALYSIS USING QUANTUM CHEMICAL CALCULATIONS

3.5.1 Bond length estimates

In dissociative electron transfer reactions, two different types of mechanism are customarily encountered viz. stepwise and concerted. The stepwise pathway refers to the formation of a stable radical anion subsequent to electron transfer. In order to validate the step wise mechanism, bond lengths and partial atomic charges were calculated using Gaussian 03 version with the help of B3LYP and 6-311++g(d,p) as the basis set. The Polarizable Continuum Model (PCM) was employed for the solvent. In the case of stepwise mechanism, the cleaving bond length of the radical anion will not be significantly different from that of the reactant. From the quantum chemical calculations using Gaussian 03, it is found that the bond lengths of (a) OFMB (neutral: 1.35 Å and radical anion: 1.38 Å) and (b) PFMB (neutral: 1.34 Å and radical anion: 1.39 Å) are nearly the same. The Mulliken charge analysis yields the partial charge of fluorine in the radical anionic forms as -0.25 (OFMB) and -0.28 (PFMB). Hence the bond is not broken after the electron transfer.

3.5.2. Potential energy diagram and molecular orbital analysis

Figure 3.15 depicts the SOMO of OFMB and PFMB radical anions. It is seen that the SOMO are present above the ester group and benzene ring. This implies that the electron is first transferred to the π^* orbital of the reactants and subsequently to σ^* orbital of the C-F bond.

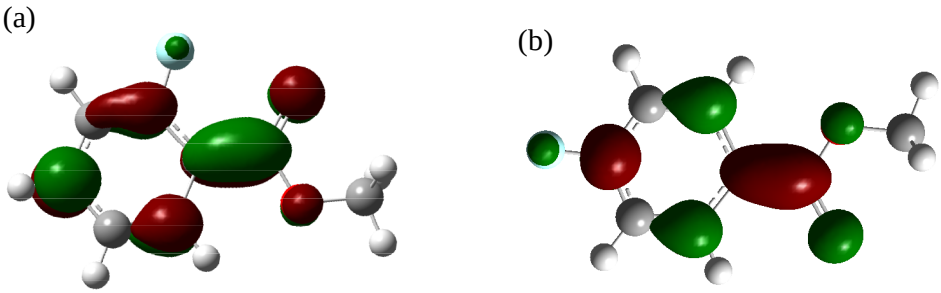

Figure 3.15 The representation of SOMO for (a) OFMB and (b) PFMB. The molecular orbital coefficients are obtained using the isosurface value of 0.05units

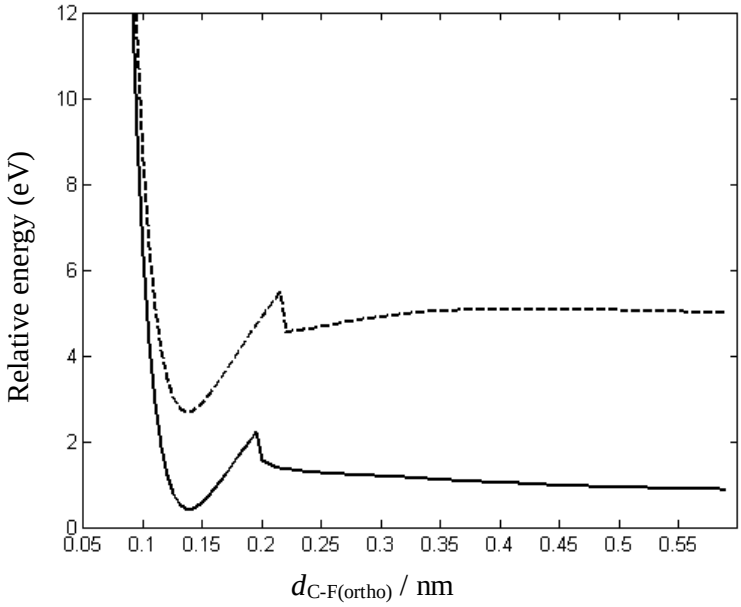

Figure 3.16 (a) Potential Energy diagram pertaining to radical anions of methyl 2-fluorobenzoate. The dashed lines denote the surfaces in vacuum while the solid line refers to the energy surfaces in the solvent (acetonitrile).

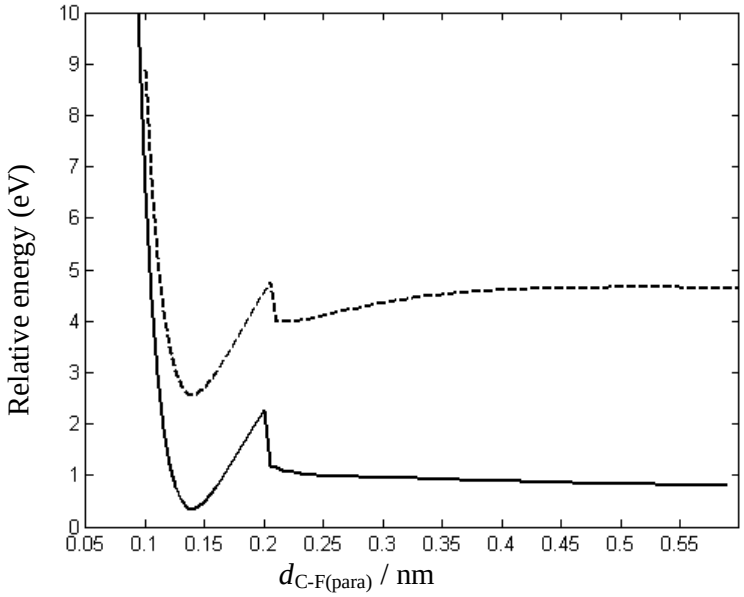

Figure 3.17 (a) Potential Energy diagram pertaining to radical anions of methyl 4-fluorobenzoate. The dashed lines denote the surfaces in vacuum while the solid line refers to the energy surfaces in the solvent (acetonitrile).

The computed potential energy surfaces in vacuum for the anionic radicals exhibit two minima (Costentin *et al*, 2004) indicating respectively the presence of (i) π-anion radical and (ii) σ-anion radical as shown in Figures 3.16 and 3.17. The first and deeper minimum denotes the strong stabilization of π-anion radical. The second minimum arises as a consequence of the ion-radical interactions. It is anticipated that electron-withdrawing groups will enhance the ion-radical interaction (Cardinale *et al*, 2002; Wentworth *et al*, 1969; Christensen *et al*, 1997; Daasbjerg *et al*, 1999) on account of the attraction of the partial positive charge (on carbon), towards the negatively charged F^-. From the investigation on the reduction of haloacetonitriles, Cardinale and coworkers (Cardinale *et al*, 2002) demonstrated that the ion-radical interaction energy decreases from Cl^- to I^-. In general, the compounds having F^- as the

functional group should have higher ion-radical interactions. In the present study, both the isomers possess the electron-withdrawing carbonyl group. In vacuum phase calculation, both the compounds exhibit two minima and the ion-radical interaction energy typically varies from 0.6 eV to 0.8 eV.

In the presence of the solvent (acetonitrile), the minimum pertaining to σ-anion complex has vanished, thus indicating that the ion-radical interaction energy is absent in the polar medium. However, both the fragments (neutral radicals and fluoride ions) and the π – anion complex become stable in the polar medium as can be seen from the corresponding minimum in the potential energy calculations. The spike appearing in the potential energy may be due to the high electronegativity of fluorine atoms.

SECTION 3.6 SUMMARY

The electron withdrawing groups play an important role in the reductive cleavage of carbon-fluorine bonds. At low scan rates, the C-F bond gets reduced yielding only one irreversible peak while an increase in the scan rates shifts the cathodic peak potential to more negative values. When the reduction potential reaches the value pertaining to that of -CN bonds at higher scan rates (~ $30Vs^{-1}$), the –CN gets reduced first while the C-F cleavage occurs leading to the subsequent dimerization. Consequently, 4-fluorobenzonitrile dimerizes only at very high scan rates in contrast to the dimerization of PFMB even at low scan rates. The reduction potential of $–COOCH_3$ in PFMB is nearly identical to that of C-F bonds. Thus, the reduction of the ester group occurs first, followed by the C-F bond cleavage due to the intra-molecular electron transfer at low scan rates although the reversible behaviour is noticed at higher scan rates.

The mechanism of C-F bond cleavage in methylfluorobenzoates is studied using the convolution potential sweep voltammetry and estimates of bond lengths. The *ortho*-isomer follows EC mechanism and the first order rate constant is estimated from the analysis of Nicholson and Shain as well as Convolution potential sweep voltammetry method. The *para*- isomer undergoes dimerization through the coupling of radical anions. The standard reduction potentials of the two compounds are also deduced. The influence of electron withdrawing groups in the mechanism of C-F bond cleavages is pointed out.

CHAPTER 4

MECHANISTIC ANALYSIS OF THE REDUCTIVE CLEAVAGE OF CARBON-HALOGEN BONDS IN HALOPENTAFLUOROBENZENES

SECTION 4.1 INTRODUCTION

The mechanism of dissociative electron transfer reactions is a fascinating investigation on account of subtle issues arising from the interplay of thermodynamic and kinetic factors, mediated by the solvent characteristics. While it is anticipated that the cleavage of carbon-halogen bonds would occur via the intermediate radical anion in simple aromatic halides, the influence of electron-withdrawing groups in the aromatic ring on the mechanistic analysis is not obvious. It is therefore of interest to study systematically, the reduction behaviour of compounds wherein the five hydrogens are replaced by the fluorines in the benzene ring while the other hydrogen is replaced by any halogen other than fluorine, thereby yielding halopentafluorobenzenes. Further, it is essential to employ different diagnostic criteria in order to obtain reliable insights.

The cleavage of aromatic halides in presence of electron withdrawing groups viz halonitrobenzenes (Pilard *et al*, 1998), halobenzophenones, haloacetophenones (Scialdone *et al*, 2005), haloacetonitriles (Cardinale *et al*, 2002) and

fluoromethylarenes (Andrieux *et al*, 1997 a) has been investigated. The nature of the functional group indeed dictates the mechanism of the reduction as in the case of arymethylhalides (Andrieux *et al*, 1992). Aryl halides in general exhibit stepwise mechanism (iodobenzene (Pause *et al*, 1999) being a notable exception). In C_6F_5X, (X=Cl,Br,I) the benzene ring becomes more electropositive leading to the formation of stable intermediate radical anion which would imply a stepwise reduction of C-X bond. Further, in the case of halopentafluorobenzenes, the C-F bond is anticipated to undergo reduction at more negative potentials and hence is unlikely to interfere with the reduction of C-X bonds. It is customary to analyse such C-X bond cleavages assuming either stepwise or concerted mechanism.

SECTION 4.2 EXPERIMENTAL AND COMPUTATIONAL METHODS

4.2.1 Experimental

The experimental set-up and the purification of the solvent and supporting electrolyte has been indicated in Chapter 2. The Electrochemical work station was CH 660 A as mentioned in Chapter 2. The electrodes have been pre-treated described in Chapter 2. The reactants chloropentafluorobenzene, bromopentafluorobenzene and iodopentafluorobenzene (Sigma Aldrich) and Ferrocene (Puriss, Spectrochem, India) were used as received.

4.2.2. Quantum Chemical Calculations

The methodology of quantum chemical calculations is similar to that described in chapter 2 while the basis set employed here is 6-311++G(d,p) for both chloro and bromo pentafluorobenzenes. However, the structure of iodo pentafluorobenzene is optimized using triple split Compact effective potential (CEP-121G) basis set (Stevens *et al*, 1984; Stevens *et al*, 1992; Cundari *et al*, 1993). The Polarized Continuum Model (PCM) was employed for the solvent and the parameters have been provided in Section 2.3.1.

SECTION 4.3 MECHANISTIC ANALYSIS OF REDUCTIVE CLEAVAGE OF C-X BONDS IN HALOPENTAFLUOROBENZENES

4.3.1. Cyclic voltammetry

Figures 4.1 to 4.3 depict the cyclic voltammogram of the compounds under study wherein an irreversible peak is noticed for each compound. The peak remains irreversible even when the scan rate (v) is increased to 1 Vs^{-1} (Figures 4.4 to 4.6). The location of the peak potential pertaining to the reduction of C_6F_5X (X=Cl,Br,I) is dictated by the nature of the halide. The peak at ca -2.6 V (vs Fc/Fc^+) corresponds to the dissociation of C-F bonds. Table 1 provides the peak potentials (E_p) and the peak widths ($E_{p/2}$-E_p). Among several methods for elucidating the reaction mechanism, the dependence of E_p on log(v) and the magnitude of the peak widths plays a crucial role (Figures 4.7, 4.8 and 4.9). It has been suggested (Nadjo and Savéant, 1973) that if the plot between E_p vs log(v) is linear, the magnitude of the slope can serve as a clue for comprehending the reaction mechanism. Analogously, from the magnitude of peak width ($E_{p/2}$-E_p) too, the mechanism can be inferred. Table 4.1 provides the peak widths as well as $dE_p/d\log(v)$ values of the three compounds; these are respectively > 95.6 mV and > 60 mV. On the basis of these estimates, it appears that the initial electron transfer is the rate determining step and that the reaction is under kinetic control, for all the three compounds.

However, the electrode kinetic parameters viz, the rate constants and transfer coefficients too need to be analyzed in order to obtain further insights. The dependence of the rate constant on the potential indicates whether the Butler-Volmer or Marcus kinetics is obeyed. Analogously, the estimation of α is especially

convenient in deciphering the transition between the stepwise and concerted path ways.

Table 4.1 Parameters deduced from the cyclic voltammograms for halopentafluorobenzenes at the scan rate of 2 Vs^{-1}.

Parameter	C_6F_5Cl	C_6F_5Br	C_6F_5I
peak potential (V) vs Fc/Fc^+	-2.48	-2.18	-1.67
peak width (mV)	109	129	159
$dE_p/d\log(v)$ (mV)	96	102	111
Diffusion coefficient (in 10^{-5} cm^2 sec^{-1})	2.52	2.26	2.64
Heterogeneous rate constant ($cm\ s^{-1}$)	0.053	0.050	0.049
transfer coefficient from CPSV	0.33	0.31	0.27
transfer coefficient from the peak widths	0.39	0.36	0.30

A simple method of obtaining the transfer coefficients consists in employing the peak widths at various scan rates using the relation (Savéant, 1987).

$$\alpha = \frac{1.856RT}{F}\frac{1}{(E_{p/2} - E_p)} \qquad (4.1)$$

The transfer coefficient values estimated using equation (4.1), are provided in Table 4.1. Figures 4.10, 4.11 and 4.12 depict the dependence of the transfer coefficient on $\log(v)$ wherein it is seen that for C_6F_5Cl, the dependence of α on $\log(v)$ is linear. However, In the case of C_6F_5Br and C_6F_5I, α increases with lowering of scan rates and reaches a maximum value and subsequently decreases. This indicates the concerted mechanism at lower scan rates and stepwise cleavage at higher scan rates for these two compounds. Such a transition between step-wise and concerted pathways, influenced by the scan rates has been already demonstrated for iodobenzne

(Pause *et al*, 1999) and 4'-bromomethylbiphenyl-2-carbonitrile (Prasad and Sangaranarayanan, 2005). Figures 4.13, 4.14 and 4.15 depict the scan-rate normalized voltammograms of all three halopentafluorobenzenes.

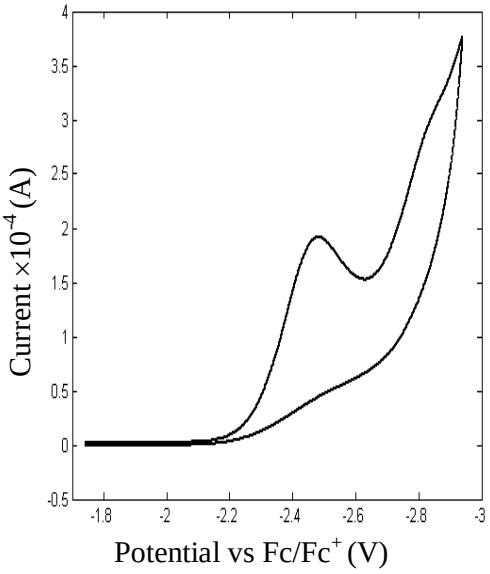

Figure 4.1 Cyclic voltammograms of C_6F_5Cl (1 mM) at the scan rate of 2 Vs^{-1}. The solvent is ACN while the supporting electrolyte is TBAP (0.1 M). The current refers to the background-subtracted current.

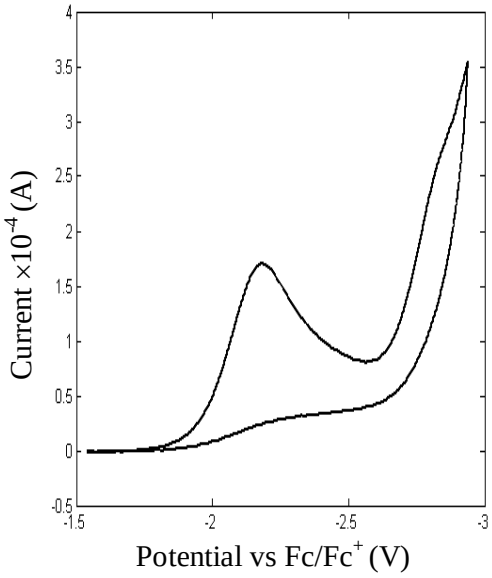

Figure 4.2 Background subtracted cyclic voltammograms of C_6F_5Br (1 mM) at the scan rate of 2 Vs^{-1}. The solvent is ACN while the supporting electrolyte is TBAP (0.1 M).

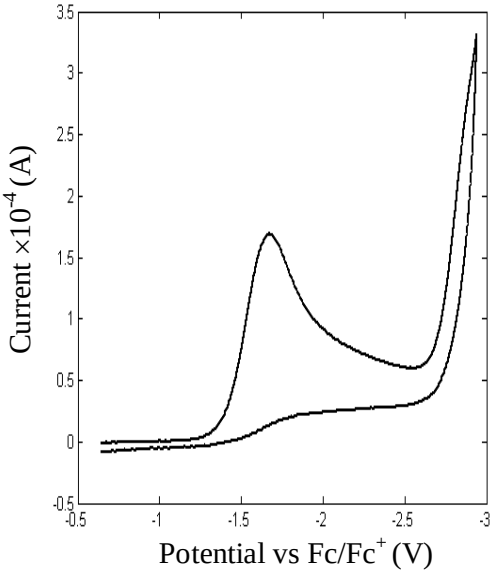

Figure 4.3 Background subtracted Cyclic voltammograms of C_6F_5I (1 mM) at the scan rate of 2 Vs^{-1}.

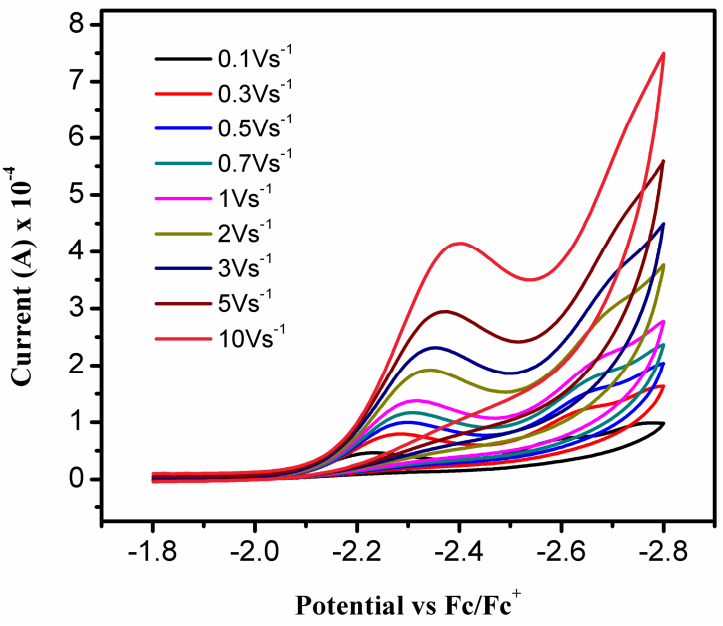

Figure 4.4 Background subtracted cyclic voltammogram of chloropentafluorobenzene at different scan rates

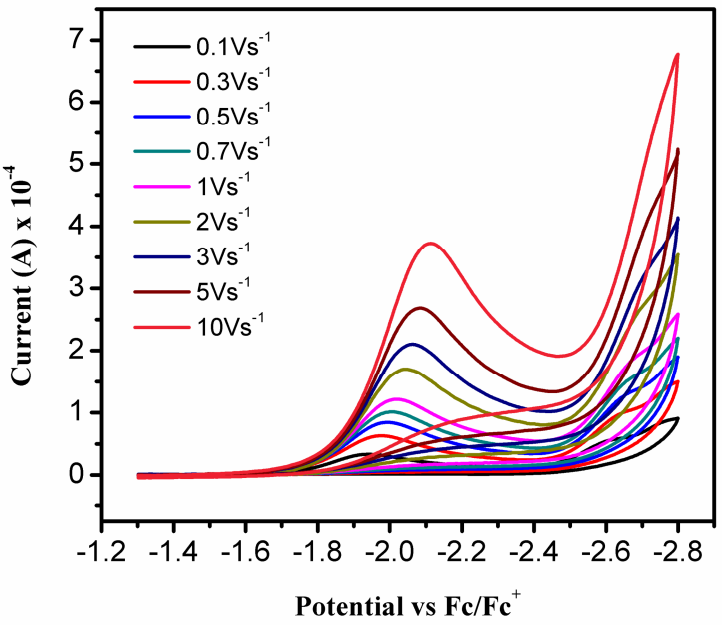

Figure 4.5 Background subtracted cyclic voltammogram of bromopentafluorobenzene at different scan rates

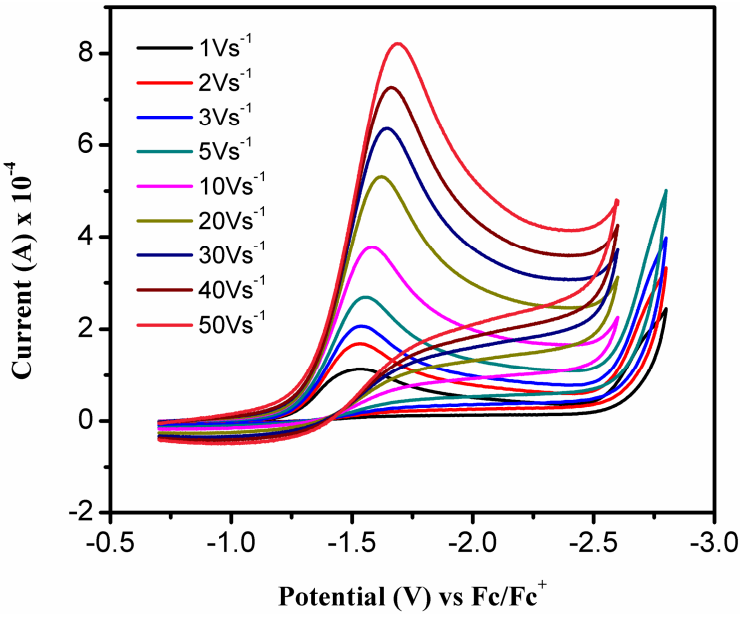

Figure 4.6 Background subtracted cyclic voltammogram of iodopentafluorobenzene at different scan rates

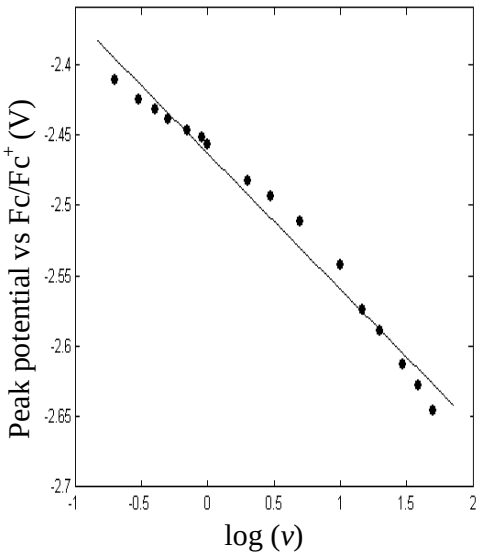

Figure 4.7 The variation of the peak potential (E_p) with log(v) for C_6F_5Cl. The points denote the values from voltammetric data. The line is obtained from the regression analysis. (v is in Vs^{-1}).

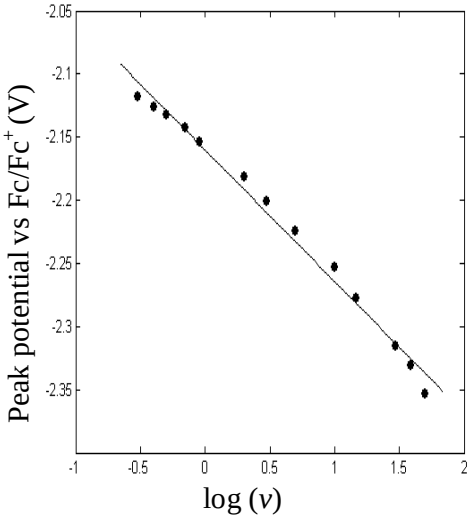

Figure 4.8 The variation of the peak potential (E_p) with log(v) for C_6F_5Br. The points denote the values from voltammetric data. The line is obtained from the regression analysis. (v is in Vs^{-1}).

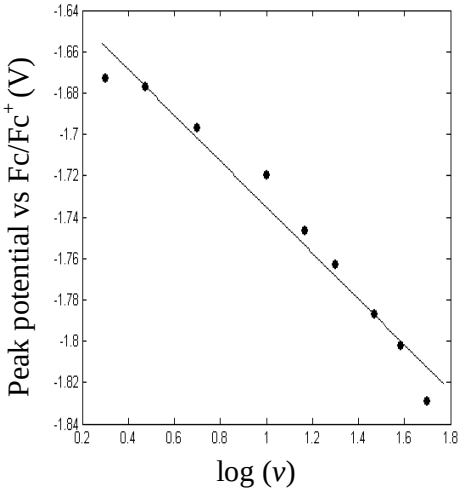

Figure 4.9 The variation of the peak potential (E_p) with log(v) for C_6F_5I. The points denote the values from voltammetric data. The line is obtained from the regression analysis. (v is in Vs^{-1}).

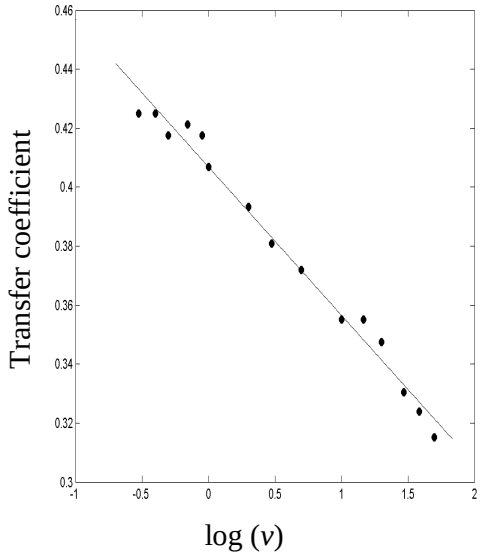

Figure 4.10 The dependence of the transfer coefficient on log(v) for C_6F_5Cl.

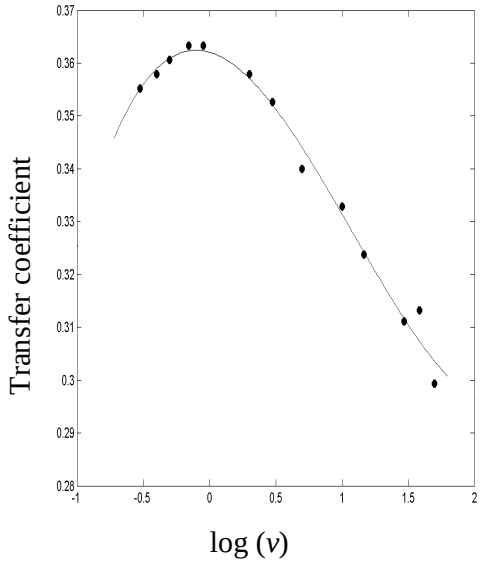

Figure 4.11 The dependence of the transfer coefficient on log(v) for C_6F_5Br. The wave-like pattern is an indication of the transition between step-wise and concerted mechanisms.

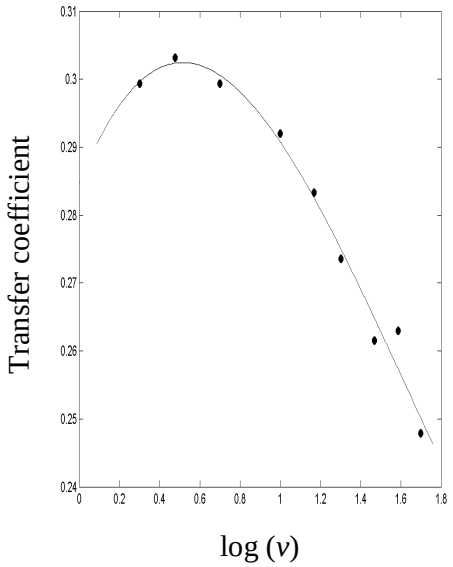

Figure 4.12 The dependence of the transfer coefficient on log(v) for C_6F_5I. The wave-like pattern is an indication of the transition between step-wise and concerted mechanisms.

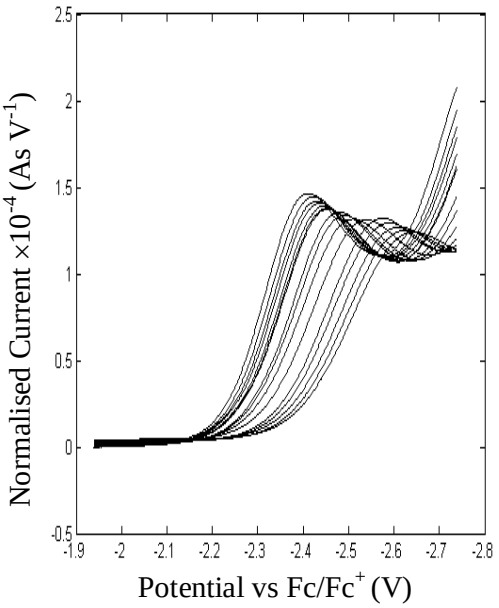

Figure 4.13 The scan-rate normalized voltammograms of C_6F_5Cl. The scan rates vary from 0.2 Vs^{-1} to 50.0 Vs^{-1}

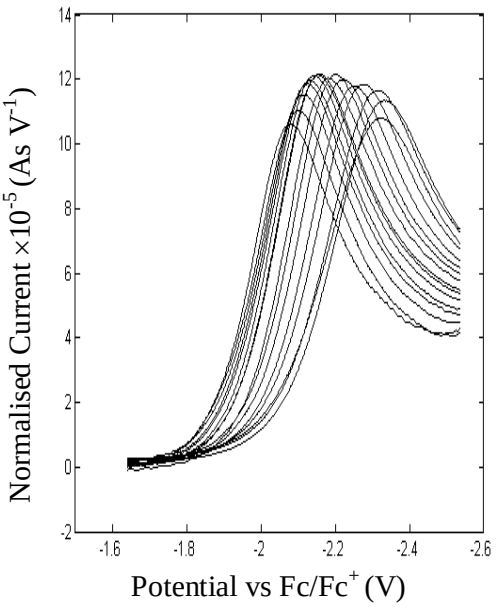

Figure 4.14 The scan-rate normalized voltammograms of C_6F_5Br. The scan rates vary from 0.2 Vs^{-1} to 50.0 Vs^{-1}

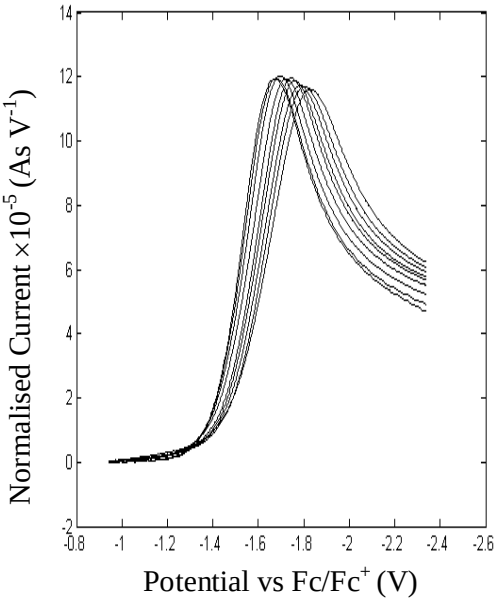

Figure 4.15 The scan-rate normalized voltammograms of C_6F_5I. The scan rates vary from 2 Vs^{-1} to 50.0 Vs^{-1}

4.3.2. Convolution Potential Sweep Voltammetry

The convolution potential sweep voltammetry (CPSV) is a valuable technique for elucidation of the reaction mechanism in so far as entire data points of the cyclic voltammograms are employed. The convolution current (I) is related to the experimentally observed current (i) through the convolution integral given by equation (1.6). By estimating the above integral using the Lawson-Maloy algorithm (Lawson and Maloy, 1974), the dependence of the convoluted current on potential is deduced in Figures 4.16, 4.17 and 4.18 for C_6F_5Cl, C_6F_5Br and C_6F_5I respectively. A typical sigmoidal curve is obtained with plateau at large negative potentials. The plateau region which represents the limiting convolution current is given by equation (1.8). The *overall* number of electrons transferred (n) equals 2. The estimated diffusion coefficients are provided in Table 4.1. In the case of C_6F_5Cl, obtaining the plateau region is difficult since the reduction occurs at large negative potentials; consequently, the limiting convoluted current is obtained by a sigmoidal fitting (Antonello *et al*, 1997 a) using the equation

$$I = a_0 + \frac{a_1}{\left(1+\exp\left[-(E-a_2)/a_3\right]\right)} \tag{4.2}$$

where a_0, a_1, a_2 and a_3 are fitting constants.

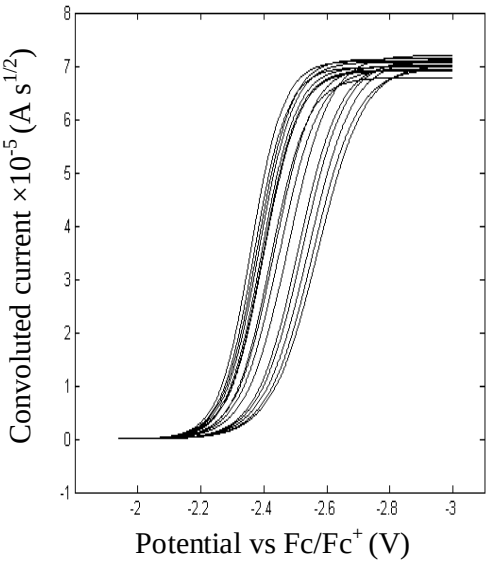

Figure 4.16 The dependence of the convoluted current on potential for C_6F_5Cl. The scan rates vary from 0.2 Vs^{-1} to 50.0 Vs^{-1}.

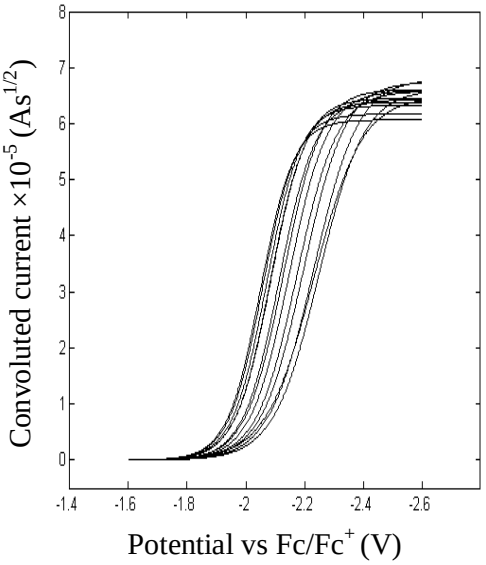

Figure 4.17 The dependence of the convoluted current on potential for C_6F_5Br. The scan rates vary from 0.2 Vs^{-1} to 50.0 Vs^{-1}.

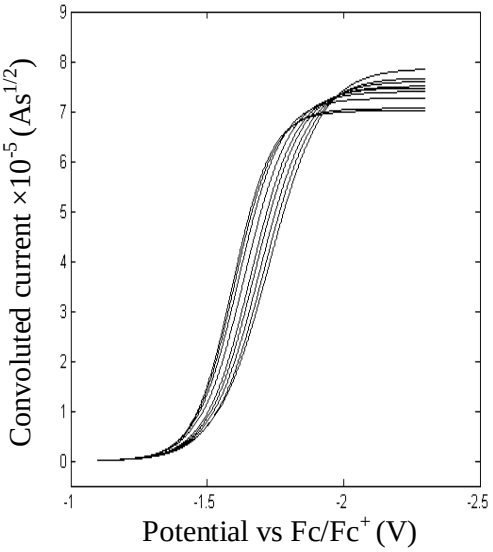

Figure 4.18 The dependence of the convoluted current on potential for C_6F_5I. The scan rates vary from 2 Vs^{-1} to 50.0 Vs^{-1}.

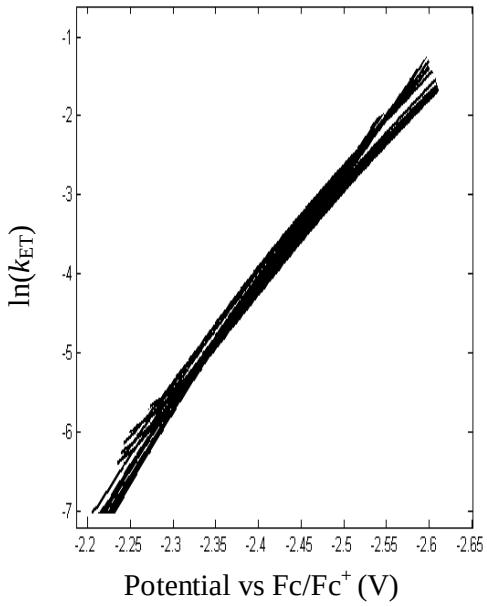

Figure 4.19 The variation of the logarithmic heterogeneous rate constant with potential for C_6F_5Cl. The scan rates vary from 0.2 Vs^{-1} to 50.0 Vs^{-1}.

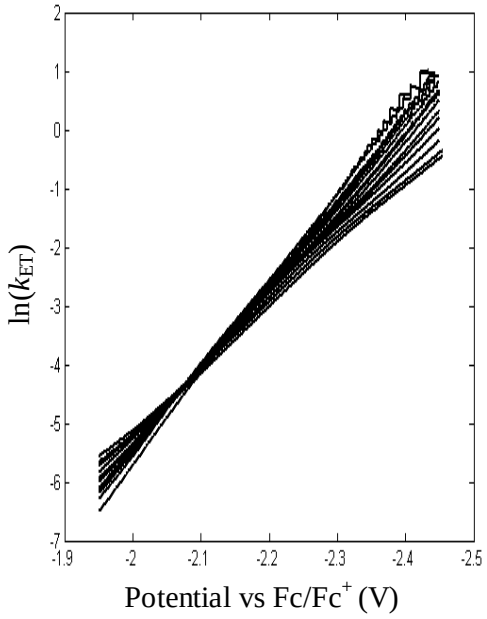

Figure 4.20 The variation of the logarithmic heterogeneous rate constant with potential for C_6F_5Br. The scan rates vary from 0.2 Vs^{-1} to 50.0 Vs^{-1}.

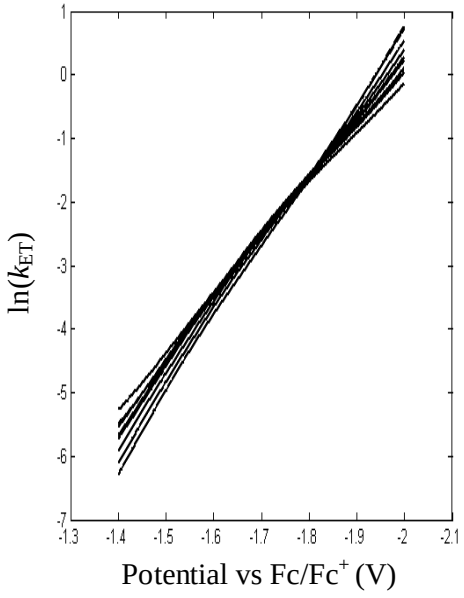

Figure 4.21 The variation of the logarithmic heterogeneous rate constant with potential for C_6F_5I. The scan rates vary from 2 Vs^{-1} to 50.0 Vs^{-1}.

The availability of the convoluted current enables the estimation of the heterogeneous electron transfer rate constants (k_{ET}) using equation (1.12). The dependence of ln(k_{ET}) on E is non-linear for halopentafluorobenzenes as shown in Figures 4.19, 4.20 and 4.21 which in turn indicates the validity of the Marcus-Hush theory of quadratic activation driving force relationship (Marcus and Sutin, 1985). The transfer coefficient is estimated from ln(k_{ET}) vs E plot using equation (1.16). In order to obtain α values, the procedure advocated by Antonello *et al* (Antonello and Maran, 1997 b) wherein successive linear fits for each 10 points with 1 mV per point were constructed. The resulting transfer coefficients are depicted in Figures 4.22, 4.23 and 4.24. The variation of the transfer coefficients with potential is quite interesting for each compound in that a maximum value is noticed with a subsequent decrease. This behaviour has been observed in the reduction of perbenzoates (Antonello and Maran, 1997 b; Antonello and Maran, 1999) and is ascribed to the occurrence of mechanistic change on account of the influence of electrode potential.

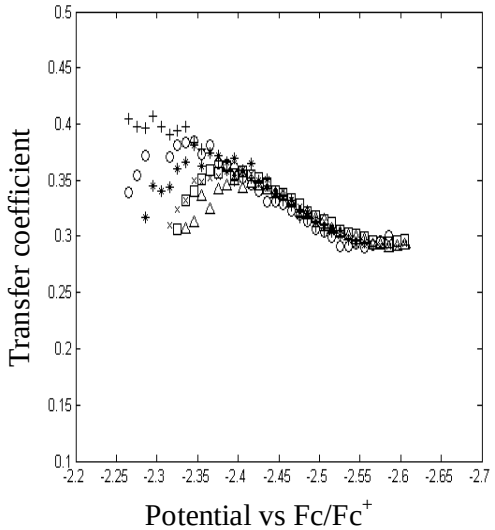

Figure 4.22 The dependence of the transfer coefficient on potential for C_6F_5Cl at the scan rates 5 Vs^{-1}(+), 10 Vs^{-1}(o), 20 Vs^{-1}(∗), 30 Vs^{-1}(×), 40 Vs^{-1}(□) and 50 Vs^{-1}(Δ).

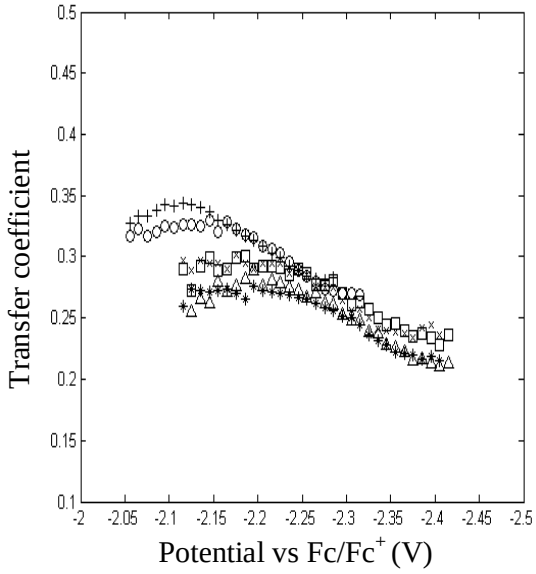

Figure 4.23 The dependence of the transfer coefficient on potential for C_6F_5Br at the scan rates 5 Vs^{-1}(+), 10 Vs^{-1}(o), 20 Vs^{-1}(∗), 30 Vs^{-1}(×), 40 Vs^{-1}(□) and 50 Vs^{-1}(Δ).

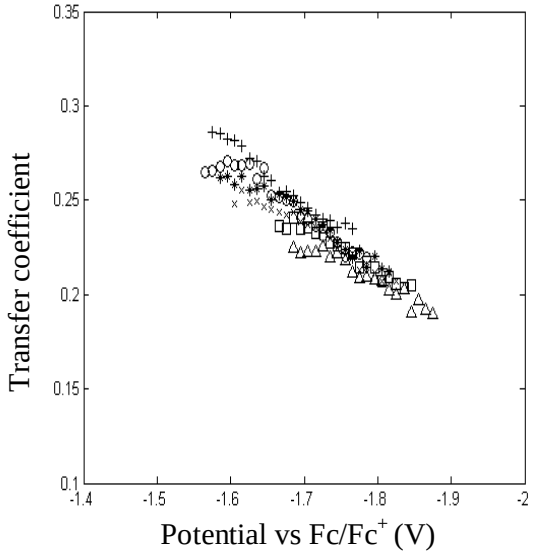

Figure 4.24 The dependence of the transfer coefficient on potential for C_6F_5I at the scan rates 5 Vs^{-1}(+), 10 Vs^{-1}(o), 20 Vs^{-1}(∗), 30 Vs^{-1}(×), 40 Vs^{-1}(□) and 50 Vs^{-1}(Δ).

4.3.3. Estimation of the bond-lengths and electron densities

The estimation of bond lengths before and after the occurrence of reactions can also provide a diagnostic criterion for distinguishing between the stepwise and concerted mechanisms (Cardinale et al, 2002). The bond lengths of neutral and anionic radicals of halopentafluorobenzenes deduced from quantum chemical calculations are provided in Table 4.2. In view of the significant differences in bond lengths, the concerted mechanism is inferred from the quantum chemical calculations as shown in Figure 4.25. The Natural Bond Orbital (NBO) analysis also indicates the absence of the bond between carbon and halogen thus suggesting a concerted mechanism for the halopentafluorobenzenes.

In order to obtain the charge density, the total charge density is estimated from the Gaussian 03 analysis. The ESP is mapped on the surface of the total electron density so as to generate the contour diagrams. It is seen that the radical anions have higher electron densities around the halogen atom indicating the presence of the extra charge in the halide (Figure 4.26). The Mulliken charge analysis denoting the partial charge of halide atoms of halopentafluorobenzene anionic radical is given in Table 4.2. Had the stepwise mechanism been obeyed, the electron density will be observed in the benzene ring rather than on the halide. The electron density mapping and the partial atomic charges estimations of neutral and anionic radicals of the halopentafluorobenznes indicate the validity of the concerted mechanism. It may be noted here that for radical anions involving sulphur, the elongation of bold length of ca. 0.7 ´ is possible despite the occurrence of the step-wise mechanism. However, in the case of carbon-halogen bonds, such a possibility is un-likely.

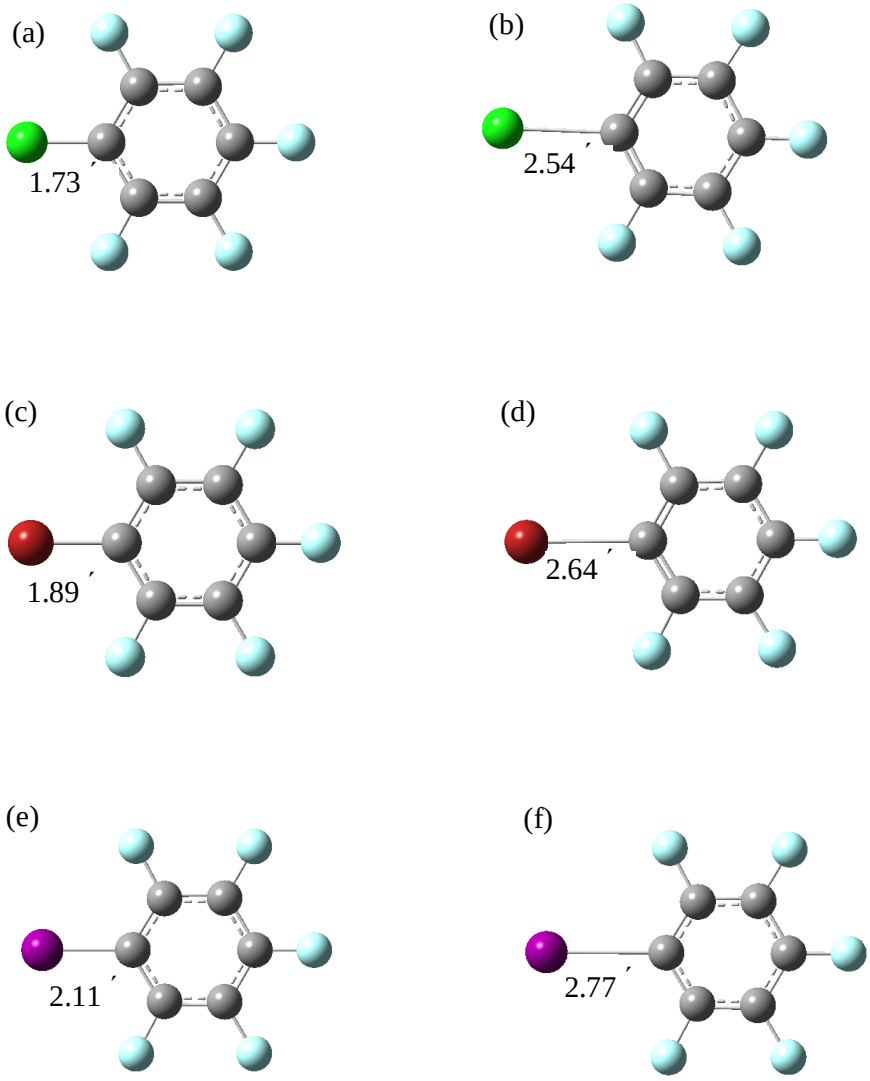

Figure 4.25 The optimized geometry of neutral and radical anions of halopentafluorobenzenes (a) C_6F_5Cl, (b) $C_6F_5Cl^{\bullet-}$, (c) C_6F_5Br, (d) $C_6F_5Br^{\bullet-}$, (e) C_6F_5I and (f) $C_6F_5I^{\bullet-}$.

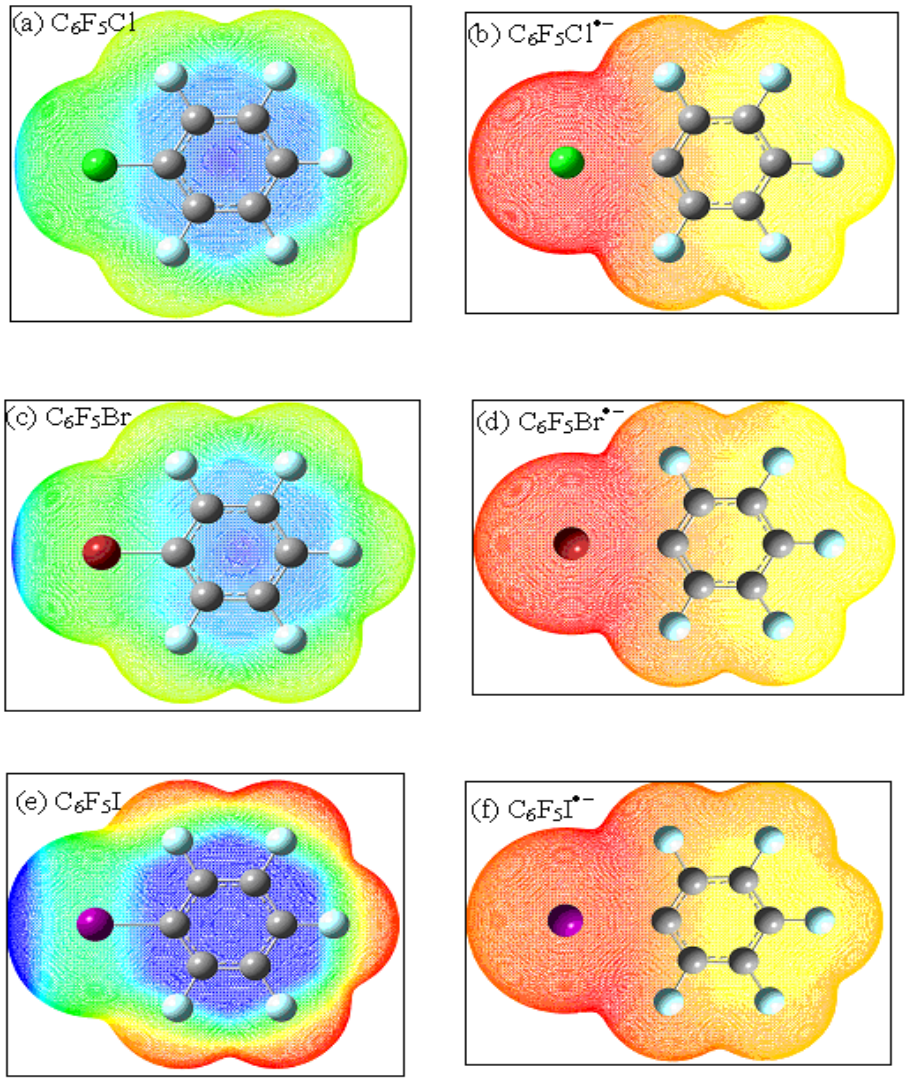

Figure 4.26 The mapping of the electrostatic potential (ESP) on the surface of the total electron density at isosurface value of 0.0004 units. (a) neutral C_6F_5Cl, blue (+0.03332 units) to red (-0.03332 units), (b) Anionic radical of C_6F_5Cl, blue (+0.191 units) to red (-0.191 units), (c) neutral C_6F_5Br, blue (+0.03048 units) to red (-0.03048 units) (d) Anionic radical of C_6F_5Br and blue (+0.185 units) to red (-0.185 units), (e) neutral C_6F_5I, blue (+0.0224 units) to red (-0.0224 units) (f) Anionic radical C_6F_5I, blue (+0.174 units) to red (-0.174 units). The red colour indicates the negative (high electron density) part of the electrostatic potential while blue indicates the positive part (low electron density) of the electrostatic potential.

Table 4.2 The bond length and partial charge of halides estimated from optimized geometries using the (a) B3LYP/6-311++G(d,p) basis for C_6F_5Cl and C_6F_5Br and (b) B3LYP/CEP-121G for C_6F_5I

Compounds	Bond length (Å)		Partial charge on the halide	
	Neutral	Radical anion	Neutral	Radical anion
C_6F_5Cl	1.73	2.54	+0.02	-0.72
C_6F_5Br	1.89	2.64	+0.08	-0.65
C_6F_5I	2.11	2.77	+0.41	-0.49

4.3.4. Estimation of the intrinsic barrier

The transfer coefficient is related to the intrinsic barrier ($\Delta G_0^{\#}$) of the reductive cleavage reaction (Savéant, 1987) can be written from equation (1.26)

$$\alpha = 0.5\left(1+\frac{\Delta G^0}{4\Delta G_0^{\#}}\right) \tag{4.3}$$

From the linear portion of the plot α vs E-E^0, the slope ($1/8\Delta G_0^{\#}$) is deduced. This value can then be compared with the theoretical prediction of the intrinsic barrier for the step wise and concerted processes. The parametric relation for theoretical estimation of $\Delta G_0^{\#}$ is different for stepwise and concerted mechanisms as represented in equations (1.23) and (1.27) (Savéant, 1990)

The bond dissociation energy (D_{RX}) is calculated either from potential energy surface or from the enthalpies of reactants and products of the reaction $RX \rightarrow R^{\bullet} + X^{\bullet}$

$$\Delta H = (H_{R^{\bullet}} + H_{X^{\bullet}}) - H_{RX} \tag{4.4}$$

λ being the total reorganization energy. Due to the occurrence of the additional term (dissociation energy), concerted reactions have higher intrinsic barrier in comparison with the stepwise mechanisms. The dissociation energies of the compounds are estimated using Gaussian 03 mentioned earlier and are shown in Table 4.3. Although the total reorganization energy consists of internal and solvent reorganization energies ($\lambda = \lambda_s + \lambda_i$), the contribution of the internal reorganization is small and is customarily neglected (Kojima and Bard, 1975). The solvent reorganization energy (in this case acetonitrile) is computed from equation (1.20) (Andrieux *et al*, 1992) as

$$\lambda_s = \frac{2.08}{a_{RX}} \tag{4.5}$$

where a_{RX} is the radius (in Å) of the compound subsequent to the electron transfer and λ_s is the solvent reorganization energy (in eV). Since the halogen atom of the molecule acquires a negative charge during the electron-transfer, the reorganization energy needs to be estimated using the relation

$$a = \frac{a_X(2a_{RX} - a_X)}{a_{RX}} \tag{4.6}$$

Here, a_{RX} and a_X denote respectively the radius of the *RX* and *X*. The numerical factor 2.08 arises from the optical and static dielectric constants of the solvent. The theoretical estimates of $\Delta G_0^{\#}$ are compared with experimentally deduced values in Table 4.3. Interestingly, this comparison of the intrinsic barrier values does not provide a clear de-markation between the step-wise and concerted mechanisms except probably in the case of C_6F_5Cl. The chloropentafluorobenzene seems to follow a stepwise mechanism since the theoretical and experimental intrinsic barriers are comparable. However, for the other two compounds, the intrinsic barriers deduced

from the experimental data are significantly deviating from the theoretical estimates pertaining to the concerted mechanism; hence a stepwise mechanism in conjunction with non-negligible inner reorganization energy may also be likely.

Table 4.3 Estimation of the intrinsic barrier ($\Delta G_0^{\#}$) for the reduction of C-X bond pertaining to the stepwise (s) and concerted (c) mechanisms

Compound	Bond dissociation energy (eV)	Reorganization energy (eV)	Intrinsic barrier (eV)	
			Theoretical	Experimental
C_6F_5Cl	3.75	0.58	1.08(c) 0.14(s)	0.29
C_6F_5Br	3.32	0.53	0.96(c) 0.13(s)	0.30
C_6F_5I	2.69	0.61	0.82(c) 0.15(s)	0.46

4.3.5. Estimation of standard reduction potentials

The estimation of the standard reduction potentials of the reactant also serves as a method of elucidating the reduction mechanism. It follows from equation (1.26), that if α is less than 0.5, E^0 is more positive than E_p. On the other hand, if α is grater than 0.5, ΔG^0 becomes positive thus indicating an unfavorable reaction. In this study, α is less than 0.5 and E^0 values as shown below are more positive than E_p. Further, E^0 can be obtained by locating the potential at which α is 0.5 in the α vs E plot. The standard reduction potentials estimated using this method are provided in Table 4.4. In the case

of concerted reactions, the thermochemical cycle for estimation of standard reduction potential as shown in the Scheme 1.2 can be employed and E^0 is estimated from equation (1.31). The entropy change is obtained from the frequency calculations using Gaussian 03.

Table 4.4 Estimated standard reduction potentials of halopentafluorobenzenes (assuming the concerted mechanism) from (i) the thermochemical cycle and (ii) α vs (E-E^0) plot

Compound	E_p vs Ag/Ag^+(1 mM) (V)	E^0 vs Ag/Ag^+(1 mM) from the thermochemical cycle (V)	E^0 vs Ag/Ag^+(1 mM) from α vs (E-E^0) plot (V)
C_6F_5Cl	-2.34	-2.05	-2.05
C_6F_5Br	-2.04	-1.97	-1.62
C_6F_5I	-1.53	-1.85	-0.75

$E^0_{X^\bullet/X^-}$ in acetonitrile is obtained from $E^0_{X^\bullet/X^-}$ in water using the following equation with SCE as the reference electrode.

$$E^{0,ACN}_{X^\bullet/X^-}(vs\ SCE) = E^{0,H_2O}_{X^\bullet/X^-}(vs\ SHE) - E^{0,H_2O}_{Ag^+/Ag}(vs\ SHE) - \left[\Delta_{tr}G^0_{X^-,(H_2O\to ACN)} + \Delta_{tr}G^0_{Ag^+,(H_2O\to ACN)}\right] + 0.44 \quad (4.7)$$

$\Delta_{tr}G^0_{X^-,(H_2O\to ACN)}$ and $\Delta_{tr}G^0_{Ag^+,(H_2O\to ACN)}$ denote the Gibbs free energy of transfer of X^- and Ag^+ ions from water to acetonitrile (Marcus, 1997). $E^{0,H_2O}_{X^\bullet/X^-}(vs\ SHE)$ follows from $E^{0,DMF}_{X^\bullet/X^-}(vs\ SCE)$ by using the above formula for DMF solvent (Cardinale *et al*, 2002).

$E^0_{RX/R^{\bullet}+X^-}$ computed with reference to SCE is converted to Ag/Ag^+(1mM) reference electrode for direct comparison with experimental data (cf. Appendix-C).

The above analysis enables the theoretical calculation of $E^0_{RX/R^{\bullet}+X^-}$ with respect to Ag/Ag^+ reference electrode for all the three compounds if concerted mechanism is valid (Table 4.4). For C_6F_5Cl, the experimental value is in agreement with the theoretical estimate suggesting the feasibility of the concerted mechanism. However, for C_6F_5Br and C_6F_5I, in view of the considerable discrepancy, concerted mechanism does not appear valid.

There exists a correspondence between E^0 and E_p values too. For concerted mechanisms ($\alpha < 0.5$), E^0 is more positive than E_p (cf. eqn. 6). Further, E^0 estimated from the thermochemical cycle is (i) significantly more positive than E_p for both C_6F_5Cl and C_6F_5Br and (ii) more negative for C_6F_5I. These features indicate the possible occurrence of concerted mechanism for C_6F_5Cl and C_6F_5Br while a borderline between the stepwise and concerted mechanisms for C_6F_5I seems likely. However, these deductions are based upon the E^0 values.

The mechanistic analysis of dissociative electron transfer reactions involving carbon-halogen, oxygen-oxygen and carbon-sulphur bonds is a challenging task in view of the significant influence offered by the nature of the solvent, substituent group as well as the electrode characteristics mediated by the driving force. Thus extensive investigations have been carried out during the past few decades in order to unravel the kinetic and thermodynamic aspects (Maran *et al*, 2001). A notable feature in such studies is the general applicability of Marcus-Hush quadratic activation-driving force relation.

In the present analysis, the reductive cleavage of carbon-halogen (Cl,Br,I) bonds in halopentafluorobenzenes is studied. The reduction potentials for chloro, bromo and iodobenzenes are -2.81 V, -2.67 V and -1.95 V in DMF (with respect to SCE) respectively (Andrieux *et al*, 1979). A significant positive shift was observed in halopentafluorobenzene in comparison with halobenzenes (after converting the potential of halopentafluorobenzenes from Ag/Ag^{+} to SCE) and is attributed to the electron withdrawing nature of fluorines. It is of interest to note that the mechanism of the C-X bond cleavages in halopentafluorobenzenes can not be classified in an unambiguous manner. The experimental data indicate the mechanism to be a borderline between stepwise and concerted. Thus a change in the mechanism (from stepwise to concerted) has occurred in halopentafluorobenznes on account of the five fluorine atoms present in the benzene ring. In this context, iodobenzene, exhibiting a mechanistic change with increase in the driving force deserves mention (Pause *et al*, 1999).

It may be emphasized that the presence of the electron-withdrawing fluorines of the pentafluorohalobenzenes has led to a departure from the expected behaviour of step wise mechanism, in comparison with the un-substituted aryl halides. Consequently, a borderline between step-wise and concerted mechanism seems to operate in the compounds studied here. It will be worthwhile to carry out further studies regarding the quantitative origin of this phenomena either as a function of polarity of the solvent or as a function of temperature so that more insights on the structure-reactivity correlation can be deduced.

SECTION 4.4 SUMMARY

The convolution potential sweep voltammetric study of C_6F_5Cl, C_6F_5Br and C_6F_5I has been carried out at glassy carbon electrodes using acetonitrile as the solvent. The potential-dependence of the heterogeneous rate constant and transfer coefficients is deduced and the kinetics is shown to obey the Marcus-Hush quadratic activation-driving force dependence. The standard reduction potentials are estimated for the halopentafluorobenzenes from the transfer coefficients. The mechanistic analysis using different criteria leads to the inference that halopentafluorobenzenes do not follow un-ambiguous stepwise or concerted pathway.

CHAPTER 5

SUMMARY AND FUTURE PERSPECTIVES

The mechanistic analysis of the reductive cleavage of carbon-halogen bonds has been studied using the Convolution Potential Sweep Voltammetry and the kinetic parameters have been interpreted with the help of the Marcus – Hush Theory of quadratic activation driving force relationship. The bond cleaving reactions have been analyzed via the dissociative electron transfer theory deduced by R. A. Marcus and J. M. Saveant. In order to comprehend the role of electron-withdrawing groups, the following substrates have been chosen: (1) 4-fluorobenzonitrile, (2) *orhto* and *para* isomers of methylfluorobenzoates and (3) halopentafluorobenzenes.

SECTION 5.1 SUMMARY

5.1.1. 4-fluorobenzonitrile

The stepwise mechanism has been inferred using Covolution potential Sweep Voltammetric analysis, solvent reorganization energies and quantum chemical calculations. The conditions under which dimerization occurs has also been delineated and a threshold concentration is deduced. The standard reduction potentials using theromochemical cycles have also been estimated.

5.1.2. Methylfluorobenzoates

These undergo reduction at potentials more positive than that pertaining to 4-fluorobenzonitrile. The *ortho* isomer undergoes reductive elimination while the *para*

isomer undergoes dimerization and the reductive elimination occurs ~100mV more positive than the dimerization of 4-methylfluorobenzoate. There is no limiting concentration for dimerization to occur. The rate constants for the ECE mechanism of 2-methylfluorobenzoate and the dimerization of 4-methylfluorobenzoate have been obtained using CPSV and the classical Nicholson and Shain analysis. The dimerization is inferred as occurring via second order anion radicals coupling. The stabilization of the radical anions is further confirmed from the potential energy studies using Gaussian analysis. The step wise mechanism is confirmed from theoretical and experimental studies. The electron withdrawing groups play an important role in the electrodimeization reaction.

5.1.3. Halopentafluorobenzenes

The halopentafluorobenzenes constitute interesting class of substrates for the study of reductive cleavage of carbon-fluorine bonds. The reductive cleavage follows ECE mechanism and the mechanistic path way has been analysed using different diagnostic criteria. The CPSV data analysis using the theory of dissociative electron transfer indicates that the reduction mechanism can not be un-ambiguously inferred for halopentafluorobenzenes. It is thus suggested that all diagnostic criteria may not be equally sensitive for elucidation of the reaction mechanism.

SECTION 5.2 FUTURE PERSPECTIVES

The mechanism of the reductive cleavage of carbon-halogen bonds is a fascinating topic of analysis. The nature of the substrate seems to play a vital role. The position of the substituent whether they are in *ortho, para or meta* position also may lead to new insights in this context. The aromatic halides having electron withdrawing substrates in general undergo electro-dimerization. The dimerization step which is dependent upon the concentration of the reactant may suppress the ECE mechanism. Hence diverse classes of substrates need to be analysed before a comprehensive theory can be formulated. The extent of dimerization needs to be estimated in future extensions of the present study.

The influence of solvents in electron transfer processes constitutes a frontier area of research in physical chemistry and chemical physics. The solvent re-organization energy has played a crucial role in the theory of electron transfer processes. The emphasis in the present investigation has been on acetonitrile - a popular solvent in electrochemical studies. It is essential to employ other polar solvents so that a correlation with the dielectric constant can be accomplished. In particular, binary solvents whose composite dielectric constants can vary over a wide range are especially crucial in order to un-ravel the influence of the polarity of the medium. While the glassy carbon electrode has been employed in the present study, it remains to be seen whether the nature of the electrodes can influence the mechanism of reduction of electro-organic compounds.

The quantum chemical calculations too need to be more extensively carried out for validating reaction mechanisms. The estimations of bond lengths has served as an important diagnostic tool in the classification of mechanism as step wise and concerted. However, other parameters such as electron density mapping, molecular orbital energies, geometric considerations etc need to be studied. The potential energy diagrams used to study the different intermediates such as π and σ anion radicals formed during the reduction. The molecular orbital analysis used to analyze and predict the stabilization of anion radicals via SOMO and LUMO mapping.

The study on the de-halogenation of polychlorobiphenyls may be useful in the environmental chemistry. Further, the regioselective reduction of carbon-chlorine bonds in polychlorobiphenyls (PCB's) is challenging in view of the *a priori* inability to predict the ease of reduction. It is anticipated that the chlorine in the *ortho* position may be eliminated more easily than *para* due to the planarity achieved during the elimination of *ortho*-chlorine. The convolution potential sweep voltammetry has been applied for the study of PCB degradation for the more number of peaks (multi nernstian) in a single voltammogram.

APPENDIX-A

MATLAB PROGRAM EMPLOYED FOR ESTIMATING THE CONVOLUTED CURRENT, RATE CONSTANT AND TRANSFER COEFFICIENT

% Estimation of the convoluted current

```
load input.txt;                                  % Input file
v =input(:,1);          % input file contains potential values in the first column
i = input(:,2);         % input file contains current values in the second column
sr=100;                                          % scan rate mentioned in mVs^-1
ne=2;                                            %number of electrons
R=8.314;                                         %gas constant
T=298;                                           % temperature
F=96500;                                         %Faraday constant
A= 0.07065                                       % Surface area of the electrode in cm^2
Cb=1;                                            % Bulk concentration of the reactant in mM
q=size(input);
delt=(1/sr);
n=q(1,1);
for k=1:n
        val1=0;
        for j=2:k
                val=(((i(j)+i(j-1))*delt)/2)/ (b=(k*delt-j*delt+0.5*delt)^0.5);
                val1=val1+val;
        end
   I=val1/(pi^0.5);
   I(k,1)=I;
end
plot(v,I)
```

%Estimation of the rate constant

```
Imax=max(I);                                % Imax is Limiting convoluted current
D=(Imax/(ne*F*A*Cb*10^-6))^2;               % D is the diffusion coefficient
for m=1:n
        val2=log(D^0.5)-log((Imax-I(m))/i(m));
        ket(n,1)=val2;
end
plot(v,ket)

% Estimation of the potential-dependent transfer coefficient


d=10;
q=fix(n/d);
for n=0:q-1
   x=v(((n*d)+1):((n*d)+d));
   y=k(((n*d)+1):((n*d)+d));
   p=polyfit(x,y,1);
   alp(n+1,1)=-((R*T)/F)*p(1,1);
   v1(n+1,1)=(min(x)+max(x))/2;
end
plot(v1,alp,'o--')
clear all
```

APPENDIX-B

ESTIMATION OF THE STANDARD REDUCTION POTENTIAL OF $X^{\bullet}/X^{-}$ IN ACETONITRILE ($E^{0,ACN}_{X^{\bullet}/X^{-}}$)

The standard reduction potential pertaining to $F^{\bullet}/F^{-}$ in acetonitrile (or any other solvent) can be computed by a suitable choice of the thermochemical cycle. The scheme depicted below is constructed for this purpose.

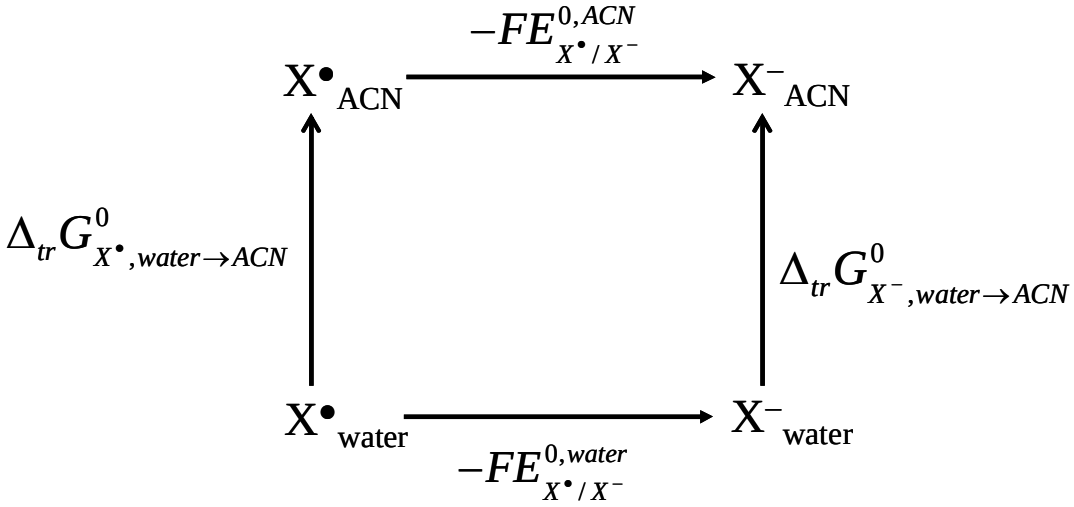

Scheme B. 1. Thermochemical cycle for the estimation Standard reduction of $X^{\bullet}/X^{-}$ in acetonitrie.

The standard reduction potential follows as

$$-FE^{0,ACN}_{X^{\bullet}/X^{-}} = -\Delta_{tr}G^{0}_{X^{\bullet},water\rightarrow ACN} - FE^{0,water}_{X^{\bullet}/X^{-}} + \Delta_{tr}G^{0}_{X^{-},water\rightarrow ACN}$$

where $\Delta_{tr}G^{0}_{X^{\bullet},water\rightarrow ACN}$ is the transfer free energy of $X^{\bullet}$ from water to acetonitrile, $\Delta_{tr}G^{0}_{X^{-},water\rightarrow ACN}$ denotes the transfer free energy of X^{-} and $E^{0,water}_{X^{\bullet}/X^{-}}$ is the standard

reduction potential of halide radical to halide anion in water and it is taken from the literature (Marcus, 1997). The Gibbs transfer free energy of halide anions are available in the literature. The transfer free energy for radical anion is unknown. It can be estimated from another thermochemical cycle depicted below:

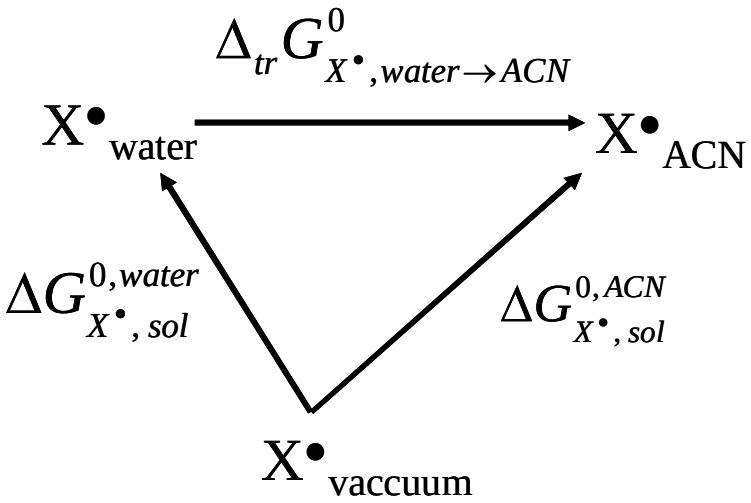

Scheme B. 2. Thermochemical cycle for the estimation Gibbs transfer free energy of $X^{\bullet}$ from water to acetonitrile.

The Gibbs transfer free energy of the radical from water to acetonitrile is given by the equation

$$\Delta_{tr}G^{0}_{X^{\bullet},water\rightarrow ACN} = -\Delta G^{0,water}_{X^{\bullet},sol} + \Delta G^{0,ACN}_{X^{\bullet},sol}$$

where $\Delta G^{0,water}_{X^{\bullet},sol}$ and $\Delta G^{0,ACN}_{X^{\bullet},sol}$ are the solvation free energies of $X^{\bullet}$ in water and acetonitrile respectively. The solvation energy values can be estimated using Gaussian 03.

APPENDIX-C

CONVERTING THE REFERENCE SCALE FROM NON-AQUEOUS Ag/Ag^+ TO AQUEOUS-SATURATED CALOMEL ELECTRODE

The standard reduction potentials deduced from thermochemical cycles are with reference to SHE, while the experimental E^0 values arise with reference to Ag/Ag^+ (1mM) in acetonitrile. However, the conversion to Ag/Ag^+ can be carried out with the help of the Nernst equation and Gibbs transfer free energies in the following manner. From the Nernst equation, we can write

$$E^0_{Ag/Ag^+(1mM,ACN)} = E^0_{Ag/Ag^+(ACN)} - 0.059\log\left[Ag^+\right]$$

$E^0_{Ag/Ag^+(ACN)}$ is estimated from the thermochemical cycle as given below

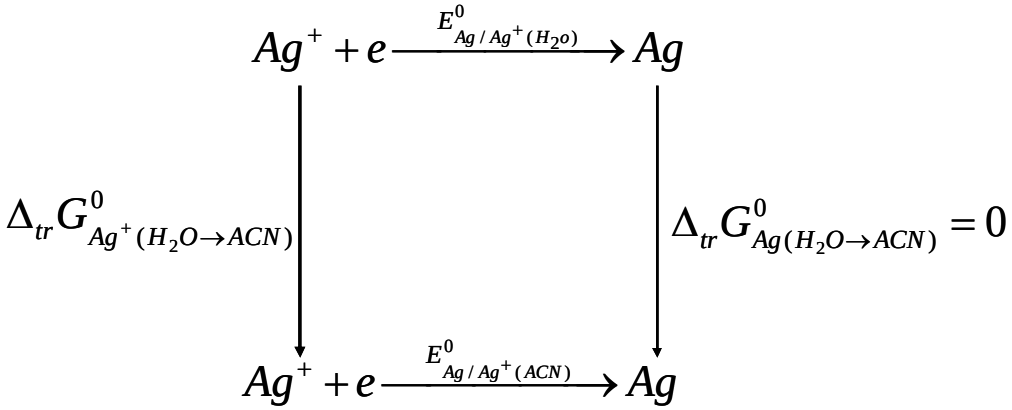

Scheme C. 1. Thermochemical cycle for the estimation of standard reduction potential of Ag/Ag+ in acetonitrile.

The standard reduction potential of Ag/Ag^+ in acetonitrile is given by

$$E^0_{Ag/Ag^+(ACN)} = E^0_{Ag/Ag^+(H_2O)} - \Delta_{tr}G^0_{Ag^+(H_2O\rightarrow ACN)}$$

$\Delta_{tr}G^0_{Ag^+,(H_2O\rightarrow ACN)}$ denotes the Gibbs free energy of transfer of Ag^+ ions from H_2O to ACN. Substituting the value of $E^0_{Ag/Ag^+(ACN)}$ in the Nernst equation, the potential

corresponding to 1 mM is obtained. The value of standard reduction potential of Ag/Ag^+ in water is 0.799V vs SHE. The value of Gibbs transfer free energy of Ag^+ from water to acetonitrile is -0.32eV. Hence, the standard reduction potential of Ag/Ag^+ in acetonitrile is 1.19V vs SHE. Since the reported values are with respect to SCE, The values are converted to SCE. The reference potential of saturated calomel electrode is 0.224V vs SHE. Finally the values are corrected to the reference potential 0.966V to convert the potentials from Ag/Ag^+ to SCE.

REFERENCES

1. **Andrieux, C. P., C. Blocman, J. M. D. Bouchiat,** and **J. M. Savéant** (1979) Heterogeneous and homogeneous electron transfers to aromatic halides. An electrochemical redox catalysis study in the halobenzene and halopyridine series. *J. Am. Chem. Soc.* **101,** 3431-3441.

2. **Andrieux, C. P., J. M. Savéant,** and **K. B. Su** (1986 a) Kinetics of dissociative electron transfer. Direct and mediated electrochemical reductive cleavage of the carbon-halogen bond. *J Phys Chem.* **90**, 3815-3823.

3. **Andrieux, C. P., I. Gallardo, J. M. Savéant,** and **K. B. Su** (1986 b) Dissociative electron transfer. Homogeneous and heterogeneous reductive cleavage of the carbon-halogen bond in simple aliphatic halides. *J Am. Chem Soc*. **108**, 638-647.

4. **Andrieux, C. P., A. L. Gorande,** and **J. M. Savéant** (1992) Electron Transfer and Bond Breaking. Examples of Passage from a Sequential to a Concerted Mechanism in the Electrochemical Reductive Cleavage of Arylmethyl Halides. *J. Am. Chem. Soc.* **114,** 6892-6904.

5. **Andrieux, C. P., A. L. Gorande,** and **J. M. Savéant** (1994 a) Reductive elimination in vicinal dibromides. Electrochemical reduction of 1,2-dibromo-3-(4-substituted)-phenylpropanes and induction of double-bond migration in the resulting olefins. *J. Electroanal. Chem.* **371,** 191-196.

6. **Andrieux, C. P., A. Batlle, M. Espin, I. Gallardo, Z. Jiang,** and **J. Marquet** (1994 b) Mechanistic studies on the electrochemical reductive coupling of some polyhalogenonitrobenzenes. A new example of a radical anion dimerization. *Tetrahedron*. **50**, 6913-6920.

7. **Andrieux, C. P., M. Robert, F. D. Saeva,** and **J. M. Savéant** (1994 c) Passage from Concerted to Stepwise Dissociative Electron Transfer as a Function of the Molecular Structure and of the Energy of the Incoming Electron. Electrochemical Reduction of Aryldialkyl Sulfonium Cations. *J. Am. Chem. Soc.* **116**, 7864-7871.

8. **Andrieux, C. P., M. Robert,** and **J. M. Savéant** (1995) Role of Environmental Factors in the Dynamics of Intramolecular Dissociative Electron Transfer. Effect of Solvation and Ion-Pairing on Cleavage Rates of Anion Radicals. *J. Am. Chem. Soc.* **117**, 9340-9346.

9. **Andrieux, C. P., C. Combellas, F. Kanoufi, J. M. Savéant,** and **A. Thiébault** (1997 a) Dynamics of Bond Breaking in Ion Radicals. Mechanisms and Reactivity in the Reductive Cleavage of Carbon-Fluorine Bonds of Fluoromethylarenes. *J. Am. Chem. Soc*. **119**, 9527-9540.

10. **Andrieux, C. P., J. M. Savéant,** and **C. Tardy** (1997 b) Transition between Concerted and Stepwise Dissociative Electron Transfers. An Example of How a Change of Temperature May Trigger a Change in Mechanism in Electrochemical Experiments. *J. Am. Chem. Soc*. **119**, 11546-547.

11. **Anson, F. C., D. N. Blauch, J. M. Savéant** and **C. F. Shu** (1991) Ion Association and Electric Field Effects on Electron Hopping in Redox Polymers. Application to the $Os(bpy)_3^{3+/2+}$ Couple in Nafion, *Journal of the American Chemical Society*, **113**, 1922-1932.

12. **Antonello, S., M. Musumeci, D. D. M. Waynerand** and **F. Maran**, (1997 a) Electroreduction of Dialkyl Peroxides. Activation−Driving Force Relationships and Bond Dissociation Free Energies. *J. Am. Chem. Soc*. **119**, 9541-9549.

13. **Antonello, S.** and **F. Maran**, (1997 b) Evidence for the Transition between Concerted and Stepwise Heterogeneous Electron Transfer−Bond Fragmentation Mechanisms. *J. Am. Chem. Soc.*, 119, 12595-12600.

14. **Antonello, S.** and **F. Maran** (1999) The Role and Relevance of the Transfer Coefficient α in the Study of Dissociative Electron Transfers: Concepts and Examples from the Electroreduction of Perbenzoates. *J. Am. Chem. Soc.* **121**, 9668-9676.

15. **Armarego, W. L. E.** and **C. L. L. Chai** (2003) Purification of laboratory chemicals, Fifth edition, Elsevier Science, USA. Chapter-4, p 85.

16. **Baizer, M. M.** and **J. L. Chruma** (1972) Electrolytic reductive coupling. XXI. Reduction of organic halides in the presence of electrophiles. *J Org Chem*. **37**, 1951-1960.

17. **Bard, A. J.** and **L. R. Faulkner** (2001) Electrochemical methods-Fundamentals and Applications John Wiley, New York, Chapter-3, 92-96.

18. **Barsoukov, E.** and **J. R. Macdonald** (2005) Impedance Spectroscopy: Theory, Experiment, and Applications, Wiley Interscience, USA.

19. **Becke, A. D.** (1993) Density-functional thermochemistry. III. The role of exact exchange. *J. Chem. Phys.* **98,** 5648-5652

20. **Bockris, J. O'M.** and **S. U. M. Khan** (1979) Quantum Electrochemistry, Plenum Press, New York.

21. **Brown, O. R.** and **K. Taylor** (1974) Adsorbed alkyl radicals in the cathodic synthesis of mercury dialkyls. *J. Electroanal. Chem*. **50**, 211-220.

22. **Bylaska, E. J., M. Dupuis,** and **P. G. Tratnyek** (2008) One-Electron-Transfer Reactions of Polychlorinated Ethylenes: Concerted and Stepwise Cleavages. *J. Phys. Chem. A.* **112**, 3712-3721

23. **Cardinale, A., A. A. Isse, A. Gennaro, M. Robert,** and **J. M. Savéant** (2002) Dissociative Electron Transfer to Haloacetonitriles. An Example of the Dependency of In-Cage Ion-Radical Interactions upon the Leaving Group. *J. Am. Chem. Soc.* **124**, 13533-13539.

24. **Chidsey, C.E.D.** and **R. W. Murray** (1986) Redox Capacity and Direct Current Electron conductivity in Electroactive materials. *Journal of Physical Chemistry*, **90**, 3850-3856.

25. **Christensen, T. B.** and **K. Daasbjerg** (1997) Investigation of the Direct and Indirect Reduction Processes of Some Disulfides by Electrochemical Means. *Acta Chem. Scand*. **51**, 307-317.

26. **Combellas, C., F. Kanoufi,** and **A. Thiébault** (1996) Reducibility of the carbon-fluorine bond in the trifluoromethyl group. *J. Electroanal. Chem.* **407**, 195-202.

27. **Costentin, C., M. Robert,** and **J. M. Savéant** (2004) Stepwise and Concerted Electron-Transfer/Bond Breaking Reactions. Solvent Control of the Existence of Unstable π-Ion Radicals and of the Activation Barriers of Their Heterolytic Cleavage. *J. Am. Chem. Soc.* **126**, 16834-16840.

28. **Costentin, C., M. Robert,** and **J. M. Savéant** (2006) Electron transfer and bond breaking: Recent advances. *Chem. Phys.* **324,** 40-56.

29. **Costentin, C., L. Donati,** and **M. Robert** (2009) Passage from Stepwise to Concerted Dissociative Electron Transfer through Modulation of Electronic States Coupling. *Chem. Eur. J.* **15**, 785 – 792.

30. **Cundari, T, R.** and **W. J. Stevens** (1993) Effective core potential methods for the lanthanides. *J. Chem. Phys.* **98,** 5555-5565.

31. **Daasbjerg, K., H. Jensen, R. Benassi, F. Taddei, S. Antonello, A. Gennaro,** and **F. Maran** (1999) Evidence for Large Inner Reorganization Energies in the Reduction of Diaryl Disulfides: Toward a Mechanistic Link between Concerted and Stepwise Dissociative Electron Transfers? *J. Am. Chem. Soc*. **121**, 1750-1751.

32. **Dahm, C. E.** and **D. G. Peters** (1994) Catalytic reduction of Iodoethane and 2-Iodopropane at Carbon Electrodes Coated with Anodically Polymerized Films of Nickel(II) Salen. *Anal Chem*. **66**, 3117-3123.

33. **Drakesmith, F. G.** (1972) Electrochemical reduction of fluorinated aromatic carboxylic acids. *J. Chem. Soc., Perkin Trans.* **1,** 184 – 189.

34. **Durante, C., A. A. Isse, G. Sandonà,** and **A. Gennaro** (2009) Electrochemical hydrodehalogenation of polychloromethanes at silver and carbon electrodes. *Applied Catalysis B: Environmental*. **88,** 479–489.

35. **Elving, P. J.** and **J. T. Leone** (1957) Electrochemical Fission of the Carbon-FIuorine Bond. pH-Dependency of the Process. *J. Am. Chem. Soc*. **79**, 1546-1550.

36. **Elving, P .J., I. Rosenthal, J. R. Hayes,** and **A. J. Martin** (1961) Effect of Structure on the Stereochemistry of Electrode Reactions. Monobromo C_4 Dibasic Acids and Esters. *Anal. Chem*. **33**, 330-334.

37. **Fillon, H., E. L. Gall, C. Gosmini,** and **J. Périchon** (2002) Pure acetonitrile as solvent for the efficient electrochemical conversion of aryl bromides in organozinc species and their coupling reaction with acetyl chloride. *Tetrahedron. Lett*. **43**, 5941-5944.

38. **Frisch, M. J., G. W. Trucks, H. B. Schlegel, G. E. Scuseria, M. A. Robb, J. R. Cheeseman, J. A. Montgomery, Jr., T. Vreven, K. N. Kudin, J. C.**

Burant, J. M. Millam, S. S. Iyengar, J. Tomasi, V. Barone, B. Mennucci, M. Cossi, G. Scalmani, N. Rega, G. A. Petersson, H. Nakatsuji, M. Hada, M. Ehara, K. Toyota, R. Fukuda, J. Hasegawa, M. Ishida, T. Nakajima, Y. Honda, O. Kitao, H. Nakai, M. Klene, X. Li, J. E. Knox, H. P. Hratchian, J. B. Cross, V. Bakken, C. Adamo, J. Jaramillo, R. Gomperts, R. E. Stratmann, O. Yazyev, A. J. Austin, R. Cammi, C. Pomelli, J. W. Ochterski, P. Y. Ayala, K. Morokuma, G. A. Voth, P. Salvador, J. J. Dannenberg, V. G. Zakrzewski, S. Dapprich, A. D. Daniels, M. C. Strain, O. Farkas, D. K. Malick, A. D. Rabuck, K. Raghavachari, J. B. Foresman, J. V. Ortiz, Q. Cui, A. G. Baboul, S. Clifford, J. Cioslowski, B. B. Stefanov, G. Liu, A. Liashenko, P. Piskorz, I. Komaromi, R. L. Martin, D. J. Fox, T. Keith, M. A. Al-Laham, C. Y. Peng, A. Nanayakkara, M. Challacombe, P. M. W. Gill, B. Johnson, W. Chen, M. W. Wong, C. Gonzalez, and J. A. Pople, Gaussian 03, Revision E.01, Gaussian, Inc., Wallingford CT, 2004

39. **Fritsch-Faules** and **L. R. Faulkner** (1989) A Microscopic model for Diffusion of Electrons by Successive Hopping Among Redox Centers in Networks, *J. Electroanal. Chem*. **236**, 237-255.

40. **Fry, A. J.** and **M. A. Mitnick** (1969) Electrochemical generation of stereoisomeric vinyl radicals. *J. Am. Chem. Soc*. **91**, 6207-6208.

41. **Farwell, S. O., F. A. Beland,** and **R. D. Geer** (1975) Interrupted-sweep voltammetry for the identification of polychlorinated biphenyls and naphthalenes, *Anal. Chem.* **47**, 895-903

42. **Fu, Y., L. Liu, H. Z. Yu, Y. M. Wang,** and **Q. X. Guo** (2005) Quantum-Chemical Predictions of Absolute Standard Redox Potentials of Diverse

Organic Molecules and Free Radicals in Acetonitrile. *J. Am. Chem. Soc.* **127**, 7227-7234.

43. **Gennaro, A., A. A. Isse, J. M. Savéant, M. G. Severin,** and **E. Vianello** (1996) Homogeneous Electron Transfer Catalysis of the Electrochemical Reduction of Carbon Dioxide. Do Aromatic Anion Radicals React in an Outer-Sphere Manner? *J. Am. Chem. Soc*. **118**, 7190-7196.

44. **Girija, T. C** and **M. V. Sangaranarayanan** (2006) Analysis of polyaniline based Nickel electrodes for Electrochemical supper capacitors. *Journal of Power Sources*, **156**, 705-711.

45. **Gomes, P., H. Fillon, C. Gosmini, E. Labbe,** and **J. Périchon,** (2002) Synthesis of unsymmetrical biaryls by electroreductive cobalt-catalyzed cross-coupling of aryl halides. *Tetrahedron*, **58**, 8417-8424.

46. **Grimshaw, J.** (2000) Electrochemical reactions and mechanisms in Organic chemistry, Elsevier, Chapter-4

47. **Houmam, A.** (2008) Electron Transfer Initiated Reactions: Bond Formation and Bond Dissociation. *Chem. Rev.* **108**, 2180-2237.

48. **Houser, K. J., D. E. Bartak,** and **M. D. Hawley** (1973) Electrochemical studies of the formation and decomposition of the fluorobenzonitrile radical anions. *J. Am. Chem. Soc*. **95**, 6033-6040.

49. **Hush, N. S.** (1958) Adiabatic Rate Processes at Electrode. I. Energy-Charge Relationship. *J. Chem. Phys.* **28**, 962-972.

50. **Hush, N. S.** (1961) Adiabatic theory of outer sphere electron transfer reactions in solution. *Trans. Faraday Soc.* **57**, 557-580.

51. **Imbeaux, J. C.** and **J. M. Savéant** (1973) Convolutive Potential Sweep Voltammetry I. Introduction, *J. Electroanal. Chem.* **44,** 169-187.

52. **Isse, A. A., P. R. Mussini,** and **A. Gennaro** (2009 a) New Insights into Electrocatalysis and Dissociative Electron Transfer Mechanisms: The Case of Aromatic Bromides. *J. Phys. Chem. C*. **113**, 14983–14992

53. **Isse, A. A., G. Berzi, L. Falciola, M. Rossi, P. R. Mussini,** and **A. Gennaro** (2009 b) Electrocatalysis and electron transfer mechanisms in the reduction of organic halides at Ag. *J. Appl. Electrochem.* **39,** 2217–2225.

54. **Jaworski, J. S., M. Cembor,** and **D. Kuck** (2007) Solvent effect on reductive bond cleavage of 1-chloro-10-methyltribenzotriquinacene: Change from the concerted to the stepwise mechanism. *Electrochim. Acta*. **52**, 2196–2202.

55. **Karrenbrock, F.** and **H. J. Schafer** (1978) Cathodic addition of tetrachloromethane and ethyl trichloroacetate to carbonyl compounds, *Tetrahedron Lett*. **19**, 1521-1522.

56. **Kojima, H.** and **A. J. Bard**, (1975) Determination of rate constants for the electroreduction of aromatic compounds and their correlation with homogeneous electron transfer rates. *J. Am. Chem. Soc.*, **97,** 6317-6324.

57. **Kuznetsov, A. M., R. R. Nazmutdinov,** and **W. Schmickler** (2002) Monte Carlo simulation of electrochemical electron transfer processes. *Journal of Electroanalytical Chemistry*, **532**, 171-180.

58. **Lawson, R. J.** and **T. Maloy** (1974) Mechanistic Studies Using Double Potential Step Chronoamperometry: The EC, ECE, and Second-Order Dimerization Mechanisms. *Anal. Chem.* **46**, 559-562.

59. **Lee, C., W. Yang** and **R. G. Parr** (1988) Development of the Colle-Salvetti correlation-energy formula into a functional of the electron density. *Phys. Rev. B.* **37,** 785-789

60. **Leopold, M. C.** and **E. F. Bowden** (2002) Influence of Gold Substrate Topography on the Voltammetry of Cytochrome c Adsorbed on Carboxylic Acid Terminated Self-Assembled Monolayers. *Langmuir*, **18**, 2239-2245.

61. **Ludwig, K.** and **B. Speiser**; (2004) EChem++ - An Object-Oriented Problem Solving Environment for Electrochemistry. 2. The Kinetic Facilities of Ecco - A Compiler for (Electro-) Chemistry. *J. Chem. Inf. Comput. Sci*. **44**, 2051-2060.

62. **Lund, H.** and **O. Hammerich**, (2001) Organic electrochemistry. Fourth Edition, Marcel Dekker, USA, Chapter–8.

63. **Maran, F., D. D. M. Wayner,** and **M. S. Workentin** (2001) Kinetics and mechanism of the dissociative reduction of C---X and X---X bonds (X = O, S). *Adv. Phys. Org. Chem*. **36**, 85-166.

64. **Marcus, R. A.** (1956) On the theory of oxidation reduction reactions involving Electron transfer 1. *J. Chem .Phys.* **24,** 966-978.

65. **Marcus, R. A.** (1963) Free energy of Non-Equilibrium polarization systems. III. Statistical Mechanics of Homogeneous and Electrode reactions. *J. Chem. Phys.* **39,** 1734-1740.

66. **Marcus, R. A.** (1968) Theoretical relations among rate constants barriers and Bronsted slopes of Chemical reactions. *J. Phys. Chem*. **72**, 891-899.

67. **Marcus, R. A.** (1977) Special Topics in Electrochemistry, pp-161-179. In **P. A. Rock** (Ed), Elsevier, New York.

68. **Marcus, R. A.** and **N. Sutin** (1985) Electron transfer in Chemistry and Biology. *Biochim. Biophys. Acta*, **811**, 265-322.

69. **Marcus**, **Y.** (1997) Ion Properties, Marcel Dekker, New York.

70. **Mbarak, M. S.** and **D. G. Peters** (1982) Electrochemical reduction of 2-iodooctane and 2-bromooctane at mercury cathodes in dimethylformamide. *J. Org. Chem*. **47**, 3397-3403.

71. **Macdonald, D.** (1977) Transient Techniques in Electrochemistry, Plenum Press (New York).

72. **McLean, A. D.** and **G. S. Chandler** (1980) Contracted Gaussian-basis sets for molecular calculations. 1. 2nd row atoms, Z=11-18. *J. Chem. Phys.* **72,** 5639-5648

73. **McNamee, G. M., B. C. Willett, D. M. L. Perriere,** and **D. G. Peters** (1977) Electrochemical reduction of 1-iododecane and 1-bromodecane at a mercury cathode in dimethylformamide. *J. Am. Chem. Soc*. **99**, 1831-1835.

74. **Miller, L. L.** and **R. Riekena** (1969) Electrochemical reduction of vinyl bromides. *J. Org. Chem*. **34**, 3359-3362.

75. **Miller, E. K.** and **Z. Vajtner** (1985) Electroreductive dehalogenation of fluorobenzenes. *J. Org. Chem.* **50**, 1394-1399.

76. **Nadjo, L.** and **J. M. Savéant** (1973) Linear sweep voltammetry: Kinetic control by charge transfer and/or secondary chemical reactions: I. Formal kinetics. *J. Electroanal. Chem.* **48**, 113-145.

77. **Nakano, K., T. Yoshitake, Y. Yamashita,** and **E. F. Bowden** (2007) Cytochrome c Self-Assembly on Alkanethiol Monolayer Electrodes as Characterized by AFM, IR, QCM, and Direct Electrochemistry. *Langmuir*, **23**, 6270-6275.

78. **Nicholson, R. S.** and **I. Shain** (1964) Theory of Stationary electrode polarography - Single scan cyclic methods applied to reversible, irreversible and kinetic systems. *Anal. Chem.* **36**, 706-723.

79. **Nicholson, R. S.** (1965) Theory and Application of Cyclic Voltammetry for Measurement of Electrode Reaction Kinetics. *J. Am. Chem. Soc.* **37**, 1351-1355.

80. **Nicholson, R. S.** (1966) Semiempirical Procedure for Measuring with Stationary Electrode Polarography Rates of Chemical Reactions Involving the Product of Electron Transfer. *Anal .Chem.* **38**, 1406-1406.

81. **Parker, V. D.** (1981) Electrode Mechanism Analysis by Linear Sweep Voltammetry. III. Reaction Orders, the Origin of the Response. *Acta. Chem. Scand. B.* **35**, 259-262.

82. **Pause, L., M. Robert,** and **J. M. Savéant** (1999) Can Single-Electron Transfer Break an Aromatic Carbon−Heteroatom Bond in One Step? A Novel Example of Transition between Stepwise and Concerted Mechanisms in the Reduction of Aromatic Iodides. *J. Am. Chem. Soc.* **121**, 7158-7159.

83. **Pause, L., M. Robert,** and **J. M. Savéant** (2000) Reductive Cleavage of Carbon Tetrachloride in a Polar Solvent. An Example of a Dissociative Electron Transfer with Significant Attractive Interaction between the Caged Product Fragments. *J. Am. Chem. Soc.* **122**, 9829–9835.

84. **Peover, M. E.** and **J. S. Powell** (1967) Dependence of electrode kinetics on molecular structure nitro-compounds in dimethylformamide. *J. Electroanal. Chem.* **20**, 427-433.

85. **Pilard, J. F., S. Postec, J. Simonet** and **G. Mousset** (1998) Formation and reactivity of arylradicals from cathodic cleavage of halonitrobenzenes and related compounds. *Electrochim. Acta.* **43**, 3135-3140.

86. **Prasad, M. A.** and **M. V. Sangaranarayanan** (2004a) Electrochemical reductive cleavage of carbon–halogen bonds in 5-bromo-1,3-dichloro-2-iodobenzene. *Tetrahedron*. **60**, 10967–10972.

87. **Prasad, M. A.** and **M. V. Sangaranarayanan** (2004 b) Electrochemical reductive cleavage of carbon tetrachloride in aqueous–nonaqueous binary solvents. *J. Electroanal. Chem.* ***569****,* 127–134.

88. **Prasad, M. A.** and **M. V. Sangaranarayanan** (2004 c) Cleavage of an aromatic carbon–heteroatom bond in a single step or successive steps?—A mechanistic distinction in the reduction of 5-bromo-1,3-dichloro-2-iodobenzene. *Tetrahedron. Lett.* **45**, 4741-4744.

89. **Prasad, M. A.** and **M. V. Sangaranarayanan** (2005 a) Electrochemical reductive cleavage of carbon–chlorine bond in 1-chloro-2,4-dinitrobenzene. *Electrochim. Acta.* 51, 242–246.

90. **Prasad, M. A.** and **M.V. Sangaranarayanan** (2005 b) Evidence for the formation of radical anion in the reductive cleavage of carbon–bromine bond in 4′-bromomethylbiphenyl-2-carbonitrile. *Chem. Phys. Lett*. **414,** 55-60.

91. **Rabalais, J. W., L. O. Werme, T. Bergmark, L. Karlsson, M. Hussain,** and **K. Siegbahn** (1972) Electron Spectroscopy of Open-Shell Systems: Spectra of $Ni(C_5H_5)_2$, $Fe(C_5H_5)_2$, $Mn(C_5H_5)_2$, and $Cr(C_5H_5)_2$. *J. Chem. Phys*, **57**, 1185-1192.

92. **Raghavachari, K., J. S. Binkley, R. Seeger,** and **J. A. Pople** (1980) Self-Consistent Molecular Orbital Methods. 20. Basis set for correlated wave-functions. *J. Chem. Phys.* **72,** 650-654.

93. **Retter, U., A. Widmann, K. Siegler,** and **H. Kahlert** (2003) On the impedance pf potassium nickel(II) composite electrodes- the generalization

of the Randles model referring to homogeneous electrode materials. *Journal of Electroanalytical Chemistry*, **546**, 87-96.

94. **Saboureau, C., M. Troupel, S. Sibille, E. d'Incan,** and **J. Périchon** (1989) Electroformylation of organic halides in *N*,*N*-dimethylformamide: an efficient electrosynthesis of aldehydes. *J. Chem. Soc., Chem. Comm.* 895 – 896.

95. **Savéant, J. M.** and **D. Tessier** (1975 a) Convolutive Potential Sweep Voltammetry IV. Homogeneous follow-up chemical reactions. *J. Electroanal. Chem.* **61**, 251-263.

96. **Savéant, J. M.** and **D. Tessier** (1975 b) Convolution potential sweep voltammetry V. Determination of charge transfer kinetics deviating from the Butler-Volmer behaviour. *J. Electroanal. Chem.* **65**, 57-66.

97. **Savéant J. M.** (1986) Electron Hopping Between Fixed Sites. Equivalent Diffusion and Migration Laws, *Journal of Electrocnalytical Chemistry*, **201**, 211-213.

98. **Savéant, J. M.** (1987) A Simple Model for the Kinetics of Dissociative Electron Transfer in Polar Solvents. Application to the Homogeneous and Heterogeneous Reduction of Alkyl Halides. *J. Am. Chem. Soc.* **109**, 6788-6795.

99. **Savéant, J. M.** (1990) Single electron transfer and Nucleophilic Substitution, *Adv. Phys. Org. Chem.* **26**, 1-130.

100. **Savéant, J. M.** (1993) Electron Transfer, Bond Breaking, and Bond Formation *Acc. Chem. Res.* **26**, 455-461.

101. **Savéant, J. M** (2000) Electron transfer, bond breaking and bond formation. *Adv. Phys. Org. Chem*. **35**, 117-192.

102. **Scialdone, O., A. Galia, C. L. Rocca** and **G. Filardo** (2005) Influence of the nature of the substrate and of operative parameters in the electrocarboxylation of halogenated acetophenones and benzophenones. *Electrochim. Acta.,* **50,** 3231-3242.

103. **Semmelhack, M. F., R. J. DeFranco,** and **J. Stock** (1972) Selective introduction of hydrogen isotopes by electrolytic reduction of the carbon-halogen bond. *Tetrahedron Lett.* **13**, 1371-1374.

104. **Sethi, R.** and **M. V. Sangaranarayanan** (2008) Nonequilibrium Thermodynamics Formalism for Marcus Theory of Heterogeneous and Self-Exchange Electron-Transfer Rate Constants. *J. Phys. Chem. A.* **112**, 4308-4313.

105. **Shono, T., H. Ohmizu, S. Kawakami, S. Nakano,** and **N. Kise** (1981) A novel chain reaction induced by cathodic reduction. Addition of trichloromethyl anion to aldehydes or vinyl acetate. *Tetrahedron Lett*. **22**, 871-874.

106. **Shono, T., N. Kise, A. Yamazaki,** and **H. Ohmizu** (1982) Novel selective synthesis of α-chloromethyl, α,α-dichloromethyl, and α,α,α-trichloromethyl ketones from aldehyde utilizing electroreduction as key reactions. *Tetrahedron Lett*. **23**, 1609-1612.

107. **Shono, T., N. Kise,** and **T. Suzumoto** (1984) Diastereoselective addition of electrogenerated trichloromethyl and dichloro(methoxycarbonyl)methyl anions to α-branching aldehydes. *J. Am. Chem. Soc*. **106**, 259-260.

108. **Sibille, S., E d'Incan, L. Leport,** and **J. Périchon** (1986) Electrosynthesis of alcohols from organic halides and ketones or aldehydes. *Tetrahedron Lett*. **27**, 3129-3132.

109. **Stevens, W. J., H. Basch,** and **M. Krauss** (1984) Compact effective potentials and efficient shared-exponent basis-sets for the 1st-row and 2nd-row atoms. *J. Chem. Phys.* **81,** 6026-6033.

110. **Stevens, W. J., M. Krauss, H. Basch,** and **P. G. Jasien** (1992) Relativistic compact effective potentials and efficient, shared-exponent basis-sets for the 3rd-row, 4th-row, and 5th-row atoms. *Can. J. Chem.* **70,** 612-630.

111. **Taube, H.** Electron transfer reactions of complex ions in solution. Academic Press, New York, 1970.

112. **Testa, A. C.** and **W. H. Reinmuth** (1961) Stepwise Reactions in Chronopotentiometry. *Anal Chem.* **33,** 1320-1324.

113. **Volkov, A. G.** and **D. W. Deamer**, (1996) Liquid-Liquid interfaces Theory and Methods, CRC press, New York. Chapter-8.

114. **Wawzonek, S.** and **R. C. Duty** (1961) Polarographic Studies in Acetonitrile and Dimethylformamide. *J Electrochem Soc.* **108**, 1135-1138.

115. **Weast, R. C.** (1979) Hand Book of Chemistry and Physics, 59th edition. CRC Press,

116. **Webster, R. D.** (2004) In Situ Electrochemical-NMR Spectroscopy. Reduction of Aromatic Halides. *Anal. Chem.* **76** (2004) 1603-1610.

117. **Wentworth, W. E., R. George,** and **H. Keith** (1969) Dissociative Thermal Electron Attachment to Some Aliphatic Chloro, Bromo, Iodo Compounds. *J. Chem. Phys.* **51**, 1791-1801.

118. **Yasuhara, A., A. Kasano,** and **T. Sakamoto** (1998) Electrochemical Generation of Highly Reactive Nickel and Its Utilization for the Dehalogenative Coupling of Aryl Halides. *Organometallics,* **17**, 4754-4756.

119. **Yoshida, J., K. Muraki, H. Funahashi,** and **N. Kawabata** (1986) Electrochemical synthesis of organosilicon compounds. *J. Org. Chem.* **51,** 3996-4000.

LIST OF PUBLICATIONS

(1) **Muthukrishnan, A.** and **M. V. Sangaranarayanan** (2006) Differential capacitance of liquid/liquid interfaces - A lattice gas model approach. *Journal of Colloid and Interface Science,* **296,** 624-633.

(2) **Muthukrishnan, A.** and **M. V. Sangaranarayanan** (2007) Hydration energies of C_{60} and C_{70} fullerenes – A novel Monte Carlo simulation study. *Chemical Physics.,* **331,** 200-206.

(3) **Muthukrishnan, A.** and **M. V. Sangaranarayanan** (2007) Electrochemical reduction of carbon–fluorine bond in 4-fluorobenzonitrile – Mechanistic analysis employing Marcus–Hush quadratic activation-driving force relation, *Chemical Physics Letters.,* **446**, 297-303.

(4) **Muthukrishnan, A.** and **M. V. Sangaranarayanan** (2009) Mechanistic Analysis of the Reductive cleavage of Carbon-Halogen bonds in halopentafluorobenzenes, *Journal of the Electrochemical Society.,* **156(2),** F23-F28.

(5) **A. Muthukrishnan** and **M. V. Sangaranarayanan** (2010) Analysis of C-F bond cleavages in Methylfluorobenzoates- Fragmentation and dimerization of anion radicals using Convolution Potential Sweep Voltammetry. *Electrochimica Acta*., **55,** 1664-1669.

(6) **A. Muthukrishnan, M. V. Sangaranarayanan, V. P. Boyarskiy, and I. A. Boyarskaya (2010)** Regioselective Electrochemical Reduction of 2,4-dichlorobiphenyl - Distinct Standard Reduction Potentials for carbon-chlorine bonds using Convolution Potential Sweep Voltammetry, *Chemical Physics Letters*., **490,** 148-153.